Systematics and biogeography of the Boana albopunctata species group (Anura, Hylidae), with the description of two new species from Amazonia

Antoine Fouquet, Pedro Marinho, Alexandre Réjaud, Thiago Carvalho, Marcel Caminer, Martin Jansen, Raíssa Rainha, Miguel Rodrigues, Fernanda Werneck, Albertina Lima, et al.

TSAB#1873869, VOL 0, ISS 0

Systematics and biogeography of the *Boana albopunctata* species group (Anura, Hylidae), with the description of two new species from Amazonia

Antoine Fouquet, Pedro Marinho, Alexandre Réjaud, Thiago R. Carvalho, Marcel A. Caminer, Martin Jansen, Raíssa N. Rainha, Miguel T. Rodrigues, Fernanda P. Werneck, Albertina P. Lima, Tomas Hrbek, Ariovaldo A. Giaretta, Pablo J. Venegas, Germán Chávez, and Santiago Ron

QUERY SHEET

This page lists questions we have about your paper. The numbers displayed at left are hyperlinked to the location of the query in your paper.

The title and author names are listed on this sheet as they will be published, both on your paper and on the Table of Contents. Please review and ensure the information is correct and advise us if any changes need to be made. In addition, please review your paper as a whole for typographical and essential corrections.

Your PDF proof has been enabled so that you can comment on the proof directly using Adobe Acrobat. For further information on marking corrections using Acrobat, please visit http://journalauthors.tandf.co.uk/production/acrobat.asp; https://authorservices.taylorandfrancis.com/how-to-correct-proofs-with-adobe/

The CrossRef database (www.crossref.org/) has been used to validate the references.

AUTHOR QUERIES

Q1 Please provide complete details for (Naka et al., 2018, Naka et al. 2018, Hime et al. 2020, Molak & Ho, 2015, Papadopoulou et al., 2010, Drummond & Rambaut, 2007, Bioacoustics Research Program 2012, Ronquist, 1997, Landis et al., 2013, Ree & Smith, 2008, Avila-Pires et al. 2010, and Avila & Kawashita -Ribeiro 2011) in the reference list or delete the citation from the text.

Q2 There is no mention of (Ceballos et al. 2015, Fouquet et al. 2007a, Fouquet et al. 2012, Günther 1858, Günther 1859, Klaus & Matzke 2020, Silva et al. 2020 and Sturaro et al. 2020) in the text. Please insert a citation in the text or delete the reference as appropriate.

Q3 Please provide the volume number and page range.

Q4 Please provide the volume number and page range.

Q5 The year of publication has been changed as per Crossref details both in the list and in the text for this reference. Please check.

Q6 The year of publication has been changed as per Crossref details both in the list and in the text for this reference. Please check.

Q7 If your paper introduces new zoological taxa at family-group level or below, you are now required to register your paper with ZooBank and insert the generated ZooBank ID (LSID) here. Individual new taxa need not be registered before publication; this can be done subsequently should you wish. Please go to http://www.zoobank.org/register to complete this task. You will need your article DOI to register. After publication, you must amend your ZooBank record of your paper to reflect the date of publication. Please see http://www.zoobank.org/help for further information.

Systematics and Biodiversity (2021), **0(0)**: 1–38

Taylor & Francis
Taylor & Francis Group

Research Article

Systematics and biogeography of the *Boana albopunctata* species group (Anura, Hylidae), with the description of two new species from Amazonia

ANTOINE FOUQUET[1], PEDRO MARINHO[2], ALEXANDRE RÉJAUD[1], THIAGO R. CARVALHO[3], MARCEL A. CAMINER[4,5], MARTIN JANSEN[6], RAÍSSA N. RAINHA[7], MIGUEL T. RODRIGUES[8], FERNANDA P. WERNECK[7], ALBERTINA P. LIMA[7], TOMAS HRBEK[9], ARIOVALDO A. GIARETTA[2], PABLO J. VENEGAS[10], GERMÁN CHÁVEZ[10] & SANTIAGO RON[4]

[1]Laboratoire Evolution et Diversité Biologique, UMR 5174, CNRS, IRD, Université Paul Sabatier, Bâtiment 4R1 31062 cedex 9, 118 Route de Narbonne, Toulouse, 31077, France
[2]Laboratório de Anuros Neotropicais, Instituto de Ciências Exatas e Naturais do Pontal, Universidade Federal de Uberlândia, Ituiutaba, MG, Brazil
[3]Laboratório de Herpetologia, Departamento de Biodiversidade e Centro de Aquicultura, I.B., Universidade Estadual Paulista, Rio Claro, SP, Brazil
[4]Museo de Zoología, Escuela de Biología, Pontificia Universidad Católica del Ecuador, Quito, Ecuador
[5]Institute of Organismic and Molecular Evolution, Johannes Gutenberg University Mainz, Germany
[6]Department of Terrestrial Zoology, Research Institute and Nature Museum Senckenberg, Frankfurt, Germany
[7]Instituto Nacional de Pesquisas da Amazônia, Coordenação de Biodiversidade, Manaus, AM, Brazil
[8]Departamento de Zoologia, Universidade de São Paulo, Instituto de Biociências, São Paulo, SP, Brazil
[9]Departamento de Genética, Universidade Federal do Amazonas, Manaus, AM, Brazil
[10]Instituto Peruano de Herpetología, Lima, Peru

The outstanding species richness of Amazonia has fascinated biologists for centuries. However, the records of actual numbers and distribution of species forming its ecosystems are so incomplete that the understanding of the historical causes and regional determinants of this diversity remain speculative. Anuran clades have repeatedly been documented to harbour many unnamed species in this region, notably the *Boana albopunctata* species group. Considering the documented distribution and the ecology of the species of that group, we hypothesized that it diversified via successive trans-riverine dispersals during the late Miocene and Pliocene, after the formation of the modern Amazon watershed. To test this hypothesis, we gathered an extensive dataset of 16S rDNA sequences sampled throughout Amazonia and a mitogenomic dataset representative of the diversity of the clade to (1) re-evaluate species boundaries and distributions, and (2) infer the spatio-temporal history of diversification within Amazonia. We delimited 14 Operational Taxonomic Units (OTUs) in an Amazonian clade, i.e., 75% higher than currently recognized (14 OTUs for eight described species). Combining molecular data with morphological and acoustic data, two new species, *Boana courtoisae* sp. nov. from the eastern Guiana Shield and *Boana eucharis* sp. nov. from Southern Amazonia, are described herein. These species belong to a clade that diversified throughout Amazonia during the last 10 Ma, thus more recently than co-distributed small terrestrial anurans but concomitantly with other more vagile vertebrates. Our time-scaled phylogeny and biogeographic analyses suggest an initial east-west divergence and confirm reciprocal trans-riverine dispersals during the last 5 Ma. The geomorphological evolution of the region and species-specific dispersal ability largely explain these distinct spatio-temporal patterns across anurans.

Key words: Amphibia, biodiversity, Guiana Shield, mitogenomics, neotropics, phylogenetics

Introduction

The Neotropics harbour the most diverse ecosystems on the planet (Jenkins et al., 2013). Within the Neotropics,

Correspondence to: Antoine Fouquet. E-mail: fouquet.antoine@gmail.com; Pedro Marinho E-mail: pmarinho50@gmail.com

ISSN 1477-2000 print / 1478-0933 online

https://dx.doi.org/10.1080/14772000.2021.1873869

Amazonia stands as a major biogeographic region covering more than 6.5 million km^2, including the largest continuous tract of tropical forest (40% of the world's tropical rainforests), encompassing the most important drainage (Amazon River basin) and probably hosting the highest continental biodiversity on earth (Myers et al., 2000). The outstanding species richness of this region has raised many questions concerning its origins and diversification mechanisms. While all agree on the astounding diversity of Amazonia, our understanding of the actual number and distribution of species forming its ecosystems is in fact so incomplete (Ficetola et al., 2014; Meyer et al., 2015; Vacher et al., 2020) that it has so far hampered investigations at the regional scale. Consequently, the understanding of the historical causes and regional determinants of this outstanding diversity remain speculative (Antonelli et al., 2018). Another consequence is that the collision between the Linnean shortfall and the biodiversity crisis is particularly evident in Amazonia (Guerra et al., 2020). With almost the entire eastern and southern parts (25%) of its extent being already deforested for agriculture, an unknown proportion of endemic species, and thus of the testimony of Amazonian history, has already vanished (Lovejoy & Nobre, 2019).

Anuran clades have repeatedly been documented to harbour many unnamed species in Amazonia (Vacher et al., 2020) and to display strikingly allopatric distribution patterns that could provide crucial insights into Amazonia's past (Fouquet, Cassini, Haddad, Pech, & Rodrigues, 2014; Réjaud et al., 2020). This is notably the case of the *Boana albopunctata* species group (Caminer & Ron, 2014; Funk et al., 2012). This group is only defined on the basis of molecular data (Faivovich et al., 2005), and currently comprises 16 valid nominal species distributed in the Caribbean and South America: *Boana albopunctata* (Spix, 1824), *Boana alfaroi* (Caminer & Ron, 2014), *Boana almendarizae* (Caminer & Ron 2014), *Boana caiapo* Pinheiro et al., 2018, *Boana calcarata* (Troschel, 1848), *Boana dentei* (Bokermann, 1967), *Boana fasciata* (Günther, 1858), *Boana heilprini* (Noble, 1923), *Boana lanciformis* (Cope, 1871), *Boana leucocheila* (Caramaschi & de Niemeyer, 2003), *Boana maculateralis* (Caminer & Ron, 2014), *Boana multifasciata* (Günther, 1859), *Boana paranaiba* (Carvalho, Giaretta & Facure, 2010), *Boana steinbachi* (Boulenger, 1905), *Boana tetete* (Caminer & Ron, 2014) and *Boana raniceps* (Cope, 1862). Within this clade, *B. heilprini* is the most distinct since it is confined to Hispaniola and is phylogenetically distant from a clade formed by all the other species of the group (Duellman, Marion, & Hedges, 2016). We can also distinguish *B. raniceps* and the *B. albopunctata* clade (*B. lanciformis*, *B. albopunctata*, *B. multifasciata*, *B. paranaiba*, *B. caiapo*, *B. leucocheila*), which occur widely in the open habitats of the Cerrado and Amazonia (Camurugi et al., 2021), from the Amazonian clade. According to Caminer and Ron (2014), this Amazonian clade is itself subdivided in two main groups, hereafter called the *B. calcarata* (*B. fasciata*, *B. calcarata*, *B. almendarizae*, *B. maculateralis*) and the *B. steinbachi* (*B. tetete*, *B. alfaroi*, *B. steinbachi*) clades.

Within this Amazonian clade, Funk, Caminer, and Ron (2012) identified no less than seven putative unnamed species based on mitochondrial divergence and acoustic data. These species add up to the 10 taxa that were valid at that time. Caminer and Ron (2014) completed this picture by documenting two additional lineages, describing four of the previously discovered species, and removing *B. steinbachi* from its synonymy with *B. fasciata*. However, sampling of both studies was circumscribed to western Amazonia (mostly Ecuador) while the species complex occurs throughout Amazonia. Populations from the eastern Guiana Shield lowlands are already assumed to belong to a yet unnamed species (Caminer & Ron, 2014), but the status of numerous other populations throughout Amazonia, generally identified as *B. fasciata*, remain virtually unknown. More recently, Vacher et al. (2020) suggested, based on 16S mitochondrial DNA (mtDNA) sequences, that up to 22 species could exist in that group and that the distribution of most species could be circumscribed to small ranges within Amazonia.

These aforementioned studies improved our understanding of the actual diversity in the *B. calcarata*/*steinbachi* clade, but left virtually unexplored the temporal and spatial context of the diversification within Amazonia. The crown age of this Amazonian clade was estimated between 16–11 million years ago (Ma) by Funk et al. (2012) and between 14–9 Ma by Duellman et al. (2016). Therefore, the initial diversification of that clade throughout Amazonia may have taken place during the final stage of the Pebas system, a freshwater lake occupying most of Western Amazonia from the early Miocene (23 Ma) until 10–9 Ma (Hoorn et al., 2017). Meanwhile, most of the diversification within the *B. calcarata*/*steinbachi* clade took place during the late Neogene (last 10 Ma). From 9 Ma onward, this system has drained eastward into the Atlantic Ocean, but enormous flooded ecosystems (Acre system) still occupied a large portion of what we currently consider as Western Amazonia until 7 Ma (Hoorn et al., 2010; Albert, et al., 2018a). Subsequent river captures were common (Ruokolainen, Moulatlet, Zuquim, Hoorn, & Tuomisto, 2018), as were climatic fluctuations that may have modified vegetation possibly to the point of forest

fragmentation, at least in some peripheral parts of Amazonia (Cheng et al., 2013; Kirschner & Hoorn, 2019). The relative roles of hydrological evolution (Albert et al., 2018b; Ribas, Aleixo, Nogueira, Miyaki, & Cracraft, 2012) and rainforest expansion and contraction due to climate oscillations (Haffer, 1969) have been the focus of intense debate (Leite & Rogers, 2013). Since the species of the *B. calcarata* and *B. steinbachi* complexes are associated with riparian forests, and these species mostly breed in pools formed on the banks of the beds of small to medium-sized rivers, very large rivers may act as barriers to dispersal, thus reducing or completely impeding gene flow and inhibiting homogenization of differentiating populations (Naka et al., 2018). However, smaller and highly dynamic meandering rivers probably represent more permeable barriers. Therefore, we assume that successive dispersals across major Amazonian rivers (parapatric speciation) (Pirani et al., 2019), as well as hydrological changes (vicariant speciation) (Naka et al., 2018), could have been major processes of diversification in these frogs.

We gathered a large mtDNA dataset for the *B. albopunctata* group sampled throughout Amazonia combined with morphological and acoustic data for a subset of this group (the *B. steinbachi* clade), to address two main goals: (1) reevaluate species boundaries (in or among members) of the *B. albopunctata* group and their respective distributions, and (2) investigate its diversification history within Amazonia using mitogenomic data for one terminal of each delimited species. Furthermore, two species in the *B. steinbachi* clade that were unnamed are described herein.

Materials and methods

Species delimitation

Our first objective was to delimit all major Operational Taxonomic Units (OTUs) based on mtDNA main lineages. Our sampling included 55 new *Boana* tissue samples, obtained through fieldwork throughout Amazonia and adjacent Dry Diagonal (DD; Chaco, Cerrado, Caatinga; Werneck, 2011) and loans from collaborators (from collections QCAZ, MPEG, INPA, CORBIDI, AAGUFU, and from personal loans JMP, SCF, FTA; Appendix 1). Samples unambiguously identified (near type locality and/or phenotypically corresponding to type material) as belonging to the currently recognized taxa were included except *B. paranaiba* and *B. caiapo*. We sequenced a ~400 bp portion of the end of the 16S rDNA gene, a locus commonly used for Neotropical amphibian taxonomy and systematics (Vences, Thomas, Bonett, & Vieites, 2005). We also retrieved homologous sequences from GenBank (389 accessions). In total, we gathered 444 16S sequences for this study (dataset details are provided in Appendix 1 and DNA extraction and sequencing protocols can be found in Appendix 2). These samples cover the whole distribution of the *B. albopunctata* species group (14 included taxa). DNA sequence alignment was conducted on the MAFFT7 online server under the E-INS-i option with default parameters, an algorithm designed for sequences with multiple conserved domains and long gaps (Katoh et al., 2019).

We applied three DNA-based single-locus species delimitation approaches: (a) a distance-based method, the Automated Barcode Gap Discovery (ABGD; Puillandre, Lambert, Brouillet, & Achaz, 2012); (b) a multi-rate coalescent based method, the multi-rate Poisson Tree Processes model approach (mPTP; Kapli et al., 2017); and (c) a single-threshold coalescent-based method, the Generalized Mixed Yule Coalescent approach (single threshold GMYC; Monaghan et al., 2009; Pons et al., 2006).

The ABGD delimitation was performed with a prior of intraspecific divergence P between 0.001 and 0.1, a proxy for minimum relative gap width, X, of 1, and a number of steps n equal to 30. We kept the partition such that $P = 0.016$, as it corresponds to the end of a plateau for group number and it matches thresholds of intraspecific divergence proposed in other vertebrate delimitation studies using 16S barcodes (Puillandre et al., 2012). For mPTP delimitation, we first reconstructed a Maximum Likelihood (ML) tree with RAxML v.8.2.4 (Stamatakis, 2014) using the GTR + G + I substitution model and estimated nodal support via 1000 parametric bootstraps. We used nine outgroups representing most other *Boana* species groups (Appendix 3). The mPTP delimitation was undertaken on the rooted ML tree, with 5 million Markov chain Monte Carlo (MCMC) iterations, sampling every 10,000th iteration, and a 10% burn-in. For the GMYC delimitation, we reconstructed a time-calibrated phylogeny using BEAST 2.5 (Bouckaert et al., 2014). We used a birth-death population model to account for extinction processes and incomplete sampling. We included the same nine *Boana* outgroups used in RAxML reconstruction and five additional representatives of other Cophomantini genera (*Nesorohyla*, *Myersiohyla*, *Hyloscirtus*, *Aplastodiscus*, *Bokermannohyla*) in order to include relationships that can be time-calibrated. We used a single partition with a GTR + G + I substitution model, with an uncorrelated relaxed lognormal clock model of rate variation among branches (Drummond, Ho, Phillips, & Rambaut, 2006). We used two calibration points, the ages of the most recent common ancestor (MRCA) of *Aplastodiscus* and

Boana, as well as the MRCA of a clade formed by *Hyloscirtus*, *Boana*, *Aplastodiscus*, and *Bokermannohyla*, which were estimated by Feng et al. (2017) and consequently constrained here assuming normal prior distributions of 25.2 Ma (standard deviation [SD] = 2.8 Ma) and 32.3 Ma (SD = 3 Ma) respectively. We considered these calibrations to represent the best prior because Feng et al. (2017) included a comprehensive dataset of nuclear loci for an extensive sampling of anurans and used many reliable fossils as calibration points. Moreover, Hime et al. (2020), analysing an even larger genomic dataset, found very similar time estimates for the TMRCA of *Boana*+*Hyloscirtus*. Instead, using fossil and/or biogeographic calibrations would have implied to expand the matrix to lineages distantly related to *Boana* and would likely lead to an overestimation of calibration dates with our mitogenomic dataset (Molak & Ho, 2015; Papadopoulou et al., 2010). For the MCMC parameters, we used four independent chains of 100 million iterations, recording every 10,000th iteration, and a 10% burn-in. We combined the log files of the independent runs using LogCombiner 2.5 (Drummond & Rambaut, 2007) and checked the convergence of our parameters, confirmed by all Effective Sample Size (ESS) being above 200. Then, we extracted the maximum clade credibility tree using Tree annotator 2.5 (Drummond & Rambaut, 2007) with a burn-in of 10%. After removing outgroups, we performed a GMYC delimitation on the ultrametric tree using the GMYC function of the splits R package v.1.0-11 (Ezard, Fujisawa, & Barraclough, 2009), with a threshold interval between 0 and 10 Ma and by using the single threshold method. Operational Taxonomic Units (OTUs) were defined using a majority-rule consensus from the results of the three methods, i.e., a lineage is considered as being an OTU if supported by at least two of the three methods.

All but five occurrence records were georeferenced and used to create distribution maps with convex polygons under QGIS 2.14 (QGIS Geographic Information System). OTUs were assigned to taxa based on the field/museum identification and sometimes corrected in accordance with type localities and known distribution (Frost, 2019; IUCN, 2020).

Morphological and acoustic variation in the *Boana steinbachi* clade

The following morphometric measurements were taken on 38 males and 9 females: snout-vent length (SVL), head length (HL), head width (HW), eye diameter (ED), tympanum diameter (TD), tibia length (TL), foot length (FL), thigh length (THL) and calcaneal appendage length (CL). In addition to these, we also measured hand length (HAL), forearm length (FLL), and eye–nostril distance (EN) for the morphometric characterization of holotypes. All measurements followed the definitions and terminology of Watters, Cummings, Flanagan, and Siler (2016). We classified the calcaneal appendage into three-character states: (i) a calcar (skin appendage with length > 1 mm, flattened or conical); a (ii) skin flap (skin appendage with length < 1 mm, flattened; or a (iii) tubercle, a conical structure with reduced size and, as such, not forming an appendage coming out of the heel. The specimens were measured by P. Marinho (Alta Floresta, Mato Grosso State and Assis Brazil, Acre State) using a Mitutoyo digital calliper (to the nearest 0.05 mm), by M.T. Rodrigues (Jirau and Pacaás Novos, Rondônia State) using a Mitutoyo digital calliper (to the nearest 0.01 mm), by A. Fouquet (French Guiana and Suriname) using a DigiMax digital calliper (nearest 0.01 mm) and by M. Caminer (Ecuador, Peru and Bolivia) using a Mannesmann digital calliper (nearest 0.01 mm). Snout shape was assessed according to Heyer et al. (1990). Digital webbing formulae followed the notation system of Savage and Heyer (1997).

Acoustic analysis of 27 recorded calling males (Appendix 4) was conducted in Raven Pro 1.5, 64-bit version (Bioacoustics Research Program 2012); sound figures were produced using Seewave version 2.1.0 (Sueur, Aubin, & Simonis, 2008) and tuneR version 1.3.2 (Ligges, Krey, Mersmann, & Schnackenberg, 2014), in R version 3.5.0 (R Core Team 2018). Raven Pro settings: window size = 512 samples; window type = Hann; 3 dB filter bandwidth = 124 Hz; window overlap = 85%; hop size = 77 ms; discrete Fourier transform (DFT) size = 1024 samples; grid spacing = 43.1 Hz; seewave settings: window type = Hanning; fast Fourier transform (FFT) size = 256 samples; FFT overlap = 90%. The analysed files are deposited in the sound collection of the 'Museu de Biodiversidade do Cerrado' (AAG-UFU), 'Fonoteca Neotropical Jacques Vielardi' (FNJV), 'La Sonothèque du Muséum National d'Histoire Naturelle' (MNHN) and the Macaulay library (MC). Detailed information about the analysed sound files and accession numbers are provided in Appendix 4.

Call types were distinguished based on the number of notes per call and pulsing. We defined as type 1 calls the multinote calls formed by nonpulsed notes, which consist of the main call type emitted by males of all studied species. Type 2 calls are emitted less often than type 1 and consist of a one-note call formed by poorly defined pulses. We only included type 1 calls in the acoustic diagnoses and the interspecific comparisons. The acoustic traits were generally analysed manually (if not stated otherwise), as follows: temporal traits (call

duration, note duration, interval between notes, number of notes, and call rise time; the latter using the 'Peak Time' function); frequency traits (dominant frequency, using the 'Peak Frequency' function; minimum and maximum frequency using the 'Frequency 5%' and 'Frequency 95%' functions, respectively). Call traits used in the description followed the definitions and terminology of Köhler et al. (2017), using a note-centred approach.

Time-calibrated species phylogeny

We selected a representative for each of the 25 OTUs identified by the species delimitation (see Results), for complete mitogenome sequencing to investigate interrelationships and divergence times. Mitogenomic sequences were obtained using low-coverage shotgun sequencing. We recovered high-quality mitochondrial genome assemblies for 18 OTU representatives (see Appendix 2 for details regarding mitogenome sequencing, assembling and annotation). For the remaining seven OTUs for which we could not obtain tissue samples (Appendix 3), we gathered all the available mitochondrial loci (12S, 16S, ND1, COI, and Cytb) from GenBank; four of these OTUs were represented by 16S only. We also selected 14 species as outgroups (nine with complete mitogenomes), including representatives for other *Boana* species groups and most other Cophomantini genera (Appendix 3).

We extracted 12S, 16S and all protein-coding sequence regions (CDS, thus removing D-Loop and tRNAs) from complete mitogenomes as well as GenBank accessions and aligned each locus independently using the MAFFT7 online server. For rRNA genes, we chose the E-INS-i strategy, recommended for sequences with multiple conserved domains and long gaps. For the protein-coding genes, we chose the G-INS-i strategy, designed for sequences with global homology (Katoh et al., 2019). Realignments of CDS considering the reading frame were done and concatenated in Geneious v.9.1.8 (https://www.geneious.com). Our final matrix totalled 39 terminals and 13,620 aligned nucleotide sites. Among these terminals, 27 were complete and nine had fewer than 3,000 nucleotides (20%) but all were putatively closely related to terminals with complete data.

We selected the best-fit partition scheme and model of evolution for each partition using PartitionFinder V2.1.1 (Lanfear et al., 2016), based on the Bayesian Information Criterion (BIC). We predefined four data blocks, one for rRNA genes (12S and 16S) and one for each codon position of all CDS regions and found the GTR + I + G model to best-fit all partitions. We reconstructed a time-calibrated tree using a birth-death tree prior using BEAST 2.5, to account for extinction processes and incomplete sampling. We parameterized unlinked substitution models according to the estimates obtained in the PartitionFinder V2.1.1 analysis (Lanfear et al., 2016). We used the same two calibration points as in the previous BEAST analysis. Analyses were undertaken using uncorrelated relaxed lognormal clock model of distribution of rate variation among branches for each partition (Drummond et al., 2006). The Markov chain Monte Carlo (MCMC) parameters were set with four independent chains of 100 million iterations, storing every 10,000th iteration and a 10% burn-in. We combined the log files of the independent runs using LogCombiner 2.5 and confirmed the convergence of our parameters as all ESS were above 200. Finally, we extracted the maximum clade credibility tree using Tree annotator 2.5. We acknowledge that our phylogenetic reconstruction solely based on mtDNA sequences prioritizes spatial and taxonomic completeness over genomic coverage and can lead to overestimated divergence times (e.g., McCormack, Heled, Delaney, Peterson, & Knowles, 2011; Near et al., 2012).

Biogeographic analysis

Biogeographic inferences were undertaken on the time-calibrated phylogeny using the BioGeoBEARS R package (Matzke, 2013). This package reconstructs ancestral geographic distributions and investigates the role of each biogeographic event with a maximum likelihood algorithm. We compared three different models: (i) a likelihood version of the Dispersal-Vicariance (DIVALIKE) model (Ronquist, 1997); (ii) a likelihood version of the BayArea (BBM) model (Landis et al., 2013); and (iii) the Dispersal Extinction Cladogenesis (DEC) model (Ree & Smith, 2008). We also compared versions of these models allowing jump dispersal as described by the J parameter (Matzke, 2013). Models were compared with the Akaike Information Criterion (AIC). We ran 50 independent BioGeoBEARS biogeographic stochastic mapping, to determine biogeographic event counts for the best-fit model (Dupin et al., 2017). Ree and Sanmartín (2018) voiced several criticisms against the use of J parameter arguing that it inflates the contribution of cladogenetic events to the likelihood, and minimizes the contribution of anagenetic, time-dependent range evolution. We thus also compared the results from the best model without jump dispersal.

Since this work focuses on the historical biogeography of the Amazonian clade, we discarded the two early diverging lineages *B. heilprini* and *B. raniceps* from the biogeographic analyses since their distribution

ranges lie mostly outside of Amazonia. We considered three areas within Amazonia: Western Amazonia, the Brazilian Shield, and the Guiana Shield. These areas correspond to major geological features roughly delimited by modern riverine barriers: the Madeira River, the Negro River, and the lower course of the Amazon River and to three large biogeographic regions known as Wallace's districts (Hoorn et al., 2010; Wallace, 1854). These districts were recently confirmed as major breaks in birds' species composition (Oliveira, Vasconcelos, & Santos, 2017) and amphibians (Godinho & da Silva, 2018; Vacher et al., 2020), strengthening their status of biogeographic regions. Because the distribution range of the *B. albopunctata* group extends outside Amazonia, we included in the ancestral range reconstruction one additional non-Amazonian Neotropical area, the Dry Diagonal.

Results

Species delimitation

Of the three tested methods of species delimitation, the ABGD method was found to be the most conservative, delimiting 21 OTUs while mPTP and GMYC delimited 24 and 47 OTUs, respectively (Appendix 1). In one case, the consensual partitioning was overly conservative given that *B. leucocheila* and *B. multifasciata* were considered as a single OTU which is contradicted by the fact that these two taxa are phenotypically distinct. Therefore, we kept the different lineages delimited by GMYC in this group as distinct OTUs. The final delimitation led to 25 OTUs (including *B. heilprini*) in the *B. albopunctata* species group (Fig. 1, Appendix 1). Thirteen of these OTUs could be linked to nominal species (except *B. caiapo* and *B. paranaiba* that were not included in the analysis because material was not available). Conversely, 11 could not be linked to any nominal species, representing a possible 44% increase in the species richness of the group. The Amazonian clade itself was represented by 14 OTUs including eight nominal species and six putative new species (Fig. 1). These results also imply important changes to the geographic distribution of the species of the group. In Appendix 5, we detail and justify the identification of these OTUs and their respective geographic ranges.

Taxonomic accounts

The Amazonian clade of the *B. albopunctata* group, previously reported as the *B. calcarata–B. fasciata* species complex by Caminer and Ron (2014), is composed of two major clades (the *B. calcarata* and the *B. steinbachi* clades), defined by the following combination of character states: (1) truncate snout in dorsal view; (2) rounded head shape; and (3) presence of calcaneal appendage on heel.

The *B. calcarata* clade (Fig. 1) is composed of four species possessing a calcar and having advertisement calls formed by a single type of call (Caminer & Ron, 2014). The *B. steinbachi* clade, on the other hand, includes three described and two undescribed species (Fig. 1). Members of this clade lack a calcar (skin flap or tubercle present, or the complete absence of calcaneal appendages) and have vocal repertoires composed of more than one type of call, except for *B. alfaroi* for which a single type of call has been documented so far (Caminer & Ron, 2014).

Hyla steinbachi Boulenger, 1905, currently valid as *Boana steinbachi* (Boulenger, 1905), was described from the Bolivian Province Sara, Departament Santa Cruz de la Sierra, Bolivia. We assume that Buenavista is the type locality of *B. steinbachi*. Between 1910 and 1950 the Steinbach family collected many amphibians and reptiles in Bolivia, mainly at Buenavista in the Department of Santa Cruz (see Parker, 1927), which is the type locality of several anurans (*Hamptophryne boliviana* (Parker, 1927); *Pseudopaludicola boliviana* Parker, 1927; *Scinax parkeri* (Gaige, 1929)), and the snake *Apostolepis tenuis* Ruthven, 1927. The material collected by the Steinbach family is on display in various museums, such as the University of Michigan Museum of Zoology (UMMZ, see Gaige, 1929), the Natural History Museum, London (BMNH, see Parker, 1927), the Zoologisches Museum Berlin (ZMB, see Müller, 1924), and the Naturhistorisches Museum Basel (NBM, pers. comm. Wüest). Many decades later, De la Riva (1990) synonymized *H. steinbachi* with *H. fasciata*. Subsequently, Jansen, Bloch, Schulze, and Pfenninger (2011) found differences in call and mtDNA data between populations of *B. fasciata* from Bolivia and Ecuador and suggested that their results imply a resurrection of *B. steinbachi*. In the following years, Caminer and Ron (2014) tentatively assigned *B. steinbachi* to a genetic lineage (clade J) inhabiting Bolivian Amazonia, near its type locality. By assessing its phylogenetic relationships in the group, Caminer and Ron (2014) formally revalidated *B. steinbachi* as a distinct species from nominal *B. fasciata*. The revalidation of *B. steinbachi* was also supported by phenotypic data obtained from syntypes but did not include a reexamination of all diagnostic characters of the species.

Next, we present an amended diagnosis of *B. steinbachi* based on novel data on life colours and morphology, and describe its vocal repertoire based on topotypes from Bolivia and distinct OTUs from Peru and Brazil

COLOR Online / B&W in Print

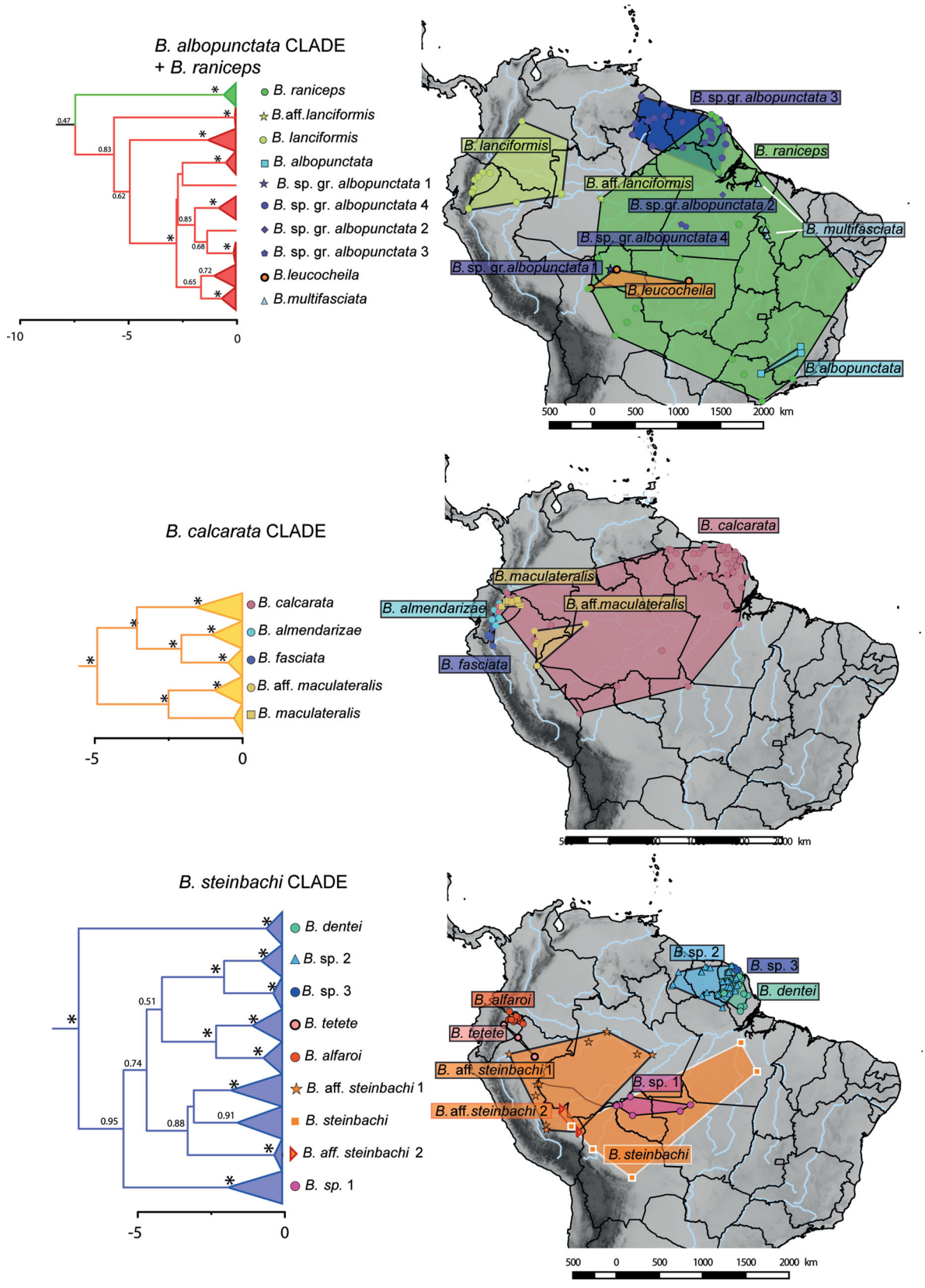

Fig. 1. Subtrees of the three main clades from the chronogram obtained from the analysis of 16S sequences using BEAST2. Terminals are collapsed according to the OTU recovered from the species delineation analysis. The distribution of each of these OTU is depicted on the maps.

also assigned to this species in this study. Specimens and calls from Acre ("*B.* aff. *steinbachi* 1") and calls from the lower Madre de Dios River ("*B.* aff. *steinbachi* 2") were included in the variation of *B. steinbachi*.

Boana steinbachi (Boulenger, 1905)
Hyla steinbachi — Boulenger, 1905
Hyla fasciata De la Riva, 1990
Hypsiboas fasciatus Jansen et al., 2011
Hypsiboas sp. (Clade G) Funk et al., 2012
Hypsiboas steinbachi Caminer & Ron, 2014
Boana steinbachi Dubois, 2017.
Boana sp. (Clade J) Meza-Joya et al., 2019
Boana fasciata Vacher et al. 2020

Syntypes. BMNH 1947.2.13.61–63, two adults of unknown sex and one juvenile, respectively, from Sara province, Department of Santa Cruz de La Sierra, Bolivia. Collected by Hf. J. Steinbach.

Diagnosis. *Boana steinbachi* is characterized by the following combination of character states: (1) skin flap on heel; (2) vocal repertoire composed of more than one call type; (3) multinote call; and (4) regular internote intervals (Figs 2, 3 & 4).

Comparisons with congeners of the Amazonian clade. *Boana steinbachi* can be distinguished from the members of the *B. calcarata* clade (*B. almendarizae*, *B. fasciata*, *B. calcarata*, and *B. maculateralis*) by the absence of a calcar and by the vocal repertoire composed of more than one type of call. Among members of the *B. steinbachi* clade, it can be distinguished from *B. dentei*, *B. alfaroi*, and *B. tetete* by the presence of a skin flap on heel (tubercle in *B. alfaroi* and *B. tetete*; tubercle on one side or completely absent in *B. dentei*), by its multinote call (one-note call in *B. dentei* and *B. tetete*), by having regular internote intervals between call notes (notes with irregular intervals, sometimes partly fused one with the next in *B. alfaroi*), and by the vocal repertoire composed of two distinct types of calls (one call type in *B. alfaroi*) (Caminer & Ron, 2014; Marinho et al., 2020).

Variation. Body size varies between 30.4 and 37.4 mm in males and between 42.5 and 48.8 mm in females (Appendix 7). Individual AAG-UFU 5918 lacks the heel skin flap on the left side, topotypes SMF 88394–95 and SMF 88397 lack the skin flap on both sides. In life (Fig. 3a, b), dorsal colouration is beige, light brown, bright yellow or orange brown in calling males, with faint brown transversal bands and dark purplish-brown, faint brown or grey longitudinal lines extending from

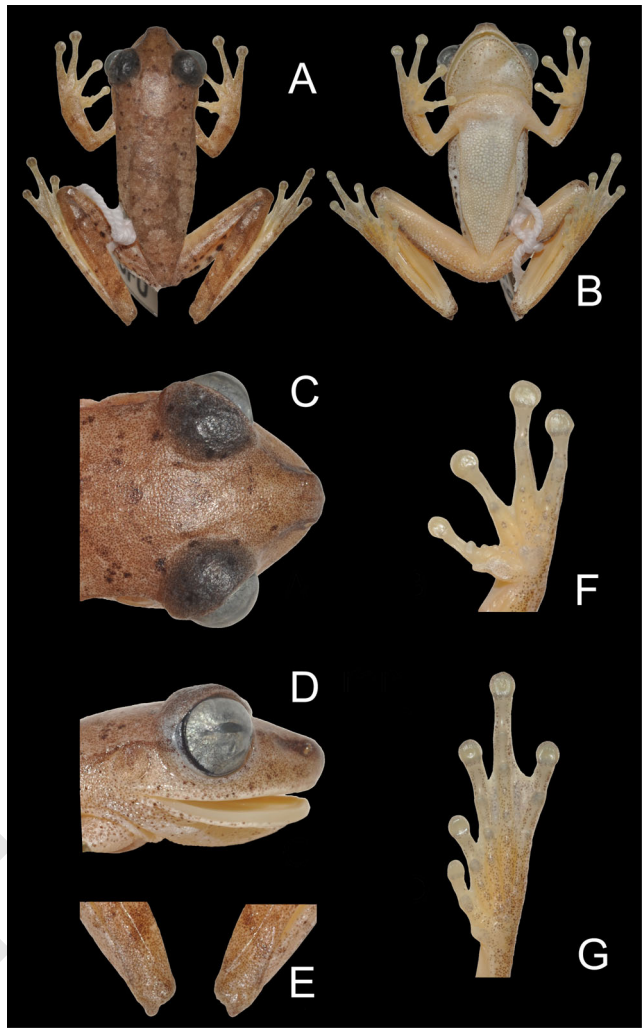

COLOR Online / B&W in Print

Fig. 2. Adult male of *Boana steinbachi* (AAG-UFU 5921) from the Assis Brasil population (Acre, Brazil): (A) dorsal and (B) ventral views of the body (SVL = 33.7 mm), (C) dorsal and (D) lateral views of the head (HL =12.3 mm; HW = 10.2 mm), (E) detail in dorsal view of the skin flap on heels, (F) palm of the hand (HAL = 10.6 mm), and (G) sole of the foot (FL = 13.9 mm).

the snout to vent, a second line extending from behind the eye to pelvic region, and a third line as a canthal stripe extending from the posterior corner of the nostril to anterior corner of the eye, and from the posterior corner of the eye to midbody length on flank (the topotypes SMF 88394–97 lack transversal bands on dorsum; individuals SMF 88394 and CORBIDI 13414 lack longitudinal lines on dorsum and the middorsal line is extending from snout to interocular region; AAG-UFU 5921 lacks longitudinal lines on dorsum). Iris cream or grey, sometimes with yellow pigmentation on the upper part of the iris. Throat varying from white to yellow, chest and anterior belly varying from white to cream. Ventral surface of hand and hind limb beige to bright

COLOR Online / B&W in Print

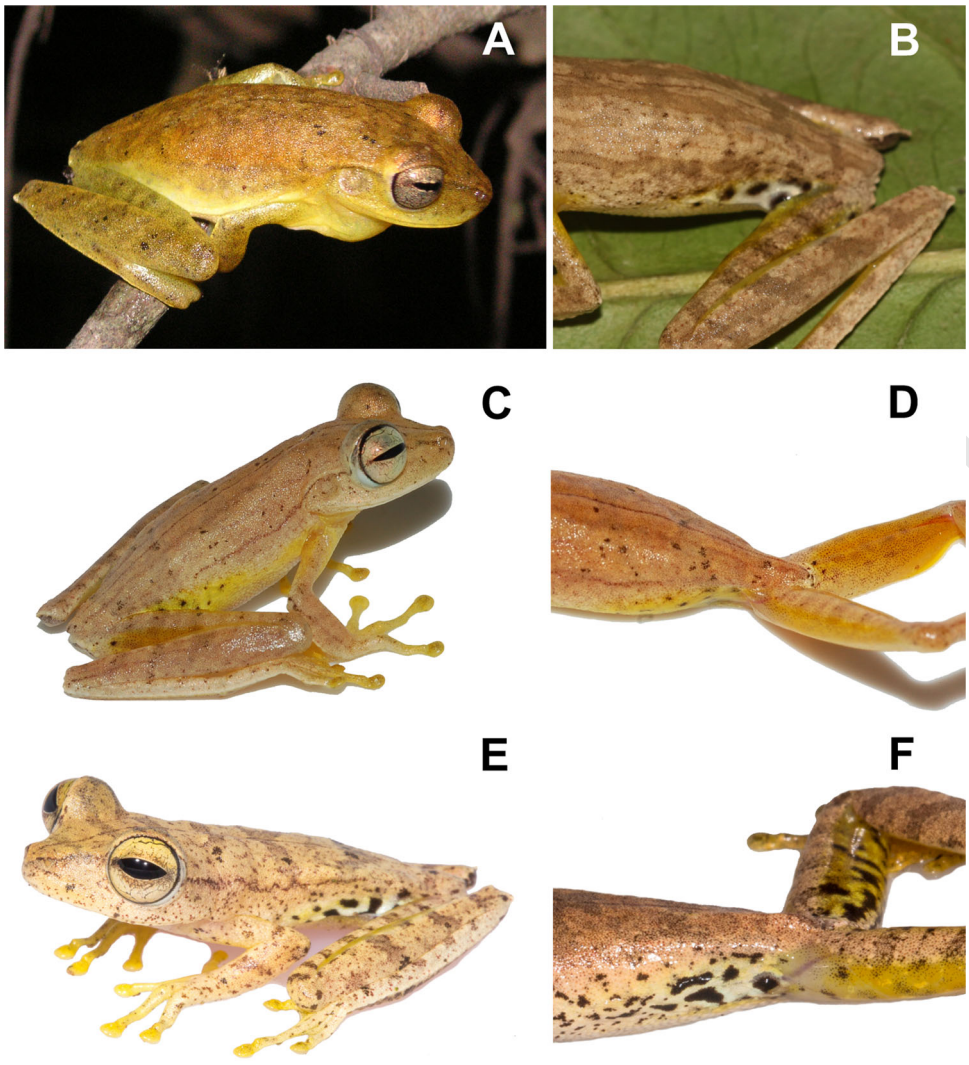

Fig. 3. Life colours in dorsolateral view and detail of the patterns on flank and groin. (A, B) *Boana steinbachi* (topotype SMF88394 and non-topotype AAG-UFU 5918, respectively), (C, D) *B. eucharis* sp. nov. (AAG-UFU 6503; holotype), and (E, F) *B. courtoisae* sp. nov. (holotype, MNHN-RA-2020.0001, and an unvouchered specimen, respectively).

yellow. Posterior surface of thigh, groin and posterior half of flank spotted in black, with a bright yellow or white background colour. Brown dots scattered on dorsum, dorsal surface of limbs, bordering the lower lip, mental region, and chest. In preservative, the colours fade: the bright yellow colour sometimes present on dorsum, ventral surfaces of limbs, groin, and flank are beige or pale cream. Iris grey. Flank and groin maculation are denser and more extensive in females.

Vocal repertoire. (Fig. 4) We analysed calls of 13 males (see Appendix 4 for information about sound recordings and Appendix 6 for the complete descriptive statistics). The vocal repertoire of *Boana steinbachi* is composed of two distinct types of calls (type 1: n = 149 calls of 13 males; type 2: n = 43 calls of five males) that are emitted sporadically at irregular intervals. The type 1 call of *B. steinbachi* lasts 130–430 ms and is composed of 3–8 nonpulsed notes lasting 4–52 ms, separated by intervals of 1–67 ms. The rise time is at 2–98% of call duration. The minimum frequency ranges from 1335–1981 Hz, the maximum frequency from 3336–4479 Hz, and the dominant frequency from 1688–3402 Hz. The type 2 call is composed of one note with poorly defined pulses. Notes last 47–87 ms. The rise time is at 18–60% of note duration. The minimum frequency ranges from 1453–2015 Hz, the maximum frequency from 2713–4522 Hz, and the dominant frequency from 1688–2813 Hz. The limited sample size for each population with recorded calls prevented us from evaluating the geographic variation of acoustic traits across populations of *B. steinbachi*.

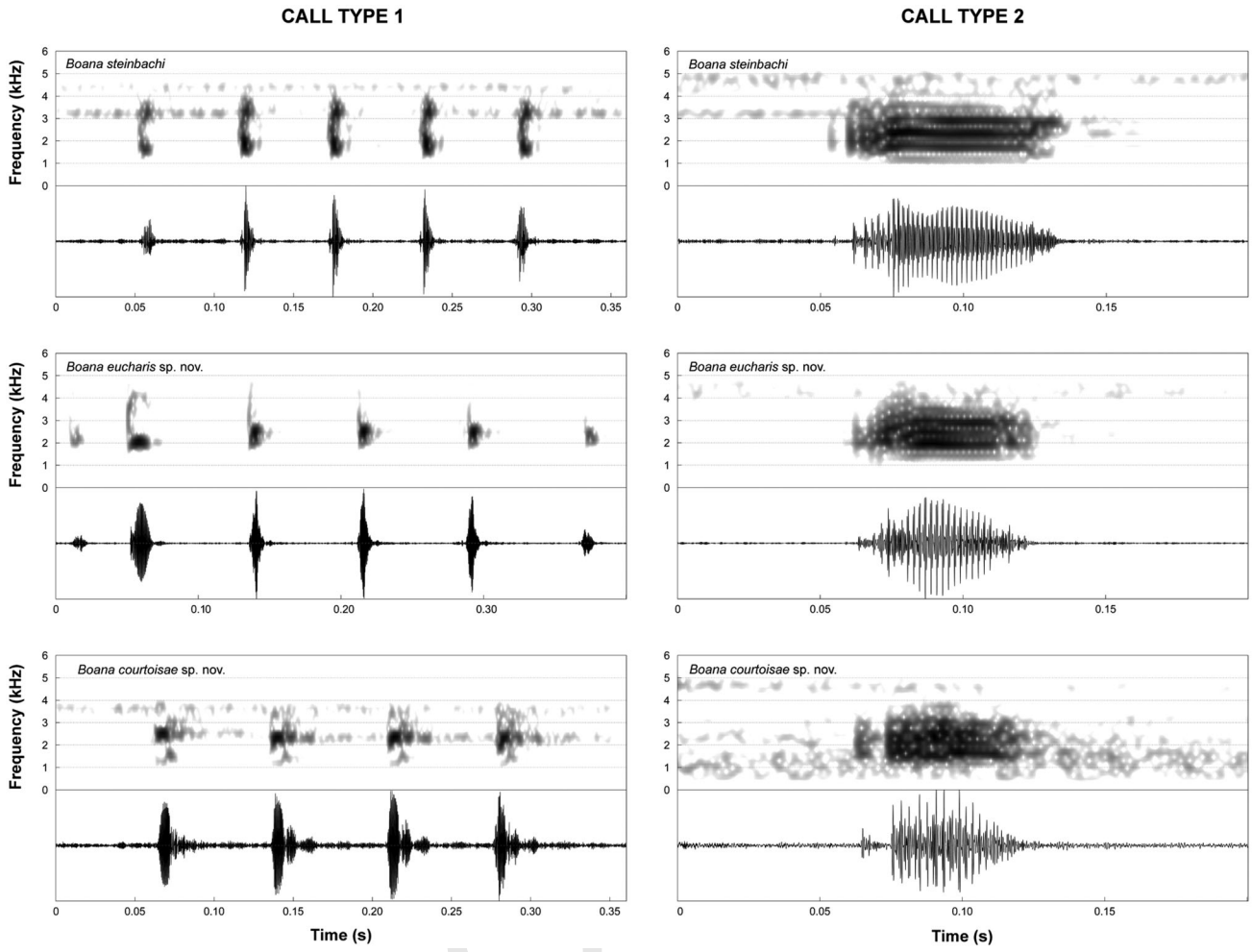

Fig. 4. Type 1 (left) and type 2 (right) calls (spectrograms and corresponding oscillograms) of *B. steinbachi* (Top; accession number MNHN-SO-2020-2934); *B. eucharis* sp. nov. (Middle; file: B_eucharisAltaFlorestaMT5hPM_AAGm671; MNHN-SO-2020-2969); and *B. courtoisae* sp. nov. (Bottom; MNHN-SO-2020-2947). See Appendix 4 for additional information on sound recordings.

Distribution and ecology. In addition to the type locality in central Bolivia, occurrence records of *B. steinbachi*, based on molecular and phenotypic data, encompass the south-western, central, and eastern Brazilian Amazonia (Acre, Amazonas, and Pará; Fig. 1), and south-western Peruvian Amazonia (Tambopata and the lower Madre de Dios River). Collected males were calling perched on shrubs in the periphery of flooded areas and in forest clearings of secondary Amazonian lowland forests. Its range is extensive and encompasses numerous protected areas. Moreover, the species seems to tolerate habitat disturbance. Therefore, its status should be considered of Least Concern.

Boana eucharis sp. nov.

Hypsiboas fasciatus Ávila & Kawashita-Ribeiro, 2011

Hypsiboas fasciatus Rodrigues et al., 2015

Boana fasciata Vacher et al., 2020

Holotype. AAG-UFU 6503, adult male collected from the municipality of Alta Floresta, Mato Grosso state, Brazil (−9.642839°, −56.271408°) by Davi L. Bang, André G. Lopes, and Pedro Marinho on 11 January 2019 (Fig. 3 & 5).

Paratopotypes. Five adult males (AAG-UFU 6504–6508) collected with the holotype. AAG-UFU 6904, adult male collected on 20 January 2020 by Ariovaldo A. Giaretta, Pedro Marinho, and André G. Lopes.

Paratypes. (1 male, 4 females). MZUSP 143323, adult male and MZUSP 143324, adult female, collected at UHE Jirau, Abunã, state of Rondônia, Brazil

COLOR Online / B&W in Print

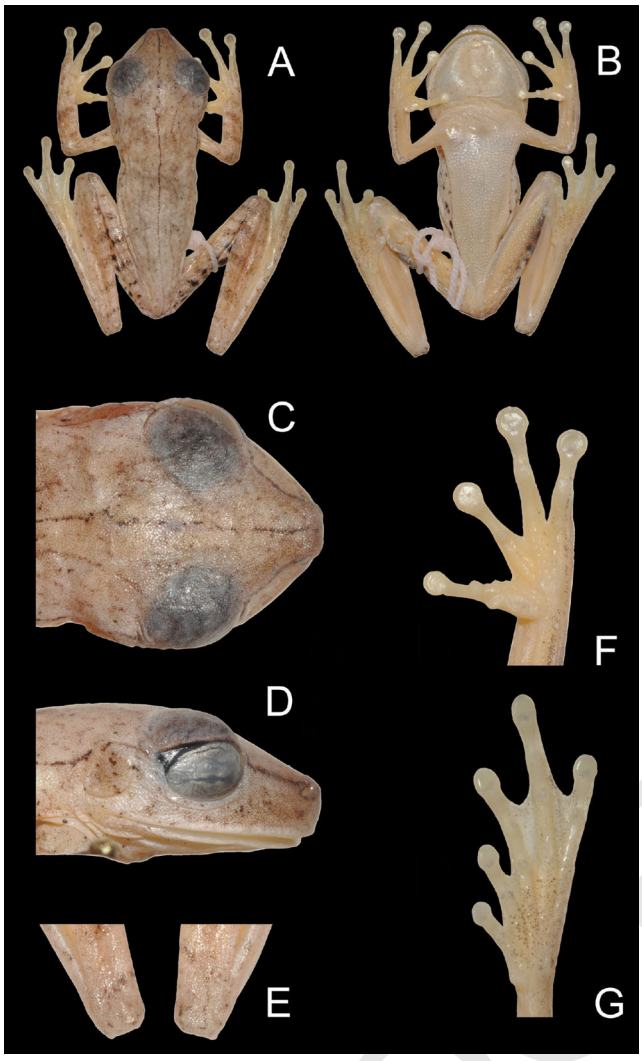

Fig. 5. Holotype of *Boana eucharis* sp. nov. (AAG-UFU 6503) from Alta Floresta (Mato Grosso, Brazil): (A) dorsal and (B) views of the body (SVL = 30.8 mm), (C) dorsal and (D) lateral views of the head (HL = 11.9 mm; HW = 10.3 mm), (E) detail in dorsal view of the tubercle on heels, (F) palm of the hand (HAL = 8.7 mm), and (G) and sole of the foot (FL = 13.1 mm).

(−9.699410°, −65.358875°); MZUSP 143238, adult female collected at UHE Jirau, Porto Velho, state of Rondônia, Brazil (−8.748483°, −63.903465°); MZUSP 159228 (field No. MTR25896), adult female collected at PARNA Pacaás Novos, state of Rondônia, Brazil (−10.786979°, −63.627305°); MZUSP 159227 (field No. MTR25798), adult female collected at Pacaás Novos, state of Rondônia, Brazil (−10.786979°, −63.627305°).

Diagnosis. *Boana eucharis* sp. nov. is characterized by the following combination of character states: (1) tubercle on heel; (2) vocal repertoire composed of more than one call type; (3) multinote call; and (4) regular internote intervals (Figs 3, 4 & 5).

Comparisons with congeners of the Amazonian clade. *Boana eucharis* sp. nov. is distinguished from the members of the *B. calcarata* clade (*B. almendarizae*, *B. fasciata*, *B. calcarata*, and *B. maculateralis*) by the absence of a calcar and by the vocal repertoire composed of more than one type of call. Within the *B. steinbachi* clade, *B. eucharis* sp. nov can be distinguished from *B. dentei*, and *B. tetete* by its multinote call (onenote calls in *B. dentei* and *B. tetete*), and from *B. alfaroi* by having regular internote intervals and vocal repertoire composed of two distinctive types of calls (in *B. alfaroi*, call notes having irregular intervals, sometimes partly fused one with the next, and repertoire formed by one call type; Caminer & Ron, 2014; Marinho et al., 2020). *Boana eucharis* sp. nov. can be distinguished in almost all cases from *B. steinbachi* by the presence of tubercle on heel (skin flap in *B. steinbachi*; but see Variation). In addition, ~~*B. eucharis* sp. nov. is sister of all remaining species of the *B. steinbachi* clade (except the allopatric *B. dentei*).~~ The phylogenetic relationships within this clade and spatial distribution strongly support the distinct specific status of *B. eucharis* sp. nov. relative to its closest relatives (Fig. 1).

Description of holotype. (Figs 3 & 5) Adult male, SVL 30.8 mm, FL 12.0 mm, ED 3.8 mm, TD 2.0 mm, TL 17.8 mm, THL 15.8 mm, CL 0.2 mm, HAL 10.4 mm, FLL 5.9 mm, EN 3.3 mm, head slightly longer (HL 11.9 mm) than wide (HW 10.3 mm), and wider than body; snout rounded in lateral view, truncate in dorsal view; EN shorter than ED; canthus rostralis indistinct, rounded; loreal region concave; internarial area convex; nostril slightly protuberant, directed laterally; interorbital area slightly convex; eye large, strongly protuberant; ED 1.9 times TD; tympanic membrane undifferentiated; tympanic annulus evident, rounded, concealed posteriorly by the supratympanic fold, running from the posterior corner of the eye to arm insertion. Tongue ovoid, widely attached to mouth floor; six vomerine teeth on each vomer, vomers barely separated, posteromedial to choanae; choanae ovoid. Arm slender, axillary membrane absent; ill-defined, low tubercles present along ventrolateral edge of forearm; relative length of fingers I < II < IV < III; fingers bearing large, oval discs; subarticular tubercles prominent, ovoid to conical, single; supernumerary tubercles present; palmar tubercle small, elongated; prepollical tubercle large, flat, elliptical; prepollex enlarged, covered by skin; nuptial excrescences absent; webbing absent between fingers. Tubercle on tibiotarsal articulation; scattered tubercles along the

external edge of tarsus and foot; toes bearing discs slightly wider than long, smaller than those of fingers; relative length of toes I < II < V < III < IV; outer metatarsal tubercle ill-defined, small, rounded; inner metatarsal tubercle large, ovoid; subarticular tubercles single, low, rounded; supernumerary tubercles restricted to the sole of foot; webbing formula of toes I 2–$2^{1/2}$ II 1^{+}–$2^{1/2}$ III $1^{1/2}$–$2^{1/2}$ IV 3–$1^{1/2}$ V. Skin on dorsum, head, and dorsal surfaces of limbs and flank mostly smooth; skin on belly and thigh coarsely granular; skin on throat and chest finely granular, arm, forearm, and shank smooth. Cloacal opening directed posteriorly at upper level of thigh; short simple cloacal sheath covering cloacal opening; round tubercles below and on the sides of the opening.

Colours of holotype. In preservative, dorsum greyish brown with scattered minute black dots; faint brown middorsal line extending from the tip of the snout to pelvic region, fragmented in interorbital region, a second line extending from behind the eye to pelvic region, fragmented and faint at midbody length, and a third line as a canthal stripe extending from the posterior corner of the nostril to anterior corner of the eye, and from the posterior corner of the eye to midbody length on flank; dorsal surface of limbs greyish brown with transversal faint brown bars; flank beige with dark irregular spots; posterior surface of thigh beige with dark irregular spots; venter cream white with brown spots on the mental region and chest; ventral surface of limbs cream with a narrow brown stripe on the outer edge of the hand, forearm, thigh, tarsal fold, and foot; limb bones partially visible through skin, white. In life (Fig. 3c, d), dorsum beige with a purplish brown middorsal line extending from the tip of snout to pelvic region, a second line extending from behind the eye to pelvic region, fragmented and faint at midbody length, and a third as canthal stripe from the posterior border of nostril to anterior corner of the eye, and from the posterior corner of the eye to midbody length on flank; dorsal surface of hindlimbs with faint brown transversal bands; minute dark brown dots scattered on the dorsal surface of limbs and dorsum; flank bright yellow with dark brown irregular blotches on groin; posterior surface of thigh pale yellowish with dark brown blotches.

Variation. Body size varies between 30.8 and 34.7 mm in males (Appendix 7). The paratopotype AAG-UFU 6504 lacks the heel tubercle on the right side, and MZUSP 80790 (from Rondônia) does not possess the tubercle on either side. In life (Fig. 3c, d), dorsal colouration varies from beige to brown, orange brown in calling males, with dark purplish-brown longitudinal lines and faint brown transversal bands (individuals MZUSP 159227 and MZUSP 159228 do not have longitudinal lines extending from snout to pelvic region or a canthal stripe). Throat varies from white to yellow, chest and anterior belly varying from white to cream. Iris cream or grey, sometimes with yellow pigmentation on the upper iris. Ventral surface of hand and hind limb mostly bright yellow. Posterior surface of thigh, groin and posterior half of flank spotted in black, with a bright yellow or white background colour. Brown dots scattered on dorsum, dorsal surface of limbs, bordering the lower lip, mental region, and chest. We did not observe dichromatic patterns between male and female specimens. In preservative, the colours become paler: the bright yellow tone occasionally on ventral surfaces of limbs, groin and flank is beige or pale cream. Iris grey.

Vocal repertoire. Calls of seven males were recorded at the type locality, in southern Brazilian Amazonia (Appendix 6). The vocal repertoire of *Boana eucharis* is composed of two distinct calls (type 1: n = 133 calls from seven males; type 2: n = 62 calls from seven males) that are emitted sporadically at irregular intervals. The type 1 call (Fig. 4) lasts 290–420 ms and consists of 3–7 non-pulsed notes that last 3–60 ms, separated by intervals of 27–82 ms. The rise time is at 2–97% of call duration. The minimum frequency ranges from 1864–2250 Hz, the maximum frequency from 2196–4220 Hz, and the dominant frequency from 2147–2462 Hz. The type 2 call consists of one note with poorly defined pulses. Notes last 29–64 ms. The rise time is at 24–78% of note duration. The minimum frequency ranges from 1593–2067 Hz, the maximum frequency from 2712–3491 Hz, and the dominant frequency from 1938–3143 Hz.

Distribution and ecology. *Boana eucharis* sp. nov. is known from southern Amazonia in the Brazilian states of Mato Grosso and Rondônia (Fig. 1). Males call perched on shrubs in flooded areas associated with the border of secondary-growth or disturbed forests. Sympatric anuran species at the type locality of *B. eucharis* sp. nov. are *Boana leuchocheila*, *B. albopunctata*, *Dendropsophus cruzi*, *Engystomops freibergi*, *Leptodactylus vastus*, *L. petersii*, *Pithecopus hypochondrialis*, *Scinax garbei*, and *S. nebulosus.* The species is not abundant. It is possible that the species range is more extensive than the five populations reported in this study, which suggests a Data Deficient conservation category for *B. eucharis* sp. nov. However, it is important to highlight that the southern limits of Amazonia are overall highly impacted by habitat conversion and this species could be classified at least as Vulnerable. Nevertheless, the known occurrence recordings comprise at least two protected conservation units: Pacaás Novos

National Park and possibly the Cristalino State Park, and the species seems to tolerate a certain extent of human disturbance to forest habitats, since calling males were sampled at forest borders and clearings.

Etymology. The specific epithet is derived from the Greek word *eúkharis*, which means gracious or charismatic, as a reference to the delicate and gracious aspect of the species.

Boana courtoisae sp. nov.
Hyla fasciata Lescure & Marty, 2000
Hyla fasciata Faivovich et al., 2005
Hypsiboas fasciatus Fouquet et al., 2007
Hyla fasciata Avila-Pires et al., 2010
Hypsiboas sp. (Clade H) Funk et al., 2012
Hypsiboas fasciatus Ouboter & Jairam, 2012
Hypsiboas fasciatus Cole et al., 2013
Hypsiboas sp. (Clade H) Caminer & Ron, 2014
Boana cf. *fasciata* Fouquet et al., 2019
Boana fasciata Vacher et al., 2020

Holotype. MNHN-RA-2020.0001 adult male, collected at Alikéné, French Guiana (3.20906°, −52.402000°) by J.P. Vacher and S. Cally on 12 February 2015 (Figs 3 & 6).

Paratopotypes. An adult female (MNHN-RA-2020.0002) collected with the holotype.

Paratypes. (12 males, 3 females). MNHN-RA-2020.0004 adult male, collected at Saut Taconet, French Guiana (4.03249°, −52.526188°); MNHN-RA-2020.0005 adult female, collected at Saut Grand Machicou, French Guiana (3.897416°, −52.583565°); MNHN-RA-2020.0006–7 two adult males, collected at Saul, French Guiana (3.615576°, −53.227093°); MNHN-RA-2020.0008 adult male, collected at Flat de la Waki, French Guiana (3.089500°, −0°,398460°); MNHN-RA-2020.0009–12 four adult males, collected at Sipaliwini, Suriname (2.097530°, −56.147200°); MNHN-RA-2020.0013 an adult male, collected at Ekini, French Guiana (4.050000°, −52.466700°); MNHN-RA-2020.0014–16 three adult males, collected at Mitaraka, French Guiana (2.235770°, −54.449280°); MNHN-RA-2020.0003 an adult female collected at Inini Tolenga, French Guiana (3.663159°, −53.928308°).

Other material. Twelve additional males and three females (Appendix 8) from French Guiana and Suriname were also assigned to *B. courtoisae*. They were examined and included in the analysis of the variation but were not deposited and not included in the type series.

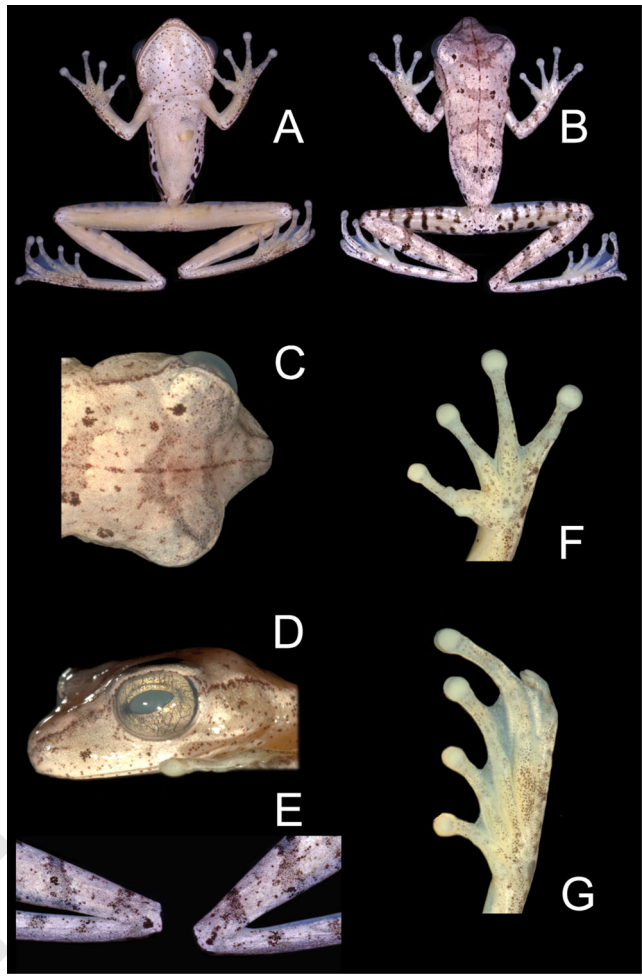

COLOR Online / B&W in Print

Fig. 6. Holotype of *Boana courtoisae* sp. nov. (MNHN-RA-2020.0001) from Alikéné (French Guiana): (A) dorsal and (B) ventral views of the body (SVL = 31.0 mm, adult male), (C) dorsal and (D) lateral views of the head (HL = 11.5 mm; HW = 10.8 mm), (E) detail in dorsal view of the skin flap on heels, (F) palm of the hand (HAL = 9.3 mm), and (G) sole of the foot (FL = 12.0 mm).

Diagnosis. *Boana courtoisae* sp. nov. is characterized by the following combination of character states: (1) skin flap on heel; (2) vocal repertoire composed of more than one call type; (3) multinote call; and (4) regular internote intervals; (5) multi-blotched pattern on groin and flank of males (Figs 3, 4 & 6).

Comparisons with congeners of the Amazonian clade. *Boana courtoisae* sp. nov. is distinguished from members of the *B. calcarata* clade (*B. almendarizae*, *B. fasciata*, *B. calcarata*, and *B. maculateralis*) by the absence of a calcar and by the vocal repertoire composed of more than one type of call. Within the *B. steinbachi* clade, *B. courtoisae* sp. nov. can be distinguished from *B. dentei*, and *B. tetete* by its multinote call (one-note calls in *B. dentei* and *B. tetete*), and from *B. alfaroi*

by its regular internote intervals and vocal repertoire composed of two distinctive types of calls (in *B. alfaroi*, call notes having irregular intervals, sometimes partly fused one with the next, and repertoire formed by one call type) (Caminer & Ron, 2014; Marinho et al., 2020). *Boana courtoisae* sp. nov. can be distinguished in almost all cases from *B. eucharis* sp. nov. by the presence of skin flap on heel (tubercle in *B. eucharis* sp. nov.; but see Variation). In addition, *B. courtoisae* sp. nov. can be distinguished from *B. eucharis* sp. nov. and *B. steinbachi* by a multi-blotched pattern on flank and groin of males (fewer blotches, or transversal bands and spots in males of the other two species; Fig. 3). Although *B. courtoisae* sp. nov. and *B. eucharis* sp. nov. are distinguished by subtle differences in morphology and colouration, the two species are not directly phylogenetically related to each other since *B. courtoisae* sp. nov. is sister of the remaining species that form the *B. steinbachi* clade (*B. steinbachi*, *B. alfaroi*, *B. tetete*, and *B. eucharis* sp. nov.), which strongly supports the distinct specific status relative to its closest relatives (Fig. 6).

Description of holotype. Adult male, SVL 31.0 mm, FL 12.0 mm, ED 4.4 mm, TD 1.8 mm, TL 18.9 mm, THL 15.8 mm, CL 0.4 mm, HAL = 9.3 mm, FLL 6.2 mm, EN 4.2 mm, head slightly longer (HL 11.5 mm) than wide (HW 10.9 mm), and wider than body; snout rounded in lateral view, truncate in dorsal view (Fig. 5); EN shorter than ED; canthus rostralis indistinct, rounded; loreal region concave; internarial area convex; nostrils slightly protuberant, directed laterally; interorbital area slightly convex; eye large, strongly protuberant; ED 2.5 times TD; tympanum membrane undifferentiated; tympanic annulus evident, rounded, concealed posteriorly by supratympanic fold, running from the posterior corner of the eye to arm insertion. Tongue ovoid, widely attached to mouth floor; vomerine odontophores triangular with arched base, barely separated, posteromedial to choanae, bearing eight vomerine teeth on each side; choanae ovoid. Arm slender, axillary membrane absent; indistinct low tubercles present along ventrolateral edge of forearm; relative length of fingers I < II < IV < III; fingers bearing large, oval discs, subarticular tubercles prominent, ovoid to conical, single; supernumerary tubercles present; palmar tubercle small, elongated; prepollical tubercle large, flat, elliptical; prepollex enlarged, claw shaped; nuptial excrescences absent; webbing absent between fingers. Skin flap on tibiotarsal articulation; scattered tubercles on tarsus and along ventrolateral edge of foot; toes bearing discs slightly wider than long, smaller than those of fingers; relative length of toes I < II < V < III < IV; outer metatarsal tubercle ill defined, small, round; inner metatarsal tubercle large, elongated and elliptical; subarticular tubercles single, low, rounded; supernumerary tubercles restricted to the sole of foot; webbing formula of toes I2$^{—}$2$^{1/2}$II1^{+}-2$^{1/2}$III1$^{1/2}$-2$^{1/2}$IV3-1$^{1/2}$V. Skin on dorsum, head, and dorsal surfaces of limbs smooth; skin on flanks smooth with weak longitudinal wrinkles posterior to the arm; skin on venter coarsely granular; skin on ventral surfaces of head and thighs granular, those of shanks smooth. Cloacal opening directed posteriorly at upper level of thighs; short simple cloacal sheath covering cloacal opening; round tubercles below and on the sides of the opening.

Colour of holotype. In preservative, dorsum beige with scattered minute black dots and spots (Fig. 6); faint brown narrow middorsal line extends from the tip of the snout to the vent; faint brown transversal bands on dorsum; dorsal surface of limbs beige with transversal faint brown bars; flank white with dark irregular spots; posterior surface of thigh white with dark irregular blotches; venter creamy white with brown spots on the throat and chest; ventral surface of limbs whitish cream with scattered dots on the forearm; ventral surface of shank cream; a discontinuous brown stripe, varying in width along its length, on the outer edge of the hand and forearm, limb bones (visible through skin) white. In life, dorsum beige with a faint brown narrow longitudinal line from snout to vent; dorsal surface of limbs beige with faint brown transversal bands; scattered minute black dots on the dorsal surfaces of limbs and dorsum; flank white to light yellow with dark irregular blotches; venter white to cream; scattered brown flecks on the throat and chest, and bordering the lower lip; ventral surface of limbs pale yellow, with bright yellow granules; discs and webbing yellow; iris cream with an undefined upper yellow band; limb bones (visible through skin) white.

Variation. Body size varies between 30.8 and 35.9 mm in males and between 43.0 and 45.9 mm in females (Appendix 7). In life (Fig. 4e–f), dorsal colouration varies from beige to bright yellow or orange brown, with faint brown transversal bands markings, purplish-brown to dark brown longitudinal lines and many scattered brown spots covering all over the dorsum. Throat, chest, and anterior belly varying from white to cream with scattered spots covering the entire ventral surface in both sexes. Flank and groin with dark brown to black blotches on a bright yellow, bluish or white background. Ventral surface of hand, foot, and legs varying from bright yellow to dark grey, covered with black spots. Posterior surface of thigh striped or spotted in black with a bright yellow or white background colour,

sometimes with tints of blue particularly pronounced in females (individual MNHN-RA-2020.0006 has no blotches or dots on the posterior surface of thigh or spots on belly). Iris grey or cream, sometimes with a yellow upper band (the individual MNHN-RA-2020.0015 has also black markings surrounding the iris). Our collected individuals exhibit a dimorphic colouration between males and females. The ventral surface of thigh in males varies from bright yellow to greenish yellow. In females, the colouration of the ventral surface of thigh is blue, bluish grey or dark grey. The groin region, flank, and posterior surface of thigh have more tints of blue in females. In addition, flank and groin maculation is denser and more extensive in females. In preservative, the colours fade, becoming pale: the bright yellow tone sometimes present on dorsum is beige or brown with brown transversal bands and lines. Ventral surfaces of body, limbs, groin and flank are beige or pale cream. The blue tints on groin, flank and posterior surface of thigh completely vanish, as well as the dark blue or grey colours on ventral surfaces of female's thigh. Iris grey.

Vocal repertoire. Calls of five males were recorded from French Guiana and Suriname. The vocal repertoire of *B. courtoisae* is composed of two types of call (type 1: n = 13 calls from five males; type 2: n = 5 calls from three males) that are emitted sporadically at irregular intervals. The type 1 call (Fig. 4) lasts 140–240 ms, consisting of 3–4 nonpulsed notes that last 5–36 ms, separated by intervals of 27–82 ms. The rise time is at 2–97% of call duration. The minimum frequency ranges from 1335–1875, the maximum frequency from 2627–3101 Hz, and the dominant frequency from 1981–2972 Hz. The type 2 call consists of one note with poorly defined pulses. Notes last 39–79 ms. The rise time is at 39–82% of note duration. The minimum frequency ranges from 1464–1723 Hz, the maximum frequency from 2713–3144 Hz, and the dominant frequency from 1680–2412 Hz.

Distribution and ecology. *Boana courtoisae* sp. nov. is distributed throughout the eastern Guiana Shield in French Guiana, Suriname, Guyana and adjacent Brazilian Amazonia in the states of Amapá, Pará (Ávila-Pires et al., 2010), and possibly Roraima (pending confirmation). The species could possibly occur in the state of Amazonas as well. The species is not abundant and found in scattered populations. Nevertheless, its range is extensive and encompasses numerous protected areas. Moreover, the species seems to tolerate habitat disturbance, indicated by the use of forest borders and clearings. Therefore, the conservation status of *B. courtoisae* sp. nov. might be classified as Least Concern (pending a formal evaluation by IUCN team). It is a nocturnal species found in primary and secondary forest associated with the flooded zones of slow streams and medium-sized rivers. The males call perched at low height on the adjacent vegetation or even overlooking the water forming small groups of 2–10 individuals separated by a few metres from each other. A single clutch was observed at Mitaraka, French Guiana and contained approximately 1,100 beige eggs deposited directly in the water and forming a film on the surface.

Etymology. This species is dedicated to our friend Elodie Courtois, in honour of her invaluable contribution to field herpetology in French Guiana, notably the monitoring of populations of threatened species and discovery of previously undocumented species and many natural history observations.

Mitogenomic phylogeny

The mitogenomic phylogeny is well resolved with the exception of the position of the clade formed by *B. cinerascens* + *B. punctata* and the position of *B. pellucens* within the genus (Fig. 7). Within the focal species group only the relationships among the different OTUs of the *B. albopunctata* clade remain ambiguous. *Boana heilprini* is strongly supported as the sister species of all other members of the *B. albopunctata* species group whose crown age is estimated to date back to 17.3 Ma (14.4–20.2). *Boana raniceps* forms a clade with all the other species of the group whose crown age is estimated to date back to 13.2 Ma (11.1–15.5). The remainder of species forms three main clades. The *B. albopunctata* clade diverges from the Amazonian species ~10.9 Ma (9.1–12.7). The two Amazonian clades diverged ~9.9 Ma (8.3–11.6).

Biogeographic inferences

Model comparisons identified DEC + J as the best-fit model (Appendix 9). According to both DEC and DEC + J models the ancestral range of the *B. albopunctata* species group remains largely ambiguous since each of the major lineages is widely distributed in Amazonia and even further for the *B. albopunctata* clade. However, the ancestral range of the *B. steinbachi* clade is supported to be located in the Guiana Shield by the DEC + J model (Fig. 8A); and while it remains ambiguous for the DEC model, all states with high likelihood encompass the Guiana Shield (Fig. 8B). This group probably dispersed southward to the Brazilian Shield ~5 Ma, as suggested by the phylogenetic position

COLOR Online / B&W in Print

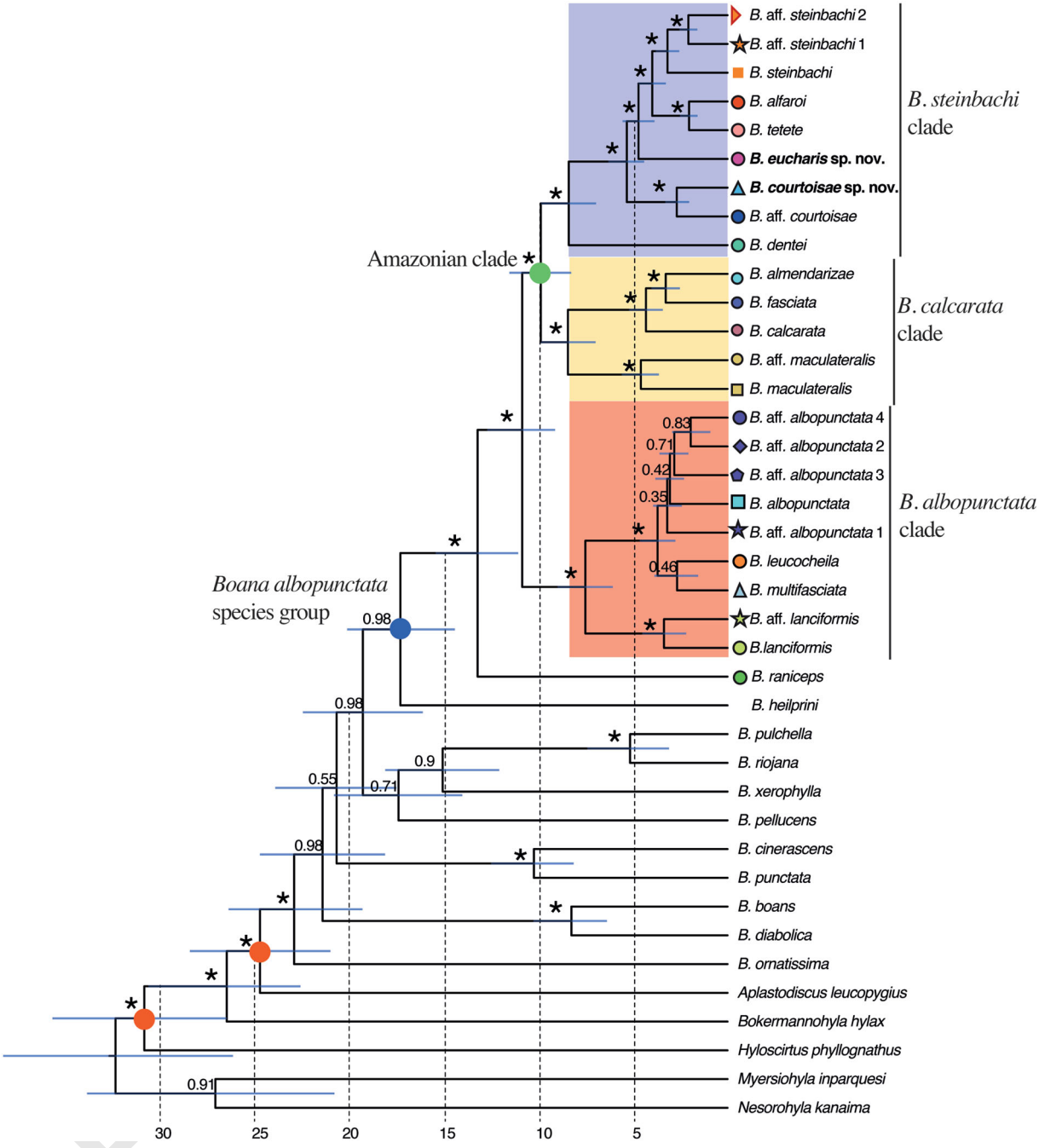

Fig. 7. Time calibrated tree inferred from the analysis of mitogenomic data in BEAST2 Nodes with maximum posterior probability (0.99 and 1) are indicated with an asterisk. Calibrated nodes are indicated with a red circle. The blue and the green circles point at major clades mentioned in the text. Node bars indicate the 95% highest posterior distributions of node dates. Symbols on the tips of the trees are the same as those used to indicate the geographic distribution of sampled species.

and range of *B. eucharis* (Fig. 8). Subsequent dispersal from the Brazilian Shield toward western Amazonia is suggested by the nested position of the clade formed by *B. tetete*, *B. alfaroi*, *B. steinbachi* and related OTUs. The occurrence of *B. steinbachi* in eastern Amazonia probably resulted from an even more recent dispersal toward the east (Pará state) from Western Amazonia (Fig. 8A, B). Mirroring that situation, the ancestral range of the *B. calcarata* clade is inferred in western Amazonia where it has exclusively diversified except for a single and recent dispersal of *B. calcarata* eastward throughout Amazonia.

The ancestral range of the *B. albopunctata* clade remains ambiguous since it also displays an east vs. west pattern

COLOR Online / B&W in Print

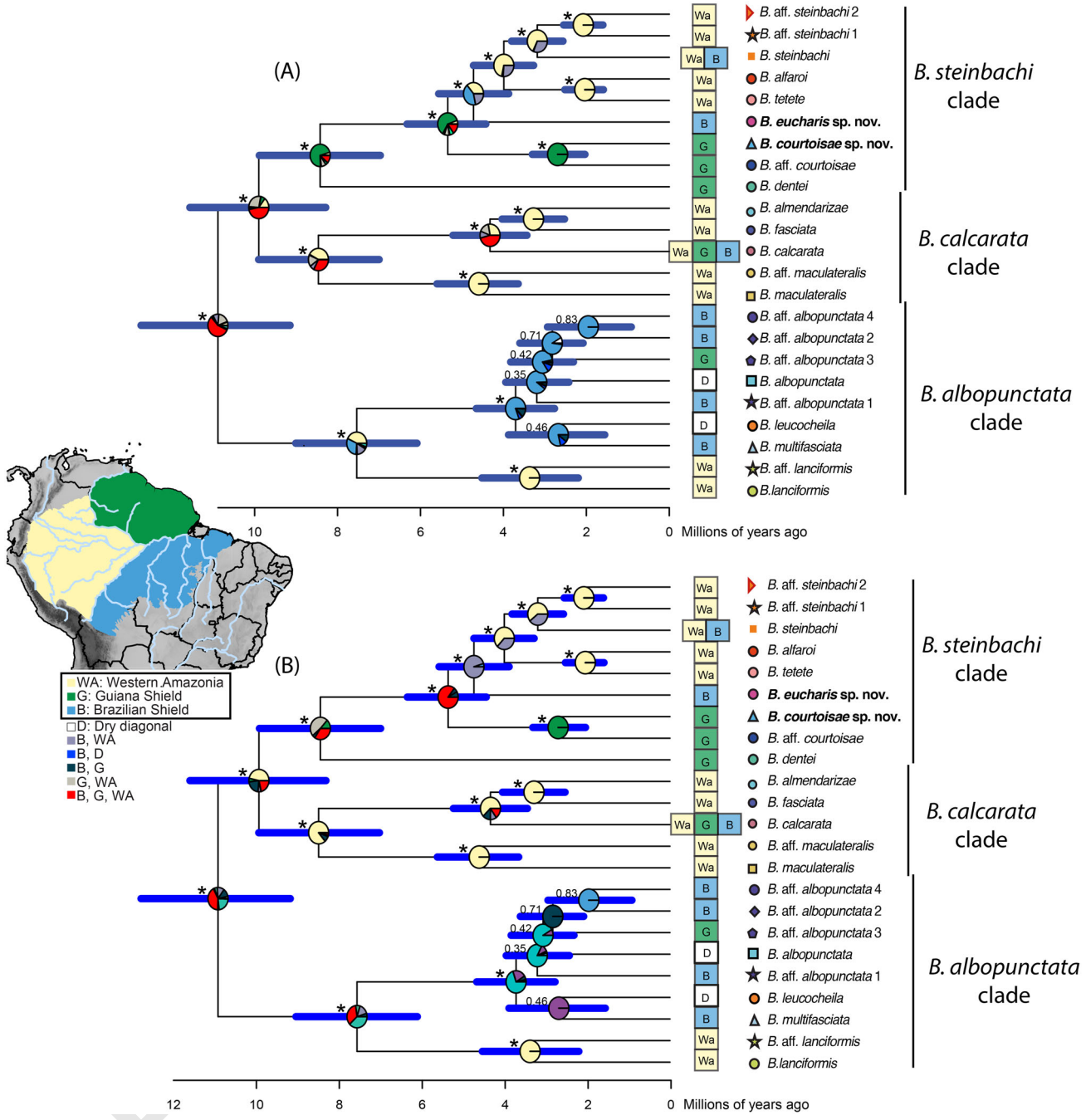

Fig. 8. Ancestral area reconstruction for the Boana albopunctata species group (B. heilprini and B. raniceps excluded) using BioGeoBears assuming (A) a DEC + J model and (B) a DEC model (Appendix 5): most likely biogeographic scenarios plotted on the chronogram obtained with BEAST 2.5, (Numbers on branches are posterior clade probabilities, those ? 0.95 are indicated with an asterisk. Node bars indicate the 95% highest posterior distributions of node dates. Squares on the tips of the trees indicate the geographic distribution of extant species sampled in the phylogeny. Pie charts on nodes show the most likely reconstructions of ancestral areas, the size of each slice proportional to the maximum likelihood. Colours corresponding to the different geographic distributions are depicted on the left.

with *B. lanciformis* occurring only in western Amazonia and the rest of the species of the clade occurring in the Cerrado and eastern Amazonia. However, this east-west divergence seems more recent in that group (7.5 Ma) than the *B. calcarata* vs. *B. steinbachi* divergence (9.9 Ma).

Discussion

Species richness and distribution

With 25 putative species and two taxa (*B. caiapo* and *B. paranaiba*) that could not be included in this study, the

species richness of the *B. albopunctata* group may actually reach 27 species, i.e., 70% higher than currently recognized (16 valid species). Within the Amazonian clade, the actual number of species may be 44% higher than currently recognized (14 OTU for 10 described/valid species including the two species described herein). We could not gather sufficient phenotypic data for the OTU identified as *B.* aff. *maculateralis*, but we are confident that such data will contribute to its taxonomic resolution. Moreover, our genetic sampling remains limited, specifically in Colombia, Venezuela, and south-eastern Amazonia, and more species in the group probably remain undocumented.

The discovery of yet undescribed species in Amazonia is not surprising, since new species descriptions of squamates and anurans keep accumulating at a fast pace (e.g. Carvalho et al., 2020; Kok et al., 2018). In fact, almost all systematic investigation of broadly distributed groups in Amazonia led to the understanding that they actually represent species complexes, often hiding narrowly distributed and remotely diverging species within Amazonia (e.g., Fouquet et al., 2014; Vacher et al., 2020). This recurrent pattern is also illustrated herein in the *B. albopunctata* species group notably by *B. fasciata*, a taxon that was used to design populations throughout Amazonia until the conclusions of Caminer and Ron (2014). The extent of the actual diversity of anurans in Amazonia remains so speculative that it could be three to four times higher than the current ~600 species occurring in that region according to the IUCN (Vacher et al., 2020).

Relationships and distribution of the species we found within the Amazonian clade strikingly mirror those found in other groups of anurans, notably *B. semilineata* group (Caminer & Ron, 2020; Fouquet et al., 2016; Peloso et al., 2018); *Osteocephalus* (Jungfer et al., 2013); *Dendropsophus minutus* (Gehara et al., 2014); *Allobates* (Réjaud et al., 2020); *Amazophrynella* (Rojas et al., 2018); *Adenomera* (Fouquet et al., 2014) and, more broadly, matches a pattern of allopatry throughout Amazonia in which communities are spatially structured forming distinct bioregions (Vacher et al., 2020). However, the history of Pan-Amazonian diversification is relatively recent in the case of the Amazonian clade of *Boana* studied herein compared with other taxa, such as *Allobates* (Réjaud et al., 2020) or *Amazophrynella* (Rojas et al., 2018). A combination of historical and contemporary climatic heterogeneity as well as species-specific dispersal ability and niche breadth (Sheu et al., 2020) is probably responsible for these common and distinct spatio-temporal patterns across taxa. Our time-scaled phylogeny and biogeographic analyses provide some insights into the historical processes responsible for the diversification of the *B. albopunctata* species group in Amazonia.

Biogeography

With nine OTUs the species richness in western Amazonia is confirmed to be higher than in the Guiana Shield (4 OTUs) and the Brazilian Shield (3 OTUs), suggesting that the climatic conditions and historical geomorphological dynamism in this region, notably hydrological changes, may have played a major role in *B.* gr. *albopunctata* diversification.

The initial diversification within the Amazonian clade between the *B. calcarata* clade in the west and the *B. steinbachi* in the east of Amazonia dates back to about 10 Ma. This estimate is relatively younger than those of Funk et al. (2012) and Duellman et al. (2016) partly because the divergences estimated by Feng et al. (2017), which were used as calibrations herein, are overall more recent than the nodes of those previous studies that were based on a lower amount of genomic data. Other east/west divergences, putatively simultaneous to the one found herein within the Amazonian clade of the *B. albopunctata* group, are documented in the *Adenomera heyeri* clade (Carvalho et al., 2020; Fouquet et al., 2014), in two instances within the *Allobates trilineatus* clade (Réjaud et al., 2020), in *Ameerega* (Guillory et al., 2020), and probably in many other lineages for which sampling and dating are still missing. This 10 Myr old node coincides with the end of the Pebas system and the transition from a western watershed drained to the north to a Pan-Amazonian system drained to the east (Hoorn et al., 2017). Available data indicate that the rise of the Vaupes Arch around 10 Ma completely separated the Western Amazon and Llanos basins (Hoorn et al., 2010; Jaramillo et al., 2017). We assume that this new configuration may have permitted the dispersal between the Guiana Shield and Western Amazonia and could be responsible for this 10 Myr old divergence in the *Boana* of the Amazonian clade and the other mentioned groups.

Subsequently, both groups have apparently diversified *in situ*, i.e., within Western Amazonia and within the Guiana Shield until some 5 Ma. This date coincides with the divergence between *B. courtoisae* sp. nov. and the other species of the *B. steinbachi* clade and suggests a dispersal from the Guiana to the Brazilian Shield across the transcontinental configuration of the Amazon River, which contradicts our expectation that such divergence would precede this configuration (9 Ma; Hoorn et al., 2017). Temporally concordant north/south divergences are documented within *Allobates tapajos* and between *A. bacurau* and *A. sumtuosus* (Réjaud et al., 2020), in *Chiasmocleis* (de Sá et al., 2019) and most likely other

lineages of terrestrial vertebrates for which the histories of diversification remain undocumented. The processes that may have fostered multiple trans-Amazon dispersals around 5 Ma remain highly speculative. Considerable uncertainty remains about the timing and amplitude of historical topographic, hydrological, and vegetational changes in Amazonia (Albert et al., 2018a; Bicudo, Sacek, de Almeida, Bates, & Ribas 2019; Campbell, Frailey, & Romero-Pittman, 2006; Hoorn et al., 2017; Latrubesse et al., 2010). The sediment discharge in the Amazon fan was relatively modest until 5 Ma and vastly increased in the Pliocene-Pleistocene (Albert et al., 2018a ; Hoorn et al., 2017). The lower course of the Amazon River may have become an impassable barrier for these taxa only from the Miocene-Pliocene boundary onward. Moreover, this period also coincides with vegetational and climatic changes, notably the expansion of grasslands not only in the Andes and the Cerrado but also within Amazonia (Kirschner & Hoorn, 2019).

Subsequently, i.e., the last 5 My, both lineages diversified extensively in Western Amazonia, notably along the foothills of the Andes. This diversification has probably been fostered by the combination of increasing availability of suitable *terra-firme* habitat due to the retreat of the lacustrine ecosystem and dynamic river capture (Albert et al., 2018a). The ancestors of the *B. calcarata* clade have presumably diversified in the western Acre system, i.e., between the Andes and the Amazon rainforest in the east (Latrubesse et al., 2010). Only recently, dispersal towards the east seems to have occurred, notably in *B. calcarata*. This last species displays the largest range in the clade, which may be explained by the large diversity of rivers used by that species and the fact that large rivers do not represent efficient barriers for its dispersal.

The diversification of the *B. albopunctata* clade has taken place both in Amazonia and in the Cerrado and appears overall more recent than within the Amazonian clade. These lineages probably originated from transitional ecosystems between the Dry Diagonal and Amazonia. This diversification may be partly related to changes in climate and probable forest retreat in the eastern part of Amazonia during the Late Pliocene and Pleistocene (Cheng et al., 2013; Ledru et al., 2000; Pennington et al., 2000; Van der Hammen & Hooghiemstra, 2000).

Acknowledgements

This study benefited from an 'Investissement d'Avenir' grant managed by the Agence Nationale de la Recherche (CEBA, ref. ANR-10-LABX-25-01; TULIP, ref. ANR-10-LABX-0041; ANAEE-France: ANR-11-INBS-0001). AF and FPW acknowledge the French/Brazilian GUYAMAZON program action (IRD, CNRS, CTG, CIRAD and Brazilian Fundação de Amparo à Pesquisa do Estado do Amazonas-FAPEAM10.13039/501100004916 062.00962/2018). MTR thanks Conselho Nacional de Desenvolvimento Científico e Tecnológico (CNPq)10.13039/501100003593, Fundação de Amparo à Pesquisa do Estado de São Paulo [FAPESP10.13039/501100001807 grant numbers: 2003/10335-8, 2011/50146-6], and NSF-FAPESP Dimensions of Biodiversity Program [grant numbers: BIOTA 2013/50297-0, NSF-DEB 1343578] and NASA10.13039/100000104. SRR acknowledges a grant from SENESCYT (Arca de Noé Initiative). FPW thanks CNPq (Productivity Fellowship), FAPEAM, Coordenação de Aperfeiçoamento de Pessoal de Nível Superior-CAPES (Visiting Professor Fellowship), and the L'Oréal-UNESCO For Women In Science Program. TH thanks CNPq (Productivity Fellowship) and CNPq/SISBIOTA [563348/2010-0]. Financial support was received through a research grant from the National Council for Scientific and Technological Development (CNPq #446935/2014-0). TRC is a recipient of a postdoctoral fellowship from FAPESP (#2017/08489-0), PM is a recipient of a Master's fellowship from Coordenação de Aperfeiçoamento de Pessoal de Nível Superior (CAPES #88887.201356/2018-00), AAG receives financial support and grants from CNPq (446935/2014-0, 300903/2015-4, and 305169/2019-0). We thank the assistance of A.G. Lopes, B.F.V. Teixeira, and D.L. Bang as field companions. We are grateful to C.F.B. Haddad, M.L. Lyra, and Centro de Estudos de Insetos Sociais (CEIS) for providing financial and logistic support and training in DNA sequencing, partly funded by a research grant from FAPESP (#2013/50741-7; CFBH). The Macaulay Library (ML) at the Cornell Lab of Ornithology, Fonoteca Neotropical Jacques Vielliard (FNJV) enabled access to sound files. The Cornell Lab of Ornithology provided a free license of Raven Pro Software. We also warmly thank members of MTR lab and Arcadis-Logos for help in fieldwork, as well as J. Lima, M. Blanc, J.-P. Vacher, E. Courtois, B. Villette, M. Dewynter, Q. Martinez, R. Jairam, and P. Ouboter for their contribution with material used in this work.

Supplemental data

Supplemental data for this article can be accessed here: https://doi.org/10.1080/14772000.2021.1873869.

ORCID

Antoine Fouquet http://orcid.org/0000-0003-4060-0281
Pedro Marinho http://orcid.org/0000-0001-6432-5312
Thiago R. Carvalho http://orcid.org/0000-0003-0910-2583
Marcel A. Caminer http://orcid.org/0000-0002-5827-7462
Miguel T. Rodrigues http://orcid.org/0000-0003-3958-9919
Ariovaldo A. Giaretta http://orcid.org/0000-0001-7054-129X
Santiago Ron http://orcid.org/0000-0001-6300-9350

References

Acosta-Galvis, A. R., Lasso, C. A., & Morales-Betancourt, M. A. (2018). First record of *Boana maculateralis* (Caminer & Ron, 2014) and *Boana tetete* (Caminer & Ron, 2014)(Anura, Hylidae) in Colombia. *Check List*, *14*(3), 549–554. https://doi.org/10.15560/14.3.549

Albert, J. S., Val, P., & Hoorn, C. (2018a). The changing course of the Amazon River in the Neogene: center stage for Neotropical diversification. *Neotropical Ichthyology*, *16*(3), e180033. https://doi.org/10.1590/1982-0224-20180033

Albert, J. S., Craig, J. M., Tagliacollo, V. A., & Petry, P. (2018b). Upland and lowland fishes: A test of the River Capture Hypothesis. In C. M. Hoorn, A. Perrigo, & A. Antonelli (Eds.), *Mountains, Climate and Biodiversity*. (pp. 273–294). Wiley.

Antonelli, A., Ariza, M., Albert, J., Andermann, T., Azevedo, J., Bacon, C., Faurby, S., Guedes, T., Hoorn, C., Lohmann, L. G., Matos-Maraví, P., Ritter, C. D., Sanmartín, I., Silvestro, D., Tejedor, M., Ter Steege, H., Tuomisto, H., Werneck, F. P., Zizka, A., & Edwards, S. V. (2018). Conceptual and empirical advances in Neotropical biodiversity research. *PeerJ.*, *6*, e5644 https://doi.org/10.7717/peerj.5644

Ávila, R. W., & Kawashita-Ribeiro, R. A. (2011). Herpetofauna of São João da Barra Hydroelectric Plant, state of Mato Grosso. *Check List*, *7*(6), 750–755. https://doi.org/10.15560/11014

Ávila-Pires, T. C. S. D., Hoogmoed, M. S., & Rocha, W. A. D. (2010). Notes on the Vertebrates of northern Pará, Brazil: a forgotten part of the Guianan Region, I. Herpetofauna. *Boletim Do Museu Paraense Emílio Goeldi*, *5*(1), 13–122.

Bicudo, T. C., Sacek, V., de Almeida, R. P., Bates, J. M., & Ribas, C. C. (2019). Andean tectonics and Mantle Dynamics as a Pervasive Influence on Amazonian ecosystem. *Scientific Reports*, *9*(1), 1–11. https://doi.org/10.1038/s41598-019-53465-y

Bokermann, W. C. A. (1967). Nova espéce de *Hyla* do Amapá (Amphibia, Hylidae). *Revista Brasileira de Biologia*, *27*, 109–112.

Bouckaert, R., Heled, J., Kühnert, D., Vaughan, T., Wu, C. H., Xie, D., Suchard, M. A., Rambaut, A., & Drummond, A. J. (2014). BEAST 2: A Software Platform for Bayesian Evolutionary Analysis. *PLoS Comput Biol*, *10*(4), e1003537 https://doi.org/10.1371/journal.pcbi.1003537

Boulenger, G. A. (1905). Descriptions of new tailless batrachians in the collection of the British Museum. *Annals and Magazine of Natural History*, *16*(92), 180–184. https://doi.org/10.1080/03745480509443666

Caminer, M. A., & Ron, S. R. (2014). Systematics of treefrogs of the *Hypsiboas calcaratus* and *Hypsiboas fasciatus* species complex (Anura, Hylidae) with the description of four new species. *Zookeys*, *370*, 1.

Caminer, M. A., & Ron, S. R. (2020). Molecular phylogeny and morphology of Ecuadorian frogs of the genus *Boana* (Anura: Hylidae) with the description of two new species. *Zoological Journal of the Linnean Society*, *190*(1), 149–180. https://doi.org/10.1093/zoolinnean/zlaa002

Campbell, K. E., Jr, Frailey, C. D., & Romero-Pittman, L. (2006). The Pan-Amazonian Ucayali Peneplain, late Neogene sedimentation in Amazonia, and the birth of the modern Amazon River system. *Palaeogeography, Palaeoclimatology, Palaeoecology*, *239*(1-2), 166–219. https://doi.org/10.1016/j.palaeo.2006.01.020

Camurugi, F., Gehara, M., Fonseca, E. M., Zamudio, K. R., Haddad, C. F. B., Colli, G. R., Thomé, M. T. C., Prado, C. P. A., Napoli, M. F., & Garda, A. A. (2021). Isolation by environment and recurrent gene flow shaped the evolutionary history of a continentally distributed Neotropical treefrog. *Journal of Biogeography*, in press.

Caramaschi, U., & de Niemeyer, H. (2003). New species of the *Hyla albopunctata* group from central Brazil (Amphibia, Anura, Hylidae). *Boletim do Museu Nacional. Nova Serie, Zoologia*, *504*, 1–8.

Carvalho, T. R., Giaretta, A. A., & Facure, K. G. (2010). A new species of *Hypsiboas* Wagler (Anura: Hylidae) closely related to *H. multifasciatus* Günther from southeastern Brazil. *Zootaxa*, *2521*, 37–52.

Carvalho, T. R., Bang, D. L., Teixeira, B. F. V., & Giaretta, A. A. (2017). First record of *Boana alfaroi* (Caminer & Ron, 2014) (Anura: Hylidae) in Brazil. *Check List*, *13*, 135–139.

Carvalho, T. R., Moraes, L. C. J. L., Lima, A. P., Fouquet, A., Peloso, P. L. V., Pavan, D., Drummond, L. O., Rodrigues, M. T., Giaretta, A. A., Gordo, M., Neckel-Oliveira, S., & Haddad, C. F. B. (2020). Systematics and historical biogeography of Neotropical foam-nesting frogs of the *Adenomera heyeri* clade (Leptodactylidae), with the description of six new Amazonian species. *Zoological Journal of the Linnean Society*, ~~in press~~, https://doi.org/10.1093/zoolinnean/zlaa051

Ceballos, G., Ehrlich, P. R., Barnosky, A. D., García, A., Pringle, R. M., & Palmer, T. M. (2015). Accelerated modern human-induced species losses: Entering the sixth mass extinction. *Science Advances*, *1*(5), e1400253 https://doi.org/10.1126/sciadv.1400253

Cheng, H., Sinha, A., Cruz, F. W., Wang, X., Edwards, R. L., d'Horta, F. M., Ribas, C. C., Vuille, M., Stott, L. D., & Auler, A. S. (2013). Climate change patterns in Amazonia and biodiversity. *Nature Communications*, *4*(1), 1–6. https://doi.org/10.1038/ncomms2415

Cole, C. J., Townsend, C. R., Reynolds, R. P., MacCulloch, R. D., & Lathrop, A. (2013). Amphibians and reptiles of Guyana, South America: illustrated keys, annotated species accounts, and a biogeographic synopsis. *Proceedings of the Biological Society of Washington*, *125*(4), 317–578. https://doi.org/10.2988/0006-324X-125.4.317

Cope, E. D. (1862 *Catalogues of the reptiles obtained during the explorations of the Parana, Paraguay, Vermejo and Uruguay Rivers, by Capt. Thos. J. Page, U.S.N.; and of those procured by Lieut. N. Michler, U.S. Top. Eng., Commander of the expedition conducting the survey of the Atrato River [Paper presentation]*. Proceedings of the Academy of Natural Sciences of Philadelphia, *14*, 346–359.

Cope, E. D. (1871). Eighth contribution to the herpetology of tropical America. *Proceedings of the American Philosophical Society*, *11*, 553–559. "1870".

De la Riva, I. (1990). Lista preliminar comentada de los anfibios de Bolivia con datos sobre su distribución. *Bollettino. Museo Regionale di Scienze Naturali. Tori*, *8*, 261–319.

de Sá, R. O., Tonini, J. F. R., van Huss, H., Long, A., Cuddy, T., Forlani, M. C., Peloso, P. L., Zaher, H., & Haddad, C. F. (2019). Multiple connections between Amazonia and Atlantic Forest shaped the phylogenetic and morphological diversity of *Chiasmocleis* Mehely, 1904 (Anura: Microhylidae: Gastrophryninae). *Molecular Phylogenetics and Evolution*, *130*, 198–210. https://doi.org/10.1016/j.ympev.2018.10.021

Dewynter, M., Marty, C., Blanc, M., Gaucher, P., Vidal, N., Frétey, T., de Massary, J. C., Fouquet, A. (2008). Liste des Amphibiens et des Reptiles de Guyane. Available online: http://www.chelidae.com/pdf/dewynter2008.pdf.

Drummond, A. J., Ho, S. Y. W., Phillips, M. J., & Rambaut, A. (2006). Relaxed phylogenetics and dating with confidence. *PLoS Biology*, *4*(5), e88 https://doi.org/10.1371/journal.pbio.0040088

Dubois, A. (2017). The nomenclatural status of *Hysaplesia, Hylaplesia, Dendrobates* and related nomina (Amphibia, Anura), with general comments on zoological nomenclature and its governance, as well as on taxonomic databases and websites. *Bionomina*, *11*(1), 1–48. https://doi.org/10.11646/bionomina.11.1.1

Duellman, W. E., Marion, A. B., & Hedges, S. B. (2016). Phylogenetics, classification, and biogeography of the treefrogs (Amphibia: Anura: Arboranae). *Zootaxa*, *4104*(1), 1–109. https://doi.org/10.11646/zootaxa.4104.1.1

Dupin, J., Matzke, N. J., Särkinen, T., Knapp, S., Olmstead, R. G., Bohs, L., & Smith, S. D. (2017). Bayesian estimation of the global biogeographical history of the Solanaceae. *Journal of Biogeography*, *44*(4), 887–899. https://doi.org/10.1111/jbi.12898

Ezard, T., Fujisawa, T., & Barraclough, T. (2009). splits: SPecies' LImits by Threshold Statistics. R package version 1.0-11/r29.

Faivovich, J., Haddad, C. F., Garcia, P. C., Frost, D. R., Campbell, J. A., & Wheeler, W. C. (2005). Systematic review of the frog family Hylidae, with special reference to Hylinae: phylogenetic analysis and taxonomic revision. *Bulletin of the American Museum of Natural History*, *294*(1), 1–240. https://doi.org/10.1206/0003-0090(2005)294[0001:SROTFF]2.0.CO;2

Feng, Y. J., Blackburn, D. C., Liang, D., Hillis, D. M., Wake, D. B., Cannatella, D. C., & Zhang, P. (2017). Phylogenomics reveals rapid, simultaneous diversification of three major clades of Gondwanan frogs at the Cretaceous-Paleogene boundary. *Proceedings of the National Academy of Sciences of the United States of America*, *114*(29), E5864–E5870. https://doi.org/10.1073/pnas.1704632114

Ficetola, G. F., Rondinini, C., Bonardi, A., Katariya, V., Padoa-Schioppa, E., & Angulo, A. (2014). An evaluation of the robustness of global amphibian range maps. *Journal of Biogeography*, *41*(2), 211–221. https://doi.org/10.1111/jbi.12206

Fouquet, A., Gilles, A., Vences, M., Marty, C., Blanc, M., & Gemmell, N. J. (2007). Underestimation of species richness in Neotropical frogs revealed by mtDNA analyses. *PLoS One*, *2*(10), e1109 https://doi.org/10.1371/journal.pone.0001109

Fouquet, A., Cassini, C. S., Haddad, C. F. B., Pech, N., & Rodrigues, M. T. (2014). Species delimitation, patterns of diversification and historical biogeography of the Neotropical frog genus *Adenomera* (Anura, Leptodactylidae). *Journal of Biogeography*, *41*(5), 855–870. https://doi.org/10.1111/jbi.12250

Fouquet, A., Martinez, Q., Zeidler, L., Courtois, E. A., Gaucher, P., Blanc, M., Lima, J. D., Souza, S. M., Rodrigues, M. T., Lima, J. D., Souza, S. M., Rodrigues, M. T., & Kok, P. J. R. (2016). Cryptic diversity in the *Hypsiboas semilineatus* species group (Amphibia, Anura) with the description of a new species from the eastern Guiana Shield. *Zootaxa*, *4084*(1), 79–104. https://doi.org/10.11646/zootaxa.4084.1.3

~~Fouquet, A., Gilles, A., Vences, M., Marty, C., Blanc, M., & Gemmell, N. J. (2007a). Underestimation of species richness in Neotropical frogs revealed by mtDNA analyses. *PLoS One*, *2*(10), e1109 https://doi.org/10.1371/journal.pone.0001109~~

~~Fouquet, A., Loebmann, D., Castroviejo-Fisher, S., Padial, J. M., Orrico, V. G., Lyra, M. L., Roberto, I. J., Kok, P. J., Haddad, C. F., & Rodrigues, M. T. (2012). From Amazonia to the Atlantic forest: Molecular phylogeny of Phyzelaphryninae frogs reveals unexpected diversity and a striking biogeographic pattern emphasizing conservation challenges. *Molecular Phylogenetics and Evolution*, *65*(2), 547–561. https://doi.org/10.1016/j.ympev.2012.07.012~~

Fouquet, A., Vidal, N., & Dewynter, M. (2019). The Amphibians of the Mitaraka massif, French Guiana. *Zoosystema*, *41*(sp1), 359–374. https://doi.org/10.5252/zoosystema2019v41a19

Frost, D. R. (2019). *Amphibian Species of the World: an Online Reference*. Version 6.1 (Date of access). Electronic Database accessible at https://amphibiansoftheworld.amnh.org/index.php. American Museum of Natural History, New York, USA.

Funk, W. C., Caminer, M., & Ron, S. R. (2012). High levels of cryptic species diversity uncovered in Amazonian frogs. *Proceedings of the Royal Society B: Biological Sciences*, *279*(1734), 1806–1814. https://doi.org/10.1098/rspb.2011.1653

Gaige, H. T. (1929). Three new tree-frogs from Panama and Bolivia. Occasional Papers of the Museum of Zoology, University of Michigan, *207*, 1–6.

Gehara, M., Crawford, A. J., Orrico, V. G. D., Rodríguez, A., Lötters, S., Fouquet, A., Barrientos, L. S., Brusquetti, F., De la Riva, I., Ernst, R., Urrutia, G. G., Glaw, F., Guayasamin, J. M., Hölting, M., Jansen, M., Kok, P. J. R., Kwet, A., Lingnau, R., Lyra, M., … Köhler, J. (2014). High levels of diversity uncovered in a widespread nominal taxon: continental phylogeography of the Neotropical tree frog *Dendropsophus minutus*. *PloS One*, *9*(9), e103958 https://doi.org/10.1371/journal.pone.0103958

Q5

Godinho, M. B. d C., & Da Silva, F. R. (2018). The influence of riverine barriers, climate, and topography on the biogeographic regionalization of Amazonian anurans. *Scientific Reports*, *8*(1), 1–11. https://doi.org/10.1038/s41598-018-21879-9

Guerra, V., Jardim, L., Llusia, D., Márquez, R., & Bastos, R. P. (2020). Knowledge status and trends in description of amphibian species in Brazil. *Ecological Indicators*, *118*, 106754. https://doi.org/10.1016/j.ecolind.2020.106754

Guillory, W. X., French, C. M., Twomey, E. M., Chávez, G., Prates, I., von May, R., De la Riva, I., Lötters, S., Reichle, S., Serrano-Rojas, S. J., Whitworth, A., & Brown, J. L. (2020). Phylogenetic relationships and systematics of the Amazonian poison frog genus *Ameerega* using ultraconserved genomic elements. *Mol Phylogenet Evol*, *142*, 106638 https://doi.org/10.1016/j.ympev.2019.106638

Günther, A. C. L. G. (1858). Neue Batrachier in der Sammlung des britischen Museums. *Archiv Für Naturgeschichte.*, *24*, 319–328. https://doi.org/10.5962/bhl.part.5288

Günther, A. C. L. G. (1859). "1858". *Catalogue of the Batrachia Salientia in the Collection of the British Museum*. Taylor and Francis.

Haffer, J. (1969). Speciation in Amazonian forest birds. *Science (New York, N.Y.).)*, *165*(3889), 131–137. https://doi.org/10.1126/science.165.3889.131

Heyer, W. R., Rand, A. S., Cruz, C. A. G., Peixoto, O. L., & Nelson, C. E. (1990). Frogs of Boracéia. *Arquivos de Zoologia*, *31*, 231–410.

Hoorn, C., Wesselingh, F. P., ter Steege, H., Bermudez, M. A., Mora, A., Sevink, J., Sanmartin, I., Sanchez-Meseguer, A., Anderson, C. L., Figueiredo, J. P., Jaramillo, C., Riff, D., Negri, F. R., Hooghiemstra, H., Lundberg, J., Stadler, T., Särkinen, T., & Antonelli, A. (2010). Amazonia through time: Andean uplift, climate change, landscape evolution, and biodiversity. *Science (New York, N.Y.).)*, *330*(6006), 927–931. https://doi.org/10.1126/science.1194585

Hoorn, C., Bogotá-A, G. R., Romero-Baez, M., Lammertsma, E. I., Flantua, S. G., Dantas, E. L., Dino, R., do Carmo, D. A., & Chemale, F. Jr., (2017). The Amazon at sea: Onset and stages of the Amazon River from a marine record, with special reference to Neogene plant turnover in the drainage basin. *Global and Planetary Change*, *153*, 51–65. https://doi.org/10.1016/j.gloplacha.2017.02.005

Jansen, M., Bloch, R., Schulze, A., & Pfenninger, M. (2011). Integrative inventory of Bolivia's lowland anurans reveals hidden diversity. *Zoologica Scripta*, *40*(6), 567–583. https://doi.org/10.1111/j.1463-6409.2011.00498.x

Jaramillo, C., Romero, I., D'Apolito, C., Bayona, G., Duarte, E., Louwye, S., Escobar, J., Luque, J., Carrillo-Briceño, J. D., Zapata, V., Mora, A., Schouten, S., Zavada, M., Harrington, G., Ortiz, J., & Wesselingh, F. P. (2017). Miocene flooding events of western Amazonia. *Science Advances*, *3*(5), e1601693 https://doi.org/10.1126/sciadv.1601693

Jenkins, C. N., Pimm, S. L., & Joppa, L. N. (2013). Global patterns of terrestrial vertebrate diversity and conservation. *Proceedings of the National Academy of Sciences*, *110*(28), E2602–E2610. https://doi.org/10.1073/pnas.1302251110

Jungfer, K.-H., Faivovich, J., Padial, J. M., Castroviejo-Fisher, S., Lyra, M. M., V. M. Berneck, B., Iglesias, P. P., Kok, P. J. R., MacCulloch, R. D., Rodrigues, M. T., Verdade, V. K., Torres Gastello, C. P., Chaparro, J. C., Valdujo, P. H., Reichle, S., Moravec, J., Gvoždík, V., Gagliardi-Urrutia, G., Ernst, R., … F. B. Haddad, C. (2013). Systematics of spiny-backed treefrogs (Hylidae: *Osteocephalus*): an Amazonian puzzle. *Zoologica Scripta*, *42*(4), 351–380. https://doi.org/10.1111/zsc.12015

Kapli, P., Lutteropp, S., Zhang, J., Kobert, K., Pavlidis, P., Stamatakis, A., & Flouri, T. (2017). Multi-rate Poisson tree processes for single-locus species delimitation under maximum likelihood and Markov chain Monte Carlo. *Bioinformatics (Oxford, England))*, *33*(11), 1630–1638. https://doi.org/10.1093/bioinformatics/btx025

Katoh, K., Rozewicki, J., & Yamada, K. D. (2019). MAFFT online service: multiple sequence alignment, interactive sequence choice and visualization. *Briefings in Bioinformatics*, *20*(4), 1160–1166. https://doi.org/10.1093/bib/bbx108

Kirschner, J. A., & Hoorn, C. (2019). The onset of grasses in the Amazon drainage basin, evidence from the fossil record. *Frontiers of Biogeography*, *12*, e44827.

Klaus, K. V., & Matzke, N. J. (2020). Statistical Comparison of Trait-dependent Biogeographical Models indicates that Podocarpaceae Dispersal is influenced by both Seed Cone Traits and Geographical Distance. *Systematic Biology*, *69*(1), 61–75. https://doi.org/10.1093/sysbio/syz034

Köhler, J., Jansen, M., Rodríguez, A., Kok, P. J. R., Toledo, L. F., Emmrich, M., Glaw, F., Haddad, C. F. B., Rödel, M.-O., & Vences, M. (2017). The use of bioacoustics in anuran taxonomy: theory, terminology, methods and recommendations for best practice. *Zootaxa*, *4251*(1), 1–124. https://doi.org/10.11646/zootaxa.4251.1.1

Kok, P. J., Bittenbinder, M. A., van den Berg, J. K., Marques-Souza, S., Sales Nunes, P. M., Laking, A. E., Teixeira, M., Jr., Fouquet, A., Means, D. B., MacCulloch, R. D., & Rodrigues, M. T. (2018). Integrative taxonomy of the gymnophthalmid lizard *Neusticurus rudis* Boulenger, 1900 identifies a new species in the eastern Pantepui region, north-eastern South America. *Journal of Natural History*, *52*(13-16), 1029–1066. https://doi.org/10.1080/00222933.2018.1439541

Lanfear, R., Frandsen, P. B., Wright, A. M., Senfeld, T., & Calcott, B. (2016). PartitionFinder 2: New methods for selecting partitioned models of evolution for molecular and morphological phylogenetic analyses. *Molecular Biology and Evolution*, *34*(3), 772–773.

Latrubesse, E. M., Cozzuol, M., da Silva-Caminha, S. A., Rigsby, C. A., Absy, M. L., & Jaramillo, C. (2010). The Late Miocene paleogeography of the Amazon Basin and the evolution of the Amazon River system. *Earth-Science Reviews*, *99*(3-4), 99–124. https://doi.org/10.1016/j.earscirev.2010.02.005

Ledru, M.-P., Blanc, P., Charles-Dominique, P., Fournier, M., Martin, L., Riera, B., & Tardy, C. (2000). Reconstitution de l'écosystème forestier guyanais au cours de l'Holocène supérieur: apport de la palynologie. In M. Servan, & S. Servant Vildar (Eds.), *Dynamique à long terme des écosystèmes forestiers intertropicaux.* (pp. 199–204). UNESCO.

Leite, R. N., & Rogers, D. S. (2013). Revisiting Amazonian phylogeography: Insights into diversification hypotheses and novel perspectives. *Organisms Diversity & Evolution*, *13*(4), 639–664. https://doi.org/10.1007/s13127-013-0140-8

Lescure, J., & Marty, C. (2000). *Atlas des amphibiens de Guyane*. Collection patrimoines naturels.

Ligges, U., Krey, S., Mersmann, O., Schnackenberg, S. (2014). TuneR: Analysis of music. Accessed May 8, 2017. Available at: http://r-forge.r-project.org/projects/tuner.

Lima, A. P., Keller, C., & Rebelo, G. H. (2017). Estudos ambientais no Rio Madeira, trecho Cachoeira de Santo Antônio-Abunã (Rondônia): Herpetofauna. Relatório elaborado para Furnas Centrais Elétricas SA como parte do Estudo de Viabilidade dos AHEs Santo Antônio e Jirau, para o Aproveitamento Hidrelétrico do Rio Madeira. INPA, Manaus.

Lovejoy, T. E., & Nobre, C. (2019). Amazon tipping point: Last chance for action. *Science Advances*, *5*(12), eaba2949 https://doi.org/10.1126/sciadv.aba2949

Marinho, P., Costa-Campos, C. E., Pezzuti, T. L., Magalhães, R. F., Souza, M. R. D., Haddad, C. F. B., Giaretta, A. A., & De Carvalho, T. R. (2020). The Amapá treefrog *Boana dentei* (Bokermann, 1967): diagnosis and redescription. *Journal of Natural History*, *54*(15-16), 971–990. https://doi.org/10.1080/00222933.2020.1777336

Matzke, N. J. (2013). BioGeoBEARS: biogeography with Bayesian (and likelihood) evolutionary analysis in R scripts. *R Package*, Version 0.2, 1, 2013.

McCormack, J. E., Heled, J., Delaney, K. S., Peterson, A. T., & Knowles, L. L. (2011). Calibrating divergence times on species trees versus gene trees: implications for speciation history of *Aphelocoma* jays. *Evolution; International Journal of Organic Evolution*, *65*(1), 184–202. https://doi.org/10.1111/j.1558-5646.2010.01097.x

Meyer, C., Kreft, H., Guralnick, R., & Jetz, W. (2015). Global priorities for an effective information basis of biodiversity distributions. *Nature Communications*, *6*(1), 1–8. https://doi.org/10.1038/ncomms9221

Medina-Rangel, G. F., Méndez-Galeano, M. A., & Calderón-Espinosa, M. L. (2019). Herpetofauna of San José del Guaviare, Guaviare, Colombia. *Biota Colombiana*, *20*(1), 75–90. https://doi.org/10.21068/c2019.v20n01a05

Medina-Rangel, G. F., Thompson, M. E., Ruiz-Valderrama, D. H., Fajardo Muñoz, W., Lombana Lugo, J., Londoño-Guarnizo, C. A., Moquena Carbajal, C., Ríos Rosero, H. D., Sánchez Pamo, J. E., & Sánchez, E. (2019). Anfibios y reptiles. In N. Pitman, A. Salazar Molano, F. Samper Samper, C. Vriesendorp, A. Vásquez Cerón, Á. del Campo, T. L. Miller, E. A. Matapi Yucuna, M. E. Thompson, L. de Souza, D. Alvira Reyes, D. F. Stotz, N. Kotlinski, T. Wachter, E. Woodward & R. Botero García. (Eds.), *Colombia: Bajo Caguán–Caquetá. Rapid Biological and Social Inventories report*. 30 (pp. 111–454). Field Museum.

Meza-Joya, F. L., Ramos-Pallares, E., & Hernández-Jaimes, C. (2019). Hidden diversity in frogs within *Boana calcarata–fasciata* and *Boana geographica* species complexes from Colombia. *Herpetology Notes*, *12*, 391–400.

Monaghan, M. T., Wild, R., Elliot, M., Fujisawa, T., Balke, M., Inward, D. J. G., Lees, D. C., Ranaivosolo, R., Eggleton, P., Barraclough, T. G., & Vogler, A. P. (2009). Accelerated species inventory on Madagascar using coalescent-based models of species delineation. *Systematic Biology*, *58*(3), 298–311. https://doi.org/10.1093/sysbio/syp027

Müller, L. (1924). Neue Batrachier aus Ost-Brasilien. *Senckenbergiana Biologica*, *6*, 169–177.

Myers, N., Mittermeier, R. A., Mittermeier, C. G., da Fonseca, G. A., & Kent, J. (2000). Biodiversity hotspots for conservation priorities. *Nature*, *403*(6772), 853–858.

Near, T. J., Eytan, R. I., Dornburg, A., Kuhn, K. L., Moore, J. A., Davis, M. P., Wainwright, P. C., Friedman, M., & Smith, W. L. (2012). Resolution of ray-finned fish phylogeny and timing of diversification. *Proceedings of the National Academy of Sciences*, *109*(34), 13698–13703. https://doi.org/10.1073/pnas.1206625109

Noble, G. K. (1923). Six new batrachians from the Dominican Republic. *American Museum Novitates*, *61*, 1–6.

Oliveira, U., Vasconcelos, M. F., & Santos, A. J. (2017). Biogeography of Amazon birds: rivers limit species composition, but not areas of endemism. *Scientific Reports*, *7*(1), 1–11. https://doi.org/10.1038/s41598-017-03098-w

Ouboter, P. E., & Jairam, R. (2012). *Amphibians of Suriname*. Brill. 376. pp.

Pansonato, A., Ávila, R. W., Kawashita-Ribeiro, R. A., & Morais, D. H. (2011). Advertisement call and new distribution records of *Hypsiboas leucocheilus* (Anura: Hylidae). *Salamandra*, *47*, 55–58.

Parker, H. W. ((1927).). The brevicipitid frogs allied to the genus *Hypopachus*. *Occasional Papers of the Museum of Zoology, University of Michigan*, *187*, 1–6.

Pennington, R. T., Prado, D. E., & Pendry, C. A. (2000). Neotropical seasonally dry forests and Quaternary vegetation changes. *Journal of Biogeography*, *27*(2), 261–273. https://doi.org/10.1046/j.1365-2699.2000.00397.x

Peloso, P. L., De Oliveira, R. M., Sturaro, M. J., Rodrigues, M. T., Lima-Filho, G. R., Bitar, Y. O., Wheeler, W. C., & Aleixo, A. (2018). Phylogeny of map tree frogs, *Boana semilineata* species Group, with a new amazonian species (Anura: Hylidae). *South American Journal of Herpetology*, *13*(2), 150–169. https://doi.org/10.2994/SAJH-D-17-00037.1

Pinheiro, P. D. P., Cintra, C. E. D., Valdujo, P. H., da Silva, H. L. R., Martins, I. A., da Silva, N. J., Jr., & Garcia, P. C. A. (2018). A new species of the *Boana albopunctata* group (Anura: Hylidae) from the Cerrado of Brazil. *South American Journal of Herpetology*, *13*(2), 170–182. https://doi.org/10.2994/SAJH-D-17-00040.1

Pirani, R. M., Werneck, F. P., Thomaz, A. T., Kenney, M. L., Sturaro, M. J., Ávila-Pires, T. C. S., Peloso, P. L. V., Rodrigues, M. T., & Knowles, L. L. (2019). Testing main Amazonian rivers as barriers across time and space within widespread taxa. *Journal of Biogeography*, *46*(11), 2444–2456. https://doi.org/10.1111/jbi.13676

Pons, J., Barraclough, T. G., Gomez-Zurita, J., Cardoso, A., Duran, D. P., Hazell, S., Kamoun, S., Sumlin, W. D., & Vogler, A. P. (2006). Sequence-based species delimitation for the DNA taxonomy of undescribed insects. *Systematic Biology*, *55*(4), 595–609. https://doi.org/10.1080/10635150600852011

Prado, C. P., Haddad, C. F. B., & Zamudio, K. R. (2012). Cryptic lineages and Pleistocene population expansion in a Brazilian Cerrado frog. *Molecular Ecology*, *21*(4), 921–941. https://doi.org/10.1111/j.1365-294X.2011.05409.x

Puillandre, N., Lambert, A., Brouillet, S., & Achaz, G. (2012). ABGD, Automatic Barcode Gap Discovery for primary species delimitation. *Molecular Ecology*, *21*(8), 1864–1877. https://doi.org/10.1111/j.1365-294X.2011.05239.x

R Core Team. (2018). R: a language and environment for statistical computing. R Foundation for Statistical Computing. Version 3.5.0. Accessed July 29, 2020. Available at: https://www.R-project.org/.

Ree, R. H., & Sanmartín, I. (2018). Conceptual and statistical problems with the DEC + J model of founder-event speciation and its comparison with DEC via model

selection. *Journal of Biogeography*, *45*(4), 741–749. https://doi.org/10.1111/jbi.13173

Réjaud, A., Rodrigues, M. T., Crawford, A. J., Castroviejo-Fisher, S., Jaramillo, A. F., Chaparro, J. C., Glaw, F., Gagliardi-Urrutia, G., Moravec, J., De la Riva, I. J., Perez, P., Lima, A. P., Werneck, F. P., Hrbek, T., Ron, S. R., Ernst, R., Kok, P. J. R., Driskell, A., Chave, J., & Fouquet, A. (2020). Historical biogeography identifies a possible role of the Pebas system in the diversification of the Amazonian rocket frogs (Aromobatidae: *Allobates*). *Journal of Biogeography*, *47*(11), 2472–2482. https://doi.org/10.1111/jbi.13937

Ribas, C. C., Aleixo, A., Nogueira, A. C. R., Miyaki, C. Y., & Cracraft, J. (2012). A palaeobiogeographic model for biotic diversification within Amazonia over the past three million years. *Proceedings. Biological Sciences*, *279*(1729), 681–689. https://doi.org/10.1098/rspb.2011.1120

Rodrigues, D. J., Noronha, J. C., Vindica, V. F., & Barbosa, F. R. (2015). *Biodiversidade do Parque Estadual do Cristalino*. *Áttema Editorial*.

Rojas-Zamora, R. R., de Carvalho, V. T., Ávila, R. W., de Almeida, A. P., de Oliveira, E. A., Menin, M., & Gordo, M. (2017). *Hypsiboas maculateralis* Caminer & Ron, 2014, new to Brazil. *Herpetozoa*, *30*, 108–114.

Rojas, R. R., Fouquet, A., Ron, S. R., Hernández-Ruz, E. J., Melo-Sampaio, P. R., Chaparro, J. C., Vogt, R. C., de Carvalho, V. T., Pinheiro, L. C., Avila, R. W., Farias, I. P., Gordo, M., & Hrbek, T. (2018). A Pan-Amazonian species delimitation: high species diversity within the genus *Amazophrynella* (Anura: Bufonidae). *PeerJ.*, *6*, e4941 https://doi.org/10.7717/peerj.4941

Ruokolainen, K., Moulatlet, G. M., Zuquim, G., Hoorn, C., & Tuomisto, H. (2018). River network rearrangements in Amazonia shake biogeography and civil security. Preprints, 2018090168.

Ruthven, A. G. (1927). Description of an apparently new species of *Apostolepis* from Bolivia. *Occasional Papers of the Museum of Zoology, University of Michigan*, *188*, 1–2.

Savage, J. M., & Heyer, W. R. (1997). Digital webbing formulae for anurans: a refinement. *Herpetological Review*, *28*, 131.

Sheu, Y., Zurano, J. P., Ribeiro-Junior, M. A., Avila-Pires, T. C. S., Rodrigue, M. Ts., Colli, G. R., & Werneck, F. P. (2020). The combined role of dispersal and niche evolution in the diversification of Neotropical lizards. *Ecology and Evolution*, *10*(5), 2608–2625. https://doi.org/10.1002/ece3.6091

Silva, L. A., Magalhães, F. M., Thomassen, H., Leite, F. S. F., Garda, A. A., Brandão, R. A., Haddad, C. F. B., Giaretta, A. A., & Carvalho, T. R. (2020). Unraveling the species diversity and relationships in the *Leptodactylus mystaceus* complex (Anura: Leptodactylidae), with the description of three new Brazilian species. *Zootaxa*, *4779*, 151–189.

Spix, J. B. v. (1824). *Animalia nova sive Species novae Testudinum et Ranarum quas in itinere per Brasiliam annis MDCCCXVII–MDCCCXX jussu et auspiciis Maximiliani Josephi I. Bavariae Regis*. F. S. Hübschmann.

Stamatakis, A. (2014). RAxML version 8: a tool for phylogenetic analysis and post-analysis of large phylogenies. *Bioinformatics (Oxford, England))*, *30*(9), 1312–1313. https://doi.org/10.1093/bioinformatics/btu033

Sturaro, M. J., Costa, J. C. L., Maciel, A. O., Lima-Filho, G. R., Rojas-Runjaic, F. J., Mejia, D. P., Ron, S. R., & Peloso, P. L. (2020). Resolving the taxonomic puzzle of *Boana cinerascens* (Spix, 1824), with resurrection of *Hyla granosa gracilis* Melin, 1941 (Anura: Hylidae). *Zootaxa*, *4750*(1), 1–30. https://doi.org/10.11646/zootaxa.4750.1.1

Sueur, J., Aubin, T., & Simonis, C. (2008). Seewave, a free modular tool for sound analysis and synthesis. *Bioacoustics*, *18*(2), 213–226. https://doi.org/10.1080/09524622.2008.9753600

Troschel, F. H. (1848). Theil 3. Versuch einer Zusammenstellung der Fauna und Flora von Britisch-Guiana. Schomburgk, R. ed., *Reisen in Britisch-Guiana in den Jahren 1840–44. Im Auftrage Sr. Majestät des Königs von Preussen ausgeführt*. : 645–661J. J. Weber.

IUCN. (2020). The IUCN Red List of Threatened Species. Version 2020-1. https://www.iucnredlist.org. Downloaded on 19 March 2020.

Vacher, J.-P., Chave, J., Ficetola, F., Sommeria-Klein, G., Tao, S., Thébaud, C., Blanc, M., Camacho, A., Cassimiro, J., Colston, T. J., Dewynter, M., Ernst, R., Gaucher, P., Gome, s J. O., Jairam, R., Kok, P. J. R., Dias Lima, J., Martinez, Q., Marty, C., … Fouquet, A. (2020). Large scale DNA-based survey of Amazonian frogs suggest a vast underestimation of species richness and endemism. *Journal of Biogeography*, *47*(8), 1781–1791. https://doi.org/10.1111/jbi.13847

Van der Hammen, T., & Hooghiemstra, H. (2000). Neogene and Quaternary history of vegetation, climate, and plant diversity in Amazonia. *Quaternary Science Reviews*, *19*(8), 725–742. https://doi.org/10.1016/S0277-3791(99)00024-4

Vences, M., Thomas, M., Bonett, R. M., & Vieites, D. R. (2005). Deciphering amphibian diversity through DNA barcoding: chances and challenges. *Philosophical Transactions of the Royal Society B: Biological Sciences*, *360*(1462), 1859–1868. https://doi.org/10.1098/rstb.2005.1717

Wallace, A. R. (1854). On the monkeys of the Amazon. *Annals and Magazine of Natural History*, *14*(84), 451–454. https://doi.org/10.1080/037454809494374

Watters, J. L., Cummings, S. T., Flanagan, R. L., & Siler, C. D. (2016). Review of morphometric measurements used in anuran species descriptions and recommendations for a standardized approach. *Zootaxa*, *4072*(4), 477–495. https://doi.org/10.11646/zootaxa.4072.4.6

Werneck, F. P. (2011). The diversification of eastern South American open vegetation biomes: historical biogeography and perspectives. *Quaternary Science Reviews*, *30*(13-14), 1630–1648. https://doi.org/10.1016/j.quascirev.2011.03.009

Associate Editor: Dr Mark Wilkinson

Appendix 1. Samples included in molecular analyses, including results from DNA-based species delineation. Some of this newly analysed material was obtained through QCAZ, MPEG, INPA (H), CORBIDI, AAGUFU collections and from personal loans from Jose Manuel Padial (JMP), Santiago Castroviejo Fisher (SCF), Jucivaldo Dias Lima (FTA), Quentin Martinez (QM); Michel Blanc (AG)

GenBank accession	Voucher	Field Number	Species_ID	mPTP	ABGD	mPTP	GMYC	Cons	Locality	State	Lat.	Long.
>AF467269		CM015	B_raniceps	1	13	1	1	1	Crique YiYi	French_Guiana	5.483333	−53.15
>AY843657	MACN37795		B_raniceps	1	13	1	2	1	Santa Fe, Vera	Argentina	−29.459031	−60.208386
>JF790127		AS0169	B_raniceps	1	13	1	2	1	nuflo de Chavez, San Sebastian	Bolivia	−16.359633	−62.000050
>JF790128		AS0218	B_raniceps	1	13	1	2	1	Velasco, Caparu	Bolivia	−14.912117	−61.082467
>JF790129		AS0303	B_raniceps	1	13	1	2	1	Velasco, Caparu	Bolivia	−14.912117	−61.082467
>JF790130		AS0304	B_raniceps	1	13	1	2	1	Velasco, Caparu	Bolivia	−14.912117	−61.082467
>JF790132		AS0306	B_raniceps	1	13	1	2	1	Velasco, Caparu	Bolivia	−14.912117	−61.082467
>JF790133		AS0468	B_raniceps	1	13	1	1	1	Yucuma, Los Lagos	Bolivia	−12.772	−65.8109
>JF790134		AS0570	B_raniceps	1	13	1	2	1	nuflo de Chavez, San Sebastian	Bolivia	−16.359633	−62.000050
>KDQF01002617		H3905	B_raniceps	1	13	1	1	1	UHE Jirau, Mutum	RO	−9.601348	−65.0574150
>KDQF01002739		LPT38	B_raniceps	1	13	1	1	1	Laranjal do Jari	AP	−0.600855	−52.38887
>KDQF01002991	MPEG36750		B_raniceps	1	13	1	2	1	Canaa dos Carajas	PA	−6.075562	−50.243245
>KDQF01004033		PNA105	B_raniceps	1	13	1	2	1	Parque Nacional do Araguaia	TO	−10.8166667	−50.1833333
>KDQF01004063		QM052	B_raniceps	1	13	1	1	1	Guatemala	French_Guiana	5.15	−52.633333
>KF723064	MNKA9349		B_raniceps	1	13	1	2	1	San Sebastian	Bolivia	−16.3596	−62.0001
>KF723065	SMF94093		B_raniceps	1	13	1	2	1	San Sebastian	Bolivia	−16.3596	−62.0001
>KF723066	SMF94094		B_raniceps	1	13	1	2	1	San Sebastian	Bolivia	−16.3596	−62.0001
>KF723067	SMF94263		B_raniceps	1	13	1	2	1	Estancia Bechler	Bolivia	−17.51720	−63.28998
>KF723068	MNKA10459		B_raniceps	1	13	1	2	1	San Sebastian	Bolivia	−16.3596	−62.0001
>KF723069	SMF94241		B_raniceps	1	13	1	2	1	San Sebastian	Bolivia	−16.3596	−62.0001
>KF723070	SMF94246		B_raniceps	1	13	1	2	1	San Sebastian	Bolivia	−16.3596	−62.0001
>KU495281	CFBHT00940		B_raniceps	1	13	1	2	1	Santa Fe do Sul	SP	−20.228	−50.944
>KU495282	CFBHT02353		B_raniceps	1	13	1	2	1	Cafelandia e Cafesopolis	SP	−21.838	−49.7
>KU495283	CFBHT13473		B_raniceps	1	13	1	2	1	campus de Veterinaria da UFBA	Bahia	−11.935	−38.112
>KU495284	CFBHT07327		B_raniceps	1	13	1	2	1	Pariquera-Acu	SP	−24.66	−47.796
>KU495285		TG146	B_raniceps	1	13	1	2	1	Estreito	MA	−6.548	−47.445
>KU495286		TG265	B_raniceps	1	13	1	2	1	Paranaita	MT	−9.671	−56.482
>KU495287	CFBHT07328	CFBHT07328	B_raniceps	1	13	1	2	1	Pariquera-Acu	SP	−24.66	−47.796
>KU495288		TG158	B_raniceps	1	13	1	2	1	Porto Franco	MA	−6.35	−47.406
>**MW370296**		AG234	B_raniceps	1	13	1	1	1	Comte, Terrain michel	French_Guiana	4.679471	−52.338531
>**MW370317**		MTR36896	B_raniceps	1	13	1	1	1	Tefé	AM	−3.36396	−64.69653
>KDQF01003728		MTR33845	B_aff.lanciformis	2	5	2	13	2	Tefe, Estrada do Abial	AM	−3.45944009	−64.7509004
>**MW370318**		MTR36907	B_aff.lanciformis	2	5	2	13	2	Tefé	AM	−3.34554	−64.71122
>AY326054		WED54081	B_lanciformis	4	6	4	3	4	Puyo, Pastaza	Ecuador	−1.375502	−78.004787
>AY843636		MJH564	B_lanciformis	4	6	4	4	4	Loreto, Alpahuayo	Peru	−3.94403	−73.606866
>JN970644	QCAZ23803		B_lanciformis	4	6	4	3	4	La Pradera, Via Gualaquiza	Ecuador	−2.285	−78.094
>JN970645	QCAZ23809		B_lanciformis	4	6	4	3	4	Mendez, River N of	Ecuador	−2.7291	−78.2849
>JN970646	QCAZ30936		B_lanciformis	4	6	4	3	4	Huino	Ecuador	−0.606	−77.173
>JN970647	QCAZ18175		B_lanciformis	4	6	4	3	4	Estacion Biologica Jatun Sacha	Ecuador	−1.0675	−77.6152778
>JN970648	QCAZ20641		B_lanciformis	4	6	4	3	4	Estacion Cientifica Yasuni	Ecuador	−0.678194	−76.3965555
>JN970649	QCAZ18237		B_lanciformis	4	6	4	3	4	Nangaritza	Ecuador	−4.335192	−78.67974
>JN970650	QCAZ31017		B_lanciformis	4	6	4	3	4	Centro Shuar Yawi	Ecuador	−4.4301	−78.631608
>KF157594		isolate7768	B_lanciformis	4	6	4	5	4		Venezuela	NA	NA
>KP149371		AJC3975	B_lanciformis	4	6	4	5	4	Casanare, Sabanalarga	Colombia	4.773	−73.037
>KP149451		AJC3373	B_lanciformis	4	6	4	5	4	Casanare, Sabanalarga	Colombia	4.773	−73.037
>KP149455		AJC3971	B_lanciformis	4	6	4	5	4	Casanare, Sabanalarga	Colombia	4.773	−73.037
>KP149465		AJC3973	B_lanciformis	4	6	4	5	4	Casanare, Sabanalarga	Colombia	4.773	−73.037
>**MW370316**		MTR36402	B_lanciformis	4	6	4	4	4	São Pedro, Rio Içá	AM	−3.03339	−68.88413
>AY843613	NMP6V71250		B_aff.maculateralis	5	11	5	45	5	Anguilla Peru	Peru	−3.662914	−73.924860
>KDQF01003645		MTR28015	B_aff.maculateralis	5	11	5	36	5	Serra do Divisor	AC	−7.44309497	−73.6576660
>KDQF01003658		MTR28077	B_aff.maculateralis	5	11	5	36	5	Serra do Divisor	AC	−7.43399298	−73.6609450
>**MW370306**	CORBIDI6182		B_aff.maculateralis	5	11	5	36	5	Jenaro Herrera, Requena	Peru	−4.903812	−73.663577
>**MW370314**		MTR35995	B_aff.maculateralis	5	11	5	46	5	Comunidade Cuiauá, Rio Içá	AM	−2.88619	−68.37169
>**MW370312**		JMP2306	B_aff.maculateralis	5	11	5	36	5	quebradas_Pinsha_y_Yanayacu	Loreto	−5.12	−73.8
>JN970541	QCAZ40082		B_maculateralis	6	12	6	37	6	Comunidad Santa Rosa	Ecuador	−1.02337	−77.48359
>JN970545	QCAZ43710		B_maculateralis	6	12	6	37	6	Coca	Ecuador	−0.47782	−76.98982
>JN970546	QCAZ43712		B_maculateralis	6	12	6	37	6	Coca	Ecuador	−0.47782	−76.98982
>JN970552	QCAZ44452		B_maculateralis	6	12	6	37	6	Chiroisla, north bank	Ecuador	−0.57564999	−75.8998299
>JN970555	QCAZ44184		B_maculateralis	6	12	6	37	6	Eden	Ecuador	−0.49833	−76.07112
>JN970556	QCAZ44185		B_maculateralis	6	12	6	37	6	Eden	Ecuador	−0.49833	−76.07112
>JN970559	QCAZ44248		B_maculateralis	6	12	6	37	6	Eden	Ecuador	−0.49833	−76.07112
>JN970562	QCAZ44636		B_maculateralis	6	12	6	37	6	Huiririma	Ecuador	−0.71163	−75.62395
>JN970563	QCAZ44651		B_maculateralis	6	12	6	37	6	Santa Teresita	Ecuador	−0.90087	−75.41357
>JN970564	QCAZ44673		B_maculateralis	6	12	6	37	6	Santa Teresita	Ecuador	−0.90087	−75.41357
>JN970568	QCAZ43825		B_maculateralis	6	12	6	37	6	La Primavera, south bank	Ecuador	−0.44427	−76.78685
>JN970570	QCAZ43827		B_maculateralis	6	12	6	37	6	La Primavera, south bank	Ecuador	−0.44427	−76.78685
>JN970572	QCAZ43897		B_maculateralis	6	12	6	37	6	La Primavera, north bank	Ecuador	−0.431	−76.78648
>JN970576	QCAZ44531		B_maculateralis	6	12	6	37	6	San Vicente	Ecuador	−0.67901	−75.65112
>JN970577	QCAZ44532		B_maculateralis	6	12	6	37	6	San Vicente	Ecuador	−0.67901	−75.65112
>JN970595	QCAZ28401		B_maculateralis	6	12	6	37	6	Cuyabeno beach	Ecuador	−0.265433	−75.891733
>JN970598	QCAZ44020		B_maculateralis	6	12	6	37	6	La Selva Lodge	Ecuador	−0.50868	−76.36493
>JN970599	QCAZ44021		B_maculateralis	6	12	6	37	6	La Selva Lodge	Ecuador	−0.50868	−76.36493
>JN970611	QCAZ27940		B_maculateralis	6	12	6	37	6	Zabalo	Ecuador	−0.318133	−75.76625

(*continued*)

Continued.

GenBank accession	Voucher	Field Number	Species_ID	mPTP	ABGD	mPTP	GMYC	Cons	Locality	State	Lat.	Long.
>JN970612	QCAZ28004		B_maculateralis	6	12	6	37	6	Zabalo	Ecuador	−0.318133	−75.76625
>JN970613	QCAZ28024		B_maculateralis	6	12	6	37	6	Zabalo	Ecuador	−0.318133	−75.76625
>JN970523	QCAZ18271		B_fasciata	7	20	7	35	7	La Pradera, Via Gualaquiza	Ecuador	−2.285	−78.094
>JN970524	QCAZ48584		B_fasciata	7	20	7	35	7	La Pradera, Via Gualaquiza	Ecuador	−2.285	−78.094
>JN970525	QCAZ48585		B_fasciata	7	20	7	35	7	La Pradera, Via Gualaquiza	Ecuador	−2.285	−78.094
>JN970526	QCAZ48593		B_fasciata	7	20	7	35	7	La Pradera, Via Gualaquiza	Ecuador	−2.285	−78.094
>JN970531	QCAZ26497		B_fasciata	7	20	7	35	7	Limon-Macas road, km 8	Ecuador	−2.8858	−78.39708
>JN970534	QCAZ17016		B_fasciata	7	20	7	35	7	Tiink	Ecuador	−3.333	−78.451806
>JN970535	QCAZ17030		B_fasciata	7	20	7	35	7	Tiink	Ecuador	−3.333	−78.451806
>JN970619	QCAZ41488		B_fasciata	7	20	7	35	7	Las Orquidias	Ecuador	−4.22903	−78.65775
>JN970620	QCAZ41575		B_fasciata	7	20	7	35	7	Miazi Alto	Ecuador	−4.25044	−78.61356
>JN970621	QCAZ41576		B_fasciata	7	20	7	35	7	Miazi Alto	Ecuador	−4.25044	−78.61356
>JN970622	QCAZ24866		B_fasciata	7	20	7	35	7	Romerillos Alto	Ecuador	−4.22725	−78.93875
>JN970623	QCAZ31037		B_fasciata	7	20	7	35	7	Centro Shuar Yawi	Ecuador	−4.4301	−78.631608
>JN970624	QCAZ23147		B_fasciata	7	20	7	35	7	Zamora	Ecuador	−4.06695	−78.950817
>JN970625	QCAZ23148		B_fasciata	7	20	7	35	7	Zamora	Ecuador	−4.06695	−78.950817
>JN970626	QCAZ48583		B_fasciata	7	20	7	35	7	Zamora	Ecuador	−4.06695	−78.950817
>JN970520	QCAZ32638		B_almendarizae	8	21	8	33	8	Guamote-Macas road	Ecuador	−2.21635	−78.28986
>JN970521	QCAZ32639		B_almendarizae	8	21	8	33	8	Guamote-Macas road	Ecuador	−2.21635	−78.28986
>JN970522	QCAZ32645		B_almendarizae	8	21	8	33	8	Guamote-Macas road	Ecuador	−2.21635	−78.28986
>JN970527	QCAZ25958		B_almendarizae	8	21	8	33	8	Limon via Gualaceo	Ecuador	−2.9796	−78.44147
>JN970528	QCAZ26300		B_almendarizae	8	21	8	33	8	Limon	Ecuador	−2.9046	−78.386931
>JN970529	QCAZ39647		B_almendarizae	8	21	8	33	8	Limon via Gualaceo	Ecuador	−2.9796	−78.44147
>JN970530	QCAZ39650		B_almendarizae	8	21	8	33	8	Limon via Gualaceo	Ecuador	−2.9796	−78.44147
>JN970532	QCAZ23810		B_almendarizae	8	21	8	33	8	Mendez, River N of	Ecuador	−2.7291	−78.2849
>JN970533	QCAZ26438		B_almendarizae	8	21	8	33	8	San Juan Bosco	Ecuador	−2.02	−77.92
>JN970538	QCAZ17944		B_almendarizae	8	9	8	34	8	Rio Hollin	Ecuador	−0.69547	−77.72958
>JN970614	QCAZ24392		B_almendarizae	8	9	8	34	8	Rio Lagarto	Ecuador	−0.678184	−76.396556
>JN970615	QCAZ24394		B_almendarizae	8	9	8	34	8	Rio Lagarto	Ecuador	−0.678184	−76.396556
>JN970616	QCAZ31449		B_almendarizae	8	9	8	34	8	Rio Pastaza	Ecuador	−1.41283	−78.26878
>JN970617	QCAZ31450		B_almendarizae	8	9	8	34	8	Rio Pastaza	Ecuador	−1.41283	−78.26878
>JN970618	QCAZ31452		B_almendarizae	8	9	8	34	8	Rio Pastaza	Ecuador	−1.41283	−78.26878
>AY326056	KU202911		B_calcarata	9	10	9	29	9	Misahualli	Ecuador	−1.033333	−77.670278
>JN970536	QCAZ40085		B_calcarata	9	10	9	29	9	8 km S of Tena	Ecuador	−1.0449	−77.76951
>JN970537	QCAZ40084		B_calcarata	9	10	9	29	9	8 km S of Tena	Ecuador	−1.0449	−77.76951
>JN970542	QCAZ43935		B_calcarata	9	10	9	29	9	anangu	Ecuador	−0.52492	−76.38445
>JN970547	QCAZ43713		B_calcarata	9	10	9	29	9	Coca	Ecuador	−0.47782	−76.98982
>JN970548	QCAZ43789		B_calcarata	9	10	9	29	9	9 km S of Coca	Ecuador	−0.49986	−77.00828
>JN970550	QCAZ44422		B_calcarata	9	10	9	29	9	Chiroisla	Ecuador	−0.57564999	−75.8998299
>JN970553	QCAZ44177		B_calcarata	9	10	9	29	9	Eden	Ecuador	−0.49833	−76.07112
>JN970558	QCAZ44247		B_calcarata	9	10	9	29	9	Eden	Ecuador	−0.49833	−76.07112
>JN970567	QCAZ43824		B_calcarata	9	10	9	29	9	La Primavera, south bank	Ecuador	−0.44427	−76.78685
>JN970575	QCAZ44530		B_calcarata	9	10	9	29	9	San Vicente	Ecuador	−0.67901	−75.65112
>JN970578	QCAZ16798		B_calcarata	9	10	9	29	9	Estacion Cientifica Yasuni	Ecuador	−0.68931	−76.42903
>JN970580	QCAZ43256		B_calcarata	9	10	9	29	9	Estacion Cientifica Yasuni	Ecuador	−0.68931	−76.42903
>JN970581	QCAZ43259		B_calcarata	9	10	9	29	9	Estacion Cientifica Yasuni	Ecuador	−0.68931	−76.42903
>JN970584	QCAZ20290		B_calcarata	9	10	9	29	9	Estacion Cientifica Yasuni	Ecuador	−0.678194	−76.3965555
>JN970585	QCAZ20305		B_calcarata	9	10	9	29	9	Estacion Cientifica Yasuni	Ecuador	−0.678194	−76.3965555
>JN970586	QCAZ17825		B_calcarata	9	10	9	29	9	Estacion Cientifica Yasuni	Ecuador	−0.678194	−76.3965555
>JN970587	QCAZ31446		B_calcarata	9	10	9	29	9	Estacion Cientifica Yasuni	Ecuador	−0.68931	−76.42903
>JN970588	QCAZ14956		B_calcarata	9	10	9	29	9	Canelos	Ecuador	−1.59	−77.75
>JN970589	QCAZ14958		B_calcarata	9	10	9	29	9	Canelos	Ecuador	−1.59	−77.75
>JN970590	QCAZ14957		B_calcarata	9	10	9	29	9	Canelos	Ecuador	−1.59	−77.75
>JN970591	QCAZ14965		B_calcarata	9	10	9	29	9	Canelos	Ecuador	−1.59	−77.75
>JN970597	QCAZ25434		B_calcarata	9	10	9	29	9	La Selva Lodge	Ecuador	−0.498167	−76.373833
>JN970606	QCAZ28181		B_calcarata	9	10	9	29	9	Cuyabeno	Ecuador	−0.0886	−76.1419
>JN970607	QCAZ28185		B_calcarata	9	10	9	29	9	Cuyabeno	Ecuador	−0.0886	−76.1419
>JN970608	QCAZ28197		B_calcarata	9	10	9	29	9	Cuyabeno	Ecuador	−0.0886	−76.1419
>JN970628		WED57649	B_calcarata	9	10	9	30	9	Cuzco Amazonico	Peru	−12.583	−69.083
>JN970630		WED58712	B_calcarata	9	10	9	30	9	Cuzco Amazonico	Peru	−12.583	−69.083
>JN970631		WED59271	B_calcarata	9	10	9	42	9	Cuzco Amazonico	Peru	−12.583	−69.083
>JN970633		CM131	B_calcarata	9	10	9	32	9	crique Margot	French_Guiana	5.443190	−53.972344
>JN970635		PG105	B_calcarata	9	10	9	32	9	Kaw, route	French_Guiana	4.516105	−52.10053
>JN970636		PG123	B_calcarata	9	10	9	32	9	Toponowini	French_Guiana	3.0521	−52.705
>JN970639		AG217	B_calcarata	9	10	9	32	9	Trinite , Crique Grand Leblond	French_Guiana	4.6709	−53.2843
>KDQF01000164		AF0605	B_calcarata	9	10	9	32	9	Trou Poisson, mare	French_Guiana	5.373475	−53.097575
>KDQF01000277		AF0848	B_calcarata	9	10	9	32	9	Chutes Voltaire, camp	French_Guiana	5.052639	−54.088444
>KDQF01000291		AF0867	B_calcarata	9	10	9	32	9	Chutes gregoire	French_Guiana	5.097472	−53.050667
>KDQF01000338		AF0941	B_calcarata	9	10	9	32	9	Matoury , Lac des Americains	French_Guiana	4.852891	−52.352092
>KDQF01000408		AF1106	B_calcarata	9	10	9	32	9	Mana, Ilet Lezard rive G	French_Guiana	5.054481	−53.8007
>KDQF01000537		AF1441	B_calcarata	9	10	9	32	9	Belizon, Mare	French_Guiana	4.368663	−52.322931
>KDQF01000583		AF1543	B_calcarata	9	10	9	32	9	Saul, roche bateau	French_Guiana	3.60654	−53.17625
>KDQF01000587		AF1549	B_calcarata	9	10	9	32	9	Matoury	French_Guiana	4.85708	−52.339175
>KDQF01000646		AF1726	B_calcarata	9	10	9	32	9	Chutes Voltaire	French_Guiana	5.03255	−54.08689
>KDQF01000760		AF1952	B_calcarata	9	10	9	31	9	Sipaliwini	Suriname	2.02439	−56.12508
>KDQF01000908		AF2341	B_calcarata	9	10	9	32	9	Ekini	French_Guiana	4.05	−52.4667
>KDQF01000986		AF2562	B_calcarata	9	10	9	32	9	RN2 PK65 mare	French_Guiana	4.487368	−52.347811
>KDQF01001120		AF2849	B_calcarata	9	10	9	31	9	Mitaraka, layon B	French_Guiana	2.23577	−54.44928
>KDQF01001145		AF2931	B_calcarata	9	10	9	32	9	Memora G	French_Guiana	3.31774	−52.19329
>KDQF01001158		AF2954	B_calcarata	9	10	9	32	9	Memora G	French_Guiana	3.31774	−52.19329
>KDQF01001159		AF2955	B_calcarata	9	10	9	32	9	Memora G	French_Guiana	3.31774	−52.19329
>KDQF01001184		AF3000	B_calcarata	9	10	9	32	9	Memora D	AP	3.31294	−52.18036
>KDQF01001185		AF3001	B_calcarata	9	10	9	32	9	Memora D	AP	3.31294	−52.18036
>KDQF01001193		AF3022	B_calcarata	9	10	9	32	9	Memora D	AP	3.31294	−52.18036
>KDQF01001194		AF3023	B_calcarata	9	10	9	32	9	Memora D	AP	3.31294	−52.18036
>KDQF01001212		AF3060	B_calcarata	9	10	9	32	9	Mitan G	French_Guiana	2.6284	−52.55404
>KDQF01001213		AF3061	B_calcarata	9	10	9	32	9	Mitan G	French_Guiana	2.6284	−52.55404

(*continued*)

Continued.

GenBank accession	Voucher	Field Number	Species_ID	mPTP	ABGD	mPTP	GMYC	Cons	Locality	State	Lat.	Long.
>KDQF01001214		AF3062	B_calcarata	9	10	9	32	9	Mitan G	French_Guiana	2.6284	−52.55404
>KDQF01001220		AF3069	B_calcarata	9	10	9	32	9	Mitan G	French_Guiana	2.6284	−52.55404
>KDQF01001277		AF3162	B_calcarata	9	10	9	32	9	Mitan D	AP	2.62764	−52.54195
>KDQF01001278		AF3164	B_calcarata	9	10	9	32	9	Mitan D	AP	2.62764	−52.54195
>KDQF01001279		AF3165	B_calcarata	9	10	9	32	9	Mitan D	AP	2.62764	−52.54195
>KDQF01001283		AF3170	B_calcarata	9	10	9	32	9	Mitan D	AP	2.62764	−52.54195
>KDQF01001323		AF3248	B_calcarata	9	10	9	32	9	Trois paletuviers	French_Guiana	4.054582	−51.677007
>KDQF01001331		AF3257	B_calcarata	9	10	9	32	9	Trois paletuviers	French_Guiana	4.054582	−51.677007
>KDQF01001341		AF3270	B_calcarata	9	10	9	32	9	Taparabo	AP	4.016066	−51.693802
>KDQF01001342		AF3271	B_calcarata	9	10	9	32	9	Taparabo	AP	4.016066	−51.693802
>KDQF01001343		AF3272	B_calcarata	9	10	9	32	9	Taparabo	AP	4.016066	−51.693802
>KDQF01001344		AF3273	B_calcarata	9	10	9	32	9	Taparabo	AP	4.016066	−51.693802
>KDQF01001345		AF3274	B_calcarata	9	10	9	32	9	Taparabo	AP	4.016066	−51.693802
>KDQF01001353		AF3287	B_calcarata	9	10	9	32	9	Trois paletuviers	French_Guiana	4.054582	−51.677007
>KDQF01001354		AF3288	B_calcarata	9	10	9	32	9	Trois paletuviers	French_Guiana	4.054582	−51.677007
>KDQF01001355		AF3289	B_calcarata	9	10	9	32	9	Trois paletuviers	French_Guiana	4.054582	−51.677007
>KDQF01001384		AF3357	B_calcarata	9	10	9	32	9	Bakhuis, Creek 10k	Suriname	4.65616	−56.78649
>KDQF01001425		AF3454	B_calcarata	9	10	9	32	9	Spari Creek	Suriname	5.23285	−55.80462
>KDQF01001842		BM335	B_calcarata	9	10	9	41	9	UHE Belo Monte	PA	−2.950584	−51.936607
>KDQF01001921		BPN0802	B_calcarata	9	10	9	31	9	Kayser	Suriname	3.048297	−56.578653
>KDQF01002023		BPN2893	B_calcarata	9	10	9	32	9	RAP Basecamp	Suriname	2.46554	−55.62955
>KDQF01002048		BPN3456	B_calcarata	9	10	9	31	9	Mapari	Guyana	3.348083	−59.275833
>KDQF01002149		CAAM38	B_calcarata	9	10	9	32	9	Montagne cacao	French_Guiana	2.349128	−53.215985
>KDQF01002510		FL45	B_calcarata	9	10	9	32	9	Plote PPBIO, Porto Grande	AP	0.979331	−51.614895
>KDQF01002600		H2487	B_calcarata	9	10	9	30	9	UHE Jirau	RO	−9.59492	−65.0650814
>KDQF01002916	MPEG30468		B_calcarata	9	10	9	31	9	Paru, FLOTA	PA	−0.9439694	−53.2363000
>KDQF01003034	MTD47753		B_calcarata	9	10	9	32	9	Kabo forestry consession	Suriname	5.378132	−55.621491
>KDQF01003057	MTD47926		B_calcarata	9	10	9	32	9	Iwokrama	Guyana	4.6713889	−58.685
>KDQF01003166		MTR10021	B_calcarata	9	10	9	44	9	Lago Cipotuba	AM	−5.8013889	−60.2211111
>KDQF01003568		MTR24073	B_calcarata	9	10	9	32	9	Oiapoque	AP	3.8355278	−51.8333333
>KDQF01003575		MTR24122	B_calcarata	9	10	9	32	9	Oiapoque	AP	3.8794167	−51.7709722
>KDQF01003750		MTR968364	B_calcarata	9	10	9	43	9	Apiacas	MT	−9.650846	−57.393665
>KDQF01003993		PK1504	B_calcarata	9	10	9	32	9	Kaieteur NP	Guyana	5.14976	−59.483128
>KDQF01004113		QM442	B_calcarata	9	10	9	32	9	Montagne de fer	French_Guiana	5.4074	−53.5548
>KDQF01004357		TJC1246	B_calcarata	9	10	9	32	9	Black Water Creek	Guyana	5.07311	−59.24635
>KR811158		MTR24072	B_calcarata	9	10	9	32	9	Oiapoque	AP	3.8355278	−51.8333333
>KR811159		DAN012	B_calcarata	9	10	9	32	9	St Georges, RN 2 PK168	French_Guiana	4.00126	−51.931057
>KU221856		??	B_calcarata	9	10	9	29	9	San Jacinto	Peru	−4.674982	−73.958995
>MF583738		LEO711	B_calcarata	9	10	9	29	9	Putumayo, Valle del Guamuez		0.4161	−76.8752
>**MW370322**		AF3769	B_calcarata	9	10	9	32	9	Voltzberg	Suriname	4.68169	−56.18568
>**MW370325**		FTA182	B_calcarata	9	10	9	32	9	Rio Amapá Grande	AP	2.127111	−51.191333
>**MW370328**		JMP1569	B_calcarata	9	10	9	29	9	Confluencia Supai_y_Sabalo	Peru	−3.065	−72.168
>AF467270		CM???	B_dentei	10	14	10	14	10	Kaw	French_Guiana	4.516105	−52.10053
>KDQF01000097		AF0233	B_dentei	10	14	10	14	10	Montagne des singes	French_Guiana	5.066667	−52.716667
>KDQF01000135		AF0540	B_dentei	10	14	10	14	10	Savane virginie, layon	French_Guiana	4.1959	−52.149
>KDQF01000227		AF0727	B_dentei	10	14	10	14	10	Paracou	French_Guiana	5.2754	−52.9236
>KDQF01000319		AF0913	B_dentei	10	14	10	14	10	Pic Coudreau du Sud	French_Guiana	2.2534	−54.3534
>KDQF01000377		AF1029	B_dentei	10	14	10	14	10	Saul, Galbao	French_Guiana	3.61125	−53.288548
>KDQF01000450		AF1212	B_dentei	10	14	10	14	10	Trinite	French_Guiana	4.6025	−53.4143
>KDQF01000495		AF1330	B_dentei	10	14	10	14	10	Saut Grand Machicou	French_Guiana	3.897416	−52.583565
>KDQF01000501		AF1337	B_dentei	10	14	10	14	10	Machicou	French_Guiana	3.890031	−52.573535
>KDQF01000578		AF1529	B_dentei	10	14	10	14	10	Savane Virginie	French_Guiana	4.1959	−52.149
>KDQF01000637		AF1695	B_dentei	10	14	10	14	10	Saul, Limonade	French_Guiana	3.56311	−53.19083
>KDQF01000846		AF2107	B_dentei	10	14	10	14	10	RN2 corridor 5	French_Guiana	4.03265	−51.99093
>KDQF01001036		AF2645	B_dentei	10	14	10	14	10	Atachi Bakka	French_Guiana	3.57236	−53.96731
>KDQF01001065		AF2697	B_dentei	10	14	10	14	10	Alikene, camp polissoir	French_Guiana	3.21792	−52.39747
>KDQF01001109		AF2797	B_dentei	10	14	10	14	10	Mitaraka, layon C	French_Guiana	2.23577	−54.44928
>KDQF01001202		AF3041	B_dentei	10	14	10	14	10	Memora G	French_Guiana	3.31774	−52.19329
>KDQF01001218		AF3066	B_dentei	10	14	10	14	10	Mitan G	French_Guiana	2.6284	−52.55404
>KDQF01001264		AF3146	B_dentei	10	14	10	14	10	Mitan D	AP	2.62764	−52.54195
>KDQF01001289		AF3180	B_dentei	10	14	10	14	10	Mitan D	AP	2.62764	−52.54195
>KDQF01001763		AP024	B_dentei	10	14	10	14	10	Plote PPBIO, Porto Grande	AP	0.979331	−51.614895
>KDQF01002148		CAAM37	B_dentei	10	14	10	14	10	Montagne cacao	French_Guiana	2.349128	−53.215985
>KDQF01002205		CM013	B_dentei	10	14	10	14	10	Kaw2	French_Guiana	4.516105	−52.10053
>KDQF01002219		CM090	B_dentei	10	14	10	14	10	Tibourou	French_Guiana	4.416667	−52.3
>KDQF01002394		DAN015	B_dentei	10	14	10	14	10	St Georges, RN 2 PK168	French_Guiana	4.00126	−51.931057
>KDQF01002403		DAN037	B_dentei	10	14	10	14	10	St Georges, piste Saut Maripa	French_Guiana	3.862884	−51.863422
>KDQF01002418		DSM064	B_dentei	10	14	10	14	10	Savane Virginie	French_Guiana	4.199878	−52.136443
>KDQF01002513		FL90	B_dentei	10	14	10	14	10	Plote PPBIO, Porto Grande	AP	0.979331	−51.614895
>KDQF01002531		FTA170	B_dentei	10	14	10	14	10	Rio Amapa Grande	AP	2.127111	−51.191333
>KDQF01003258		MTR13753	B_dentei	10	14	10	14	10	Serra do Navio	AP	0.9180556	−52.0027778
>KDQF01003277		MTR13850	B_dentei	10	14	10	14	10	Lourenco	AP	2.3236111	−51.6452778
>KDQF01003811		PG032	B_dentei	10	14	10	14	10	Kaw2	French_Guiana	4.516105	−52.10053
>KDQF01003812		PG035	B_dentei	10	14	10	14	10	Matecho	French_Guiana	3.75	−53.033333
>KDQF01003843		PG234	B_dentei	10	14	10	14	10	Haute Wanapi	French_Guiana	2.5134	−53.8211
>**MW370338**		AG428	B_dentei	10	14	10	14	10	Atachi Bakka	French_Guiana	3.6553	−53.844
>**MW370343**		AG509	B_dentei	10	14	10	14	10	Saul, Monts Belvedere	French_Guiana	3.719347	−53.412809
>**MW370344**		AG095/BM029	B_dentei	10	14	10	14	10	Kaw2, CD6/PK 47	French_Guiana	4.571	−52.2206
>**MW370346**		AG216	B_dentei	10	14	10	14	10	Trinite, Crique Grand Leblond	French_Guiana	4.6709	−53.2843
>**MW370320**		AF2984	B_dentei	10	14	10	14	10	Mémora D	AP	3.28215	−52.20263
>**MW370321**		AF3628	B_dentei	10	14	10	14	10	Itoupe_400	French_Guiana	3.02208	−53.11046
>**MW370323**		AM009	B_dentei	10	14	10	14	10	Inini_Tolenga	French_Guiana	3.663159	−53.928308
>**MW370324**		BOAM034	B_dentei	10	14	10	14	10	Borne 4	French_Guiana	2.3709	−53.7728
>**MW370326**		FTA91	B_dentei	10	14	10	14	10	Rio Vila Nova	AP	0.449335	−52.022137
>JN970539	QCAZ40080		B_tetete	13	16	13	17	13	Comunidad Santa Rosa	Ecuador	−1.02137	−77.47819
>JN970540	QCAZ40081		B_tetete	13	16	13	17	13	Comunidad Santa Rosa	Ecuador	−1.02137	−77.47819
>JN970627		WED60015	B_tetete	13	17	13	18	13	San Jacinto	Ecuador	−2.3125	−75.8628
>KU221865		???	B_tetete	13	17	13	18	13	San Jacinto	Peru	−4.674982	−73.958995

(*continued*)

Continued.

GenBank accession	Voucher	Field Number	Species_ID	mPTP	ABGD	mPTP	GMYC	Cons	Locality	State	Lat.	Long.
>JN970543	QCAZ43977		B_alfaroi	14	2	14	19	14	anangu	Ecuador	−0.52492	−76.38445
>JN970544	QCAZ43682		B_alfaroi	14	2	14	19	14	Coca	Ecuador	−0.47782	−76.98982
>JN970549	QCAZ44351		B_alfaroi	14	2	14	19	14	Chiroisla	Ecuador	−0.57997	−75.91769
>JN970551	QCAZ44425		B_alfaroi	14	2	14	19	14	Chiroisla	Ecuador	−0.57564999	−75.8998299
>JN970554	QCAZ44180		B_alfaroi	14	2	14	19	14	Eden	Ecuador	−0.49833	−76.07112
>JN970557	QCAZ44191		B_alfaroi	14	2	14	19	14	Eden	Ecuador	−0.49833	−76.07112
>JN970560	QCAZ44634		B_alfaroi	14	2	14	19	14	Huiririma	Ecuador	−0.71163	−75.62395
>JN970561	QCAZ44635		B_alfaroi	14	2	14	19	14	Huiririma	Ecuador	−0.71163	−75.62395
>JN970565	QCAZ44788		B_alfaroi	14	2	14	19	14	Nuevo Roacafuerte	Ecuador	−0.91927	−75.40103
>JN970566	QCAZ44790		B_alfaroi	14	2	14	19	14	Nuevo Roacafuerte	Ecuador	−0.91927	−75.40103
>JN970569	QCAZ43826		B_alfaroi	14	2	14	19	14	La Primavera, south bank	Ecuador	−0.44427	−76.78685
>JN970571	QCAZ43894		B_alfaroi	14	2	14	19	14	La Primavera, north bank	Ecuador	−0.431	−76.78648
>JN970573	QCAZ44527		B_alfaroi	14	2	14	19	14	San Vicente	Ecuador	−0.67901	−75.65112
>JN970574	QCAZ44528		B_alfaroi	14	2	14	19	14	San Vicente	Ecuador	−0.67901	−75.65112
>JN970579	QCAZ19328		B_alfaroi	14	2	14	19	14	Estacion Cientifica Yasuni	Ecuador	−0.68931	−76.42903
>JN970582	QCAZ43262		B_alfaroi	14	2	14	19	14	Estacion Cientifica Yasuni	Ecuador	−0.68931	−76.42903
>JN970583	QCAZ43263		B_alfaroi	14	2	14	19	14	Estacion Cientifica Yasuni	Ecuador	−0.68931	−76.42903
>JN970592	QCAZ28272		B_alfaroi	14	2	14	19	14	Cuyabeno beach	Ecuador	−0.265433	−75.891733
>JN970593	QCAZ28278		B_alfaroi	14	2	14	19	14	Cuyabeno beach	Ecuador	−0.265433	−75.891733
>JN970594	QCAZ28398		B_alfaroi	14	2	14	19	14	Cuyabeno beach	Ecuador	−0.241517	−75.930533
>JN970596	QCAZ25410		B_alfaroi	14	2	14	19	14	La Selva Lodge	Ecuador	−0.498167	−76.373833
>JN970600	QCAZ44025		B_alfaroi	14	2	14	19	14	La Selva Lodge, entrance	Ecuador	−0.50868	−76.36493
>JN970601	QCAZ44027		B_alfaroi	14	2	14	19	14	La Selva Lodge, entrance	Ecuador	−0.50868	−76.36493
>JN970602	QCAZ44851		B_alfaroi	14	2	14	19	14	Panacocha, 2.5 km S of	Ecuador	−0.4712	−76.6667
>JN970603	QCAZ44853		B_alfaroi	14	2	14	19	14	Panacocha, 2.5 km S of	Ecuador	−0.4712	−76.6667
>JN970604	QCAZ44856		B_alfaroi	14	2	14	19	14	Panacocha, 2.5 km S of	Ecuador	−0.4712	−76.6667
>JN970605	QCAZ44858		B_alfaroi	14	2	14	19	14	Panacocha, 2.5 km S of	Ecuador	−0.4712	−76.6667
>JN970609	QCAZ28240		B_alfaroi	14	2	14	19	14	Cuyabeno	Ecuador	−0.0886	−76.1419
>JN970610	QCAZ28315		B_alfaroi	14	2	14	19	14	Cuyabeno	Ecuador	−0.0886	−76.1419
>KF955305	QCAZ50785		B_alfaroi	14	2	14	19	14	Panacocha	Ecuador	−0.4712	−76.6667
>MF583737		LEO720	B_alfaroi	14	2	14	19	14	Putumayo, Valle del Guamuez	Colombia	0.4161	−76.8752
>JN970634		CM168	B_aff. courtoisae	15	4	15	16	15	Guatemala	French_Guiana	5.15	−52.633333
>JN970637		CM118	B_aff. courtoisae	15	4	15	16	15	Cayenne, Rorota	French_Guiana	4.884444	−52.258611
>KDQF01000183		AF0641	B_aff. courtoisae	15	4	15	16	15	Cayenne, Rorota	French_Guiana	4.879124	−52.257589
>KDQF01000335		AF0937	B_aff. courtoisae	15	4	15	16	15	Cayenne, Vidal	French_Guiana	4.884433	−52.288819
>KDQF01000337		AF0940	B_aff. courtoisae	15	4	15	16	15	Matoury, Lac des Americains	French_Guiana	4.852891	−52.352092
>KDQF01002239		CM149	B_aff. courtoisae	15	4	15	16	15	Guatemala	French_Guiana	5.15	−52.633333
>KDQF01002246		CM174	B_aff. courtoisae	15	4	15	16	15	Guatemala	French_Guiana	5.15	−52.633333
>KDQF01002266		CM262	B_aff. courtoisae	15	4	15	16	15	Guatemala	French_Guiana	5.15	−52.633333
>KDQF01002267		CM263	B_aff. courtoisae	15	4	15	16	15	Guatemala	French_Guiana	5.15	−52.633333
>KDQF01002271		CM273	B_aff. courtoisae	15	4	15	16	15	Guatemala	French_Guiana	5.15	−52.633333
>KDQF01002424		DSM100	B_aff. courtoisae	15	4	15	16	15	Monsinery	French_Guiana	4.80338	−52.47466
>KDQF01004062		QM051	B_aff. courtoisae	15	4	15	16	15	Matiti	French_Guiana	5.035425	−52.565573
>KDQF01004066		QM076	B_aff. courtoisae	15	4	15	16	15	Tonnegrande grenouillere	French_Guiana	4.837603	−52.444249
>AY549335	AMNHA164081	AMNHA164081	B_courtoisae	16	18	16	15	16	Iwokrama, Cowfly camp	Guyana	4.6713889	−58.685
>EU201108		CM229	B_courtoisae	16	18	16	15	16	Saul	French_Guiana	3.625556	−53.207222
>JN970638		AG213	B_courtoisae	16	18	16	15	16	Trinite	French_Guiana	4.6709	−53.2843
>JN970640		AG221	B_courtoisae	16	18	16	15	16	Trinite	French_Guiana	4.6709	−53.2843
>JN970641		AF0097	B_courtoisae	16	18	16	15	16	Road to Apura	Suriname	5.183333	−55.616667
>KDQF01000489	MNHN-RA-2020.0004	AF1322	B_courtoisae	16	18	16	15	16	Saut Taconet	French_Guiana	4.03249	−52.526188
>KDQF01000494	MNHN-RA-2020.0005	AF1328	B_courtoisae	16	18	16	15	16	Saut Grand Machicou	French_Guiana	3.897416	−52.583565
>KDQF01000584	MNHN-RA-2020.0007	AF1546	B_courtoisae	16	18	16	15	16	Saul, gros arbre	French_Guiana	3.615576	−53.227093
>KDQF01000636		AF1694	B_courtoisae	16	18	16	15	16	Saul, Limonade	French_Guiana	3.56311	−53.19083
>KDQF01000753		AF1934	B_courtoisae	16	18	16	15	16	Flat de la Waki	French_Guiana	3.0895	−53.39846
>KDQF01000829		AF2090	B_courtoisae	16	18	16	15	16	Sipaliwini	Suriname	2.09753	−56.1472
>KDQF01000830		AF2091	B_courtoisae	16	18	16	15	16	Sipaliwini	Suriname	2.09753	−56.1472
>KDQF01000847	MNHN-RA-2020.0009	AF2114	B_courtoisae	16	18	16	15	16	Sipaliwini	Suriname	2.09753	−56.1472
>KDQF01000898		AF2319	B_courtoisae	16	18	16	15	16	Trinite	French_Guiana	4.6025	−53.4143
>KDQF01000909	MNHN-RA-2020.0013	AF2342	B_courtoisae	16	18	16	15	16	Ekini	French_Guiana	4.05	−52.4667
>KDQF01001002		AF2584	B_courtoisae	16	18	16	15	16	Sinnamary	French_Guiana	5.372835	−52.960608
>KDQF01001038	MNHN-RA-2020.0002	AF2654	B_courtoisae	16	18	16	15	16	Alikene, camp 1	French_Guiana	3.20906	−52.402
>KDQF01001059	MNHN-RA-2020.0001	AF2686	B_courtoisae	16	18	16	15	16	Alikene, camp 1	French_Guiana	3.20906	−52.402
>KDQF01001118	MNHN-RA-2020.0014	AF2839	B_courtoisae	16	18	16	15	16	Mitaraka, layon B	French_Guiana	2.23577	−54.44928
>KDQF01001211		AF3059	B_courtoisae	16	18	16	15	16	Mitan G	French_Guiana	2.6284	−52.55404
>KDQF01001424		AF3452	B_courtoisae	16	18	16	15	16	Spari Creek	Suriname	5.23285	−55.80462
>KDQF01001456		AF3695	B_courtoisae	16	18	16	15	16	Itoupe	French_Guiana	3.01498	−53.13286
>KDQF01001686	MNHN-RA-2020.0003	AM007	B_courtoisae	16	18	16	15	16	Inini Tolenga	French_Guiana	3.663159	−53.928308
>KDQF01001687		AM008	B_courtoisae	16	18	16	15	16	Inini Tolenga	French_Guiana	3.663159	−53.928308
>KDQF01001733		AMS394	B_courtoisae	16	18	16	15	16	Ants Creek	Guyana	3.305817	−59.324067
>KDQF01001735		AMS420	B_courtoisae	16	18	16	15	16	Land Turtle Landing Swamp	Guyana	3.180717	−59.421967
>KDQF01001918		BPN0794	B_courtoisae	16	18	16	15	16	Ralleighvallen	Suriname	4.7166667	−56.2166667
>KDQF01002020		BPN2861	B_courtoisae	16	18	16	15	16	RAP Basecamp 1,	Suriname	2.477	−55.62941
>KDQF01002044		BPN3448	B_courtoisae	16	18	16	15	16	Mapari	Guyana	3.348083	−59.275833
>KDQF01002140		CAAM28	B_courtoisae	16	18	16	15	16	Montagne cacao	French_Guiana	2.349128	−53.215985
>KDQF01002908	MPEG30336		B_courtoisae	16	18	16	15	16	REBIO Maicuru	PA	0.8286194	−53.9312000
>KDQF01002909	MPEG30341		B_courtoisae	16	18	16	15	16	REBIO Maicuru	PA	0.8286194	−53.9312000
>KDQF01002910	MPEG30342		B_courtoisae	16	18	16	15	16	REBIO Maicuru	PA	0.8286194	−53.9312000
>KDQF01003773	NZCS45		B_courtoisae	16	18	16	15	16	rosebel	Suriname	5.124392	−55.249254
>KDQF01004011		PK3520	B_courtoisae	16	18	16	15	16	Turtle Camp, Iwokrama	Guyana	4.6718	−58.6847
>**MW370337**		AG422	B_courtoisae	16	18	16	15	16	Atachi Bakka	French_Guiana	3.6553	−53.844
>**MW370339**		AG444	B_courtoisae	16	18	16	15	16	Alikene	French_Guiana	3.220044	−52.37855
>**MW370340**		AG446	B_courtoisae	16	18	16	15	16	Alikene	French_Guiana	3.220044	−52.37855
>**MW370342**		AG485	B_courtoisae	16	18	16	15	16	Saul, Monts Belvedere	French_Guiana	3.719347	−53.412809
>**MW370345**		AG072	B_courtoisae	16	18	16	15	16	Trinite, Crique Grand Leblond	French_Guiana	4.6709	−53.2843
>**MW370333**		AF3775	B_courtoisae	16	18	16	15	16	Voltzberg_CI camp	Suriname	4.68169	−56.18568
>**MW370334**		AF3791	B_courtoisae	16	18	16	15	16	Voltzberg_CI camp	Suriname	4.68169	−56.18568
>KDQF01002632		HJ071	B_eucharis	17	1	17	40	17	UHE Jirau	RO	−8.748483	−63.903465

(*continued*)

Continued.

GenBank accession	Voucher	Field Number	Species_ID	mPTP	ABGD	mPTP	GMYC	Cons	Locality	State	Lat.	Long.
>KDQF01002656		HJ443	B_eucharis	17	1	17	28	17	UHE Jirau	RO	−9.69941	−65.358875
>KDQF01002657		HJ447	B_eucharis	17	1	17	28	17	UHE Jirau	RO	−9.69941	−65.358875
>KDQF01003636		MTR25798	B_eucharis	17	1	17	27	17	Pacaas Novos, PARNA	RO	−10.7869789	−63.6273050
>KDQF01003752		MTR968510	B_eucharis	17	1	17	27	17	Apiacas	MT	−9.650846	−57.393665
>KDQF01003759		MTR977049	B_eucharis	17	1	17	27	17	Juruena	MT	−10.3236111	−58.4927778
>**MW370327**		H2472	B_eucharis	17	1	17	28	17	UHE Jirau	RO	−9.60283365	−65.0583638
>**MW370329**	MZUSP 159228	MTR25896	B_eucharis	17	1	17	27	17	Pacaás Novos_PARNA	RO	−10.7815800	−63.6267350
>AY843632	AMNHA168405		B_heilprini	18	15	18	47	25	pet_trade	NA		
>JN970629		WED57865	B_aff.steinbachi(2)	12	3	19	26	18	Cuzco Amazonico	Peru	−12.583	−69.083
>JN970632		WED59350	B_aff.steinbachi(2)	12	3	19	26	18	Cuzco Amazonico	Peru	−12.583	−69.083
>KU205472		WED55554	B_aff.steinbachi(2)	12	3	19	26	18	Puerto Maldonado	Peru	−12.618187	−69.167000
>**MW370330**	AAGUFU5917		B_aff.steinbachi(2)	12	3	19	26	18	Assis	AC	−10.933098	−69.594418
>**MW370331**	AAGUFU5918		B_aff.steinbachi(2)	12	3	19	26	18	Assis	AC	−10.933098	−69.594418
>**MW370350**		SCF395	B_aff.steinbachi(2)	12	3	19	26	18	Cocama	Peru	−10.399	−71.165
>KDQF01003399		MTR18819	B_aff.steinbachi(1)	11	3	11	22	11	Lago Chaviana	AM	−4.18314	−61.48801
>KDQF01003402		MTR18844	B_aff.steinbachi(1)	11	3	11	22	11	Lago Chaviana	AM	−4.18314	−61.48801
>KDQF01003646		MTR28018	B_aff.steinbachi(1)	11	3	11	21	11	Serra do Divisor	AC	−7.43707300	−73.6571960
>KDQF01003722		MTR33822	B_aff.steinbachi(1)	11	3	11	23	11	Japura, Trilha da Anta	AM	−1.77207062	−66.3725554
>**MW370297**	CORBIDI11192		B_aff.steinbachi(1)	11	3	11	20	11	Saniri Malvinas	Peru	−11.846765	−72.94
>**MW370298**	CORBIDI12128		B_aff.steinbachi(1)	11	3	11	20	11	Rio Tapiche	Peru	−7.448717	−73.940944
>**MW370299**	CORBIDI13035		B_aff.steinbachi(1)	11	3	11	21	11	Coronel Pontillo	Peru	−8.662599	−74.059897
>**MW370307**	CORBIDI8542		B_aff.steinbachi(1)	11	3	11	20	11	Poyentimari	Peru	−12.3175	−72.8922
>**MW370308**	CORBIDI8698		B_aff.steinbachi(1)	11	3	11	39	11	Datem del Maranon	Peru	−4.171196	−76.932370
>**MW370309**	CORBIDI8974		B_aff.steinbachi(1)	11	3	11	20	11	Rio Corrientes	Peru	−2.735647	−76.031778
>**MW370310**	CORBIDI8975		B_aff.steinbachi(1)	11	3	11	20	11	Rio Corrientes	Peru	−2.735647	−76.031778
>**MW370313**		MTR35970	B_aff.steinbachi(1)	11	3	11	23	11	Comunidade Cachoeirinha	AM	−2.87148	−68.34707
>**MW370315**		MTR36143	B_aff.steinbachi(1)	11	3	11	23	11	Açaí, Rio Içá	AM	−2.90452	−68.33869
>**MW370319**		MTR36968	B_aff.steinbachi(1)	11	3	11	22	11	Coari	AM	−4.08864	−63.09844
>JF790135		MJ1300	B_steinbachi	12	3	12	24	12	Sara, Buenavista	Bolivia	−17.481683	−63.684867
>JF790136		MJ1301	B_steinbachi	12	3	12	24	12	Sara, Buenavista	Bolivia	−17.481683	−63.684867
>JF790137		MJ1302	B_steinbachi	12	3	12	24	12	Sara, Buenavista	Bolivia	−17.481683	−63.684867
>JF790138		MJ1310	B_steinbachi	12	3	12	24	12	Sara, Buenavista	Bolivia	−17.481683	−63.684867
>KDQF01001813		BM048	B_steinbachi	12	3	12	25	12	UHE Belo Monte	PA	−2.950584	−51.936607
>KDQF01001848		BM355	B_steinbachi	12	3	12	25	12	UHE Belo Monte	PA	−2.950584	−51.936607
>KDQF01002994	MPEG36753	MPEG36753	B_steinbachi	12	3	12	25	12	Canaa dos Carajas	PA	−6.075562	−50.243245
>**MW370300**	CORBIDI13415	CORBIDI13415	B_steinbachi	12	3	12	24	12	Tambopata	Peru	−11.962370	−70.213704
>**MW370301**	CORBIDI13417	CORBIDI13417	B_steinbachi	12	3	12	24	12	Tambopata	Peru	−11.962370	−70.213704
>**MW370302**	CORBIDI13453	CORBIDI13453	B_steinbachi	12	3	12	24	12	Tambopata	Peru	−11.962370	−70.213704
>**MW370303**	CORBIDI13454	CORBIDI13454	B_steinbachi	12	3	12	24	12	Tambopata	Peru	−11.962370	−70.213704
>**MW370304**	CORBIDI13482	CORBIDI13482	B_steinbachi	12	3	12	24	12	Tambopata	Peru	−11.962370	−70.213704
>**MW370305**	CORBIDI15138	CORBIDI15138	B_steinbachi	12	3	12	24	12	Tambopata	Peru	−11.962370	−70.213704
>**MW370311**		JMP088	B_steinbachi	12	3	12	24	12	Chalalan._Franz_Tamayo	Bolivia	−14.428168	−67.922330
>AY549317	ZUEC12053		B_albopunctata	3	7	3	6	19	Campinas	SP	−22.926527	−47.002675
>JQ627203		10	B_albopunctata	3	7	3	6	19	Sao Carlos	SP	−21.98	−47.87
>JQ627205		114	B_albopunctata	3	7	3	6	19	Sao Carlos	SP	−21.98	−47.87
>KY002929	MCNAM19674		B_albopunctata	3	7	3	6	19		MG	−19.1694	−43.7148
>KY002930	MCNAM19670		B_albopunctata	3	7	3	6	19		MG	−19.1694	−43.7148
>KY002955	MCNAM19624		B_albopunctata	3	7	3	6	19		MG	−19.815346	−43.661281
>KY007134	MCNAM17920		B_albopunctata	3	7	3	6	19		MG	−19.1694	−43.7148
>KY911220	MCNAM19707		B_albopunctata	3	7	3	6	19		MG	−19.815346	−43.661281
>KDQF01002967	MPEG33422		B_sp.gralbopunctata4	3	7	21	10	20	Projeto Tocantizinho	PA	−6.061700	−56.296620
>KDQF01002983	MPEG36699		B_sp.gralbopunctata4	3	7	21	10	20	Itaituba	PA	−6.31731705	−55.7986444
>JF790116		AS0470	B_leucocheila	3	7	20	11	21A	Yucuma, Los Lagos	Bolivia	−12.772	−65.8109
>JF790117		MJ1326	B_leucocheila	3	7	20	11	21A	Yucuma, Los Lagos	Bolivia	−12.771967	−65.810933
>KDQF01003124		MTR00212	B_leucocheila	3	7	20	11	21A	Claudia	MT	−11.585	−55.1355556
>KDQF01003634		MTR25723	B_leucocheila	3	7	20	11	21A	Pacaas Novos	RO	−10.8158520	−63.6260410
>KDQF01002443		ESTR00081	B_multifasciata	3	7	20	12	21B	Carolina	MA	−7.22941	−47.26147
>KDQF01002465		ESTR0652	B_multifasciata	3	7	20	12	21B	Estreito	MA	−6.56055555	−47.4511111
>**MW370347**		H02	B_multifasciata	3	7	20	12	21B	Belem	PA	−1.439224	−48.417892
>**MW370348**		H13	B_multifasciata	3	7	20	12	21B	Belem	PA	−1.439224	−48.417892
>KDQF01001810		BM044	B_sp.gralbopunctata2	3	7	22	25	22	UHE Belo Monte	PA	−2.950584	−51.936607
>KDQF01003631		MTR25676	B_sp.gralbopunctata1	3	8	23	38	23	Pacaas Novos	RO	−10.7805610	−63.6266239
>AY843648	AMCC101446		B_sp.gr.albopunctata3	3	19	24	7	24	Demerara	Guyana	6.505246	−58.108209
>EU201110		AF0047	B_sp.gr.albopunctata3	3	19	24	7	24	Petit Saut	French_Guiana	5.066667	−53.05
>EU201111		CM241	B_sp.gr.albopunctata3	3	19	24	9	24	Saul	French_Guiana	3.625556	−53.207222
>JN970642	ROM22756		B_sp.gr.albopunctata3	3	19	24	7	24	Baramita	Guyana	7.3666	−60.4833
>JN970643	ROM28435		B_sp.gr.albopunctata3	3	19	24	8	24	Paramakatoi	Guyana	4.69722	−59.78666
>KDQF01000029		AF0048	B_sp.gr.albopunctata3	3	19	24	7	24	Petit Saut	French_Guiana	5.066667	−53.05
>KDQF01000041		AF0079	B_sp.gr.albopunctata3	3	19	24	9	24	St Georges	French_Guiana	3.888232	−51.807804
>KDQF01000163		AF0603	B_sp.gr.albopunctata3	3	19	24	9	24	St elie, pist PK∼8	French_Guiana	5.357068	−53.035859
>KDQF01000340		AF0943	B_sp.gr.albopunctata3	3	19	24	9	24	Matoury	French_Guiana	4.852891	−52.352092
>KDQF01000479		AF1272	B_sp.gr.albopunctata3	3	19	24	9	24	Matiti	French_Guiana	5.035425	−52.565573
>KDQF01000592		AF1570	B_sp.gr.albopunctata3	3	19	24	7	24	St elie, piste	French_Guiana	5.357068	−53.035859
>KDQF01000700		AF1832	B_sp.gr.albopunctata3	3	19	24	9	24	Montagne des Singes	French_Guiana	5.07148	−52.6927
>KDQF01000870		AF2173	B_sp.gr.albopunctata3	3	19	24	9	24	Sipaliwini, air strip	Suriname	2.02682	−56.12564
>KDQF01001448		AF3666	B_sp.gr.albopunctata3	3	19	24	9	24	Itoupe	French_Guiana	3.02208	−53.11046
>KDQF01002087		BPN3687	B_sp.gr.albopunctata3	3	19	24	7	24	Parabara, BC	Guyana	2.181833	−59.337017
>KDQF01002218		CM088	B_sp.gr.albopunctata3	3	19	24	9	24	Tibourou	French_Guiana	4.416667	−52.3
>KDQF01002220		CM093	B_sp.gr.albopunctata3	3	19	24	9	24	Cayenne, Montjoly	French_Guiana	4.916667	−52.266667
>KDQF01002262		CM242	B_sp.gr.albopunctata3	3	19	24	9	24	Saul	French_Guiana	3.625556	−53.207222
>KDQF01002301		CM338	B_sp.gr.albopunctata3	3	19	24	9	24	Cayenne, Montjoly	French_Guiana	4.916667	−52.266667
>KDQF01002415		DSM048	B_sp.gr.albopunctata3	3	19	24	9	24	Monsinery	French_Guiana	4.80338	−52.47466
>KDQF01002423		DSM097	B_sp.gr.albopunctata3	3	19	24	9	24	Monsinery	French_Guiana	4.80338	−52.47466
>KDQF01003251		MTR13743	B_sp.gr.albopunctata3	3	19	24	9	24	Serra do Navio	AP	0.9180556	−52.0027778
>KDQF01003256		MTR13750	B_sp.gr.albopunctata3	3	19	24	9	24	Serra do Navio	AP	0.9180556	−52.0027778
>KDQF01003257		MTR13751	B_sp.gr.albopunctata3	3	19	24	9	24	Serra do Navio	AP	0.9180556	−52.0027778
>KDQF01003259		MTR13769	B_sp.gr.albopunctata3	3	19	24	9	24	Serra do Navio	AP	0.9180556	−52.0027778

(*continued*)

Continued.

GenBank accession	Voucher	Field Number	Species_ID	mPTP	ABGD	mPTP	GMYC	Cons	Locality	State	Lat.	Long.
>KDQF01003260		MTR13776	B_sp.gr.albopunctata3	3	19	24	9	24	Serra do Navio	AP	0.9180556	−52.0027778
>KDQF01003264		MTR13793	B_sp.gr.albopunctata3	3	19	24	9	24	Serra do Navio	AP	0.9180556	−52.0027778
>KDQF01003299		MTR13953	B_sp.gr.albopunctata3	3	19	24	9	24	Laranjal do Jari	AP	−0.7166667	−52.3833333
>KDQF01003454		MTR20411	B_sp.gr.albopunctata3	3	19	24	7	24	E.E. Maraca	RR	3.36977	−61.44177
>KDQF01003472		MTR20525	B_sp.gr.albopunctata3	3	19	24	7	24	E.E. Maraca	RR	3.3326	−61.3824
>KDQF01003486		MTR20658	B_sp.gr.albopunctata3	3	19	24	8	24	Pacaraima	RR	4.46905	−61.13607
>KDQF01003491		MTR20680	B_sp.gr.albopunctata3	3	19	24	8	24	Pacaraima	RR	4.473034897	−61.1352092
>KDQF01003809		PG026	B_sp.gr.albopunctata3	3	19	24	9	24	Cayenne, Rorota	French_Guiana	4.874784	−52.261119
>KDQF01003813		PG036	B_sp.gr.albopunctata3	3	19	24	9	24	Kaw2	French_Guiana	4.516105	−52.10053
>KDQF01003845		PG248	B_sp.gr.albopunctata3	3	19	24	9	24	Haute Wanapi	French_Guiana	2.5134	−53.8211
>KDQF01004238	SMNS12093		B_sp.gr.albopunctata3	3	19	24	7	24	Bamboo landing	Guyana	5.325	−58.0455556
>KDQF01004356		TJC1243	B_sp.gr.albopunctata3	3	19	24	7	24	Black Water Creek	Guyana	5.07297	−59.24899
>KDQF01004364		TJC1268	B_sp.gr.albopunctata3	3	19	24	7	24	NARIL	Guyana	5.12324	−59.11266
>KR811154		PG779	B_sp.gr.albopunctata3	3	19	24	9	24	St Georges, Savane 14 juillet	French_Guiana	3.967639	−51.87225
>KR811155		MTR24173	B_sp.gr.albopunctata3	3	19	24	9	24	Oiapoque	AP	3.7960278	−51.8629167
>KR811156		MTR24194	B_sp.gr.albopunctata3	3	19	24	9	24	Lourenco	AP	2.3526389	−51.6152222
>KR811157		AF0749	B_sp.gr.albopunctata3	3	19	24	9	24	St Georges, savane	French_Guiana	3.925482	−51.788964
>**MW370336**		AG334	B_sp.gr.albopunctata3	3	19	24	9	24	RN2 PK103	French_Guiana	4.36387	−52.27747
>**MW370341**		AG480	B_sp.gr.albopunctata3	3	19	24	9	24	Saul, Monts Belvedere	French_Guiana	3.719347	−53.412809
>**MW370332**		AF3704	B_sp.gr.albopunctata3	3	19	24	9	24	Itoupe_200	French_Guiana	3.01498	−53.13286
>**MW370335**		AF3816	B_sp.gr.albopunctata3	3	19	24	7	24	Voltzberg_CI camp	Suriname	4.68169	−56.18568
>**MW370349**		QM108	B_sp.gr.albopunctata3	3	19	24	9	24	Matiti	French_Guiana	5.035425	−52.565573

Appendix 2. Molecular data acquisition

We extracted DNA from liver or muscle tissue (thigh or toe-clip) of the 307 samples using the Wizard Genomic extraction protocol (Promega; Madison, WI, USA). We targeted a ∼400 bp fragment of the 16S rDNA. We used primers N16R and N16F (Salducci et al., 2005), to which we added NNN + 8-nucleotide labels (hereafter designated as 'tags') for sample identification as all resulting PCR products were mixed into single libraries: 32 tags for forward primer (N16R) and 36 tags for reverse primer (N16F). The final volume of PCRs was 20 µl, and contained 2 µl of DNA extract diluted 10-fold, 10 µl of Amplitaq Gold® 360 Master Mix (Life Technologies, Carlsbad, CA, USA), 5.84 µl of Nuclease Free Water Ambion (Thermo Fisher Scientific, MA, USA), 0.25 µM of each primer and 3.2 µg of Bovine Serum Albumin (Roche Diagnostic, Basel, Switzerland). We ran the PCR in duplicate for each sample, and we included blank PCR controls in the analysis using nuclease-free water as template. First, the mixture was denaturated at 95 °C for 10 min, followed by 40 cycles of 30 s at 95 °C, 30 s at 55 °C and 1 min at 72 °C; followed by a final step of 7 min at 72 °C. Libraries of mixed PCR products were sequenced using 2 × 250 paired-end reads sequencing technology through MiSeq high throughput sequencing (Illumina) at the Génopole (Toulouse, France). The resulting outputs were analysed with the OBITOOLS software suite (Boyer et al., 2016a). Paired-end reads were assembled and merged, and we used the tag attached to the primer to assign each reads to its label. Then we removed low quality reads (alignment scores <50, containing Ns or shorter than 50 bp). The resulting batch of reads was dereplicated while keeping the coverage information (number of reads merged). All sequences <100 bp were discarded. Eventually, all the sequences that we included in our dataset were >380 bp long.

Mitogenome sequencing, assembling, and annotation

For complete mitochondrial sequencing we used 200 ng of genomic DNA per sample to build libraries at the Genotoul-GeT-PlaGe core facility (Toulouse, France). Genomic DNA was fragmented by sonication, fragments were size-selected (50–400 bp), adenylated and ligated to indexed sequencing adapters. Eight cycles of Polymerase Chain Reaction (PCR) were applied to amplify libraries before library quantification and validation. A total of 48 libraries were multiplexed to be sequenced on one lane on an Illumina HiSeq 3000 flow cell (Illumina Inc., San Diego, CA). Read assembly was performed using the ORGanelle ASseMbler (Boyer et al., 2016b), a python program developed especially for organelle and ribosomal DNA reconstructions from a genome skimming dataset. The first step is to sort and index the reads with the *oa index* command. Then, with the *oa buildgraph* command, the program uses a seed (reference sequence) to assemble the reads and creates a graph with all the fragments assembled. Finally, the *oa unfold* command finds an optimal path in the assembly graph and reconstructs the consensus sequence (Boyer et al., 2016b).

For the *oa index* command, we used two options: (i) *–estimate-length 0.9*, which estimates the reads' length using 90% of the reads; and (ii) *–bypass-filtering* when the read indexing failed due to an over-filtering that resulted in an empty index. For the *oa buildgraph* command we used default settings in most cases, except if the assembly graph was empty due to errors in coverage estimation. In these cases, we modified the *–coverage* value to be slightly lower than the estimate. For the *oa unfold* command we used the default options as long as it was able to find the optimal assembly path. If not, we checked the assembling graph with the yEd

Graph Editor (organic layout, default parameters) and selected the green fragments (that correspond to similar seed fragments) and extracted them with the *–path–* option in the *oa unfold* command. The fragments were then mapped onto a seed with the Geneious (R9.1.7; Biomatters Ltd, Auckland, New Zealand) *map to reference* function with medium-low sensitivity and one iteration. The mapping consensus was extracted and considered as a mitochondrial genome assembly.

For annotation, sequences were aligned on the MAFFT7 online server under default parameters except the use of E-INS-i strategy for rDNA, which is designed for sequences with multiple conserved domains and long gaps (Katoh et al., 2019). Then, using the Geneious R9.1.7 *transfer annotation* function, we annotated all the alignment sequences from a reference sequence (*Anomaloglossus baeobatrachus*; NC_030054). Finally, we checked that each coding sequence (CDS) began with a methionine (ATA or ATG codon for vertebrate mitochondrial genomes) and ended with a stop codon. For the final alignment, we kept the CDS, 12S–16S loci.

Supplementary references

Boyer, F., Coissac, E., Viari, A. (2016b). The ORGanelle ASseMbler. *Retrieved from* https://pypi.org/project/ORG.asm/

Boyer, F., Mercier, C., Bonin, A., Le Bras, Y., Taberlet, P., & Coissac, E. (2016a). obitools: A unix-inspired software package for DNA metabarcoding. *Mol Ecol Resour*, *16*(1), 176–182. https://doi.org/10.1111/1755-0998.12428

Salducci, M.-D., Marty, C., Fouquet, A., & Gilles, A. (2005). Phylogenetic relationships and biodiversity in Hylids (Anura: Hylidae) from French Guiana. *Comptes Rendus Biologies*, *328*(10-11), 1009–1024. https://doi.org/10.1016/j.crvi.2005.07.005

Appendix 3. Completion for the mitogenomic matrix

Terminals	Cons	voucher	mtDNA				
			12S	16S	ND1	COI	CytB
Boana_eucharis	1	MZUSP 159227			MTR25798		
Boana aff. *lanciformis*	2	MTR33845			MTR33845		
Boana aff. *maculateralis*	16	MTR28015			MTR28015		
Boana aff. *steinbachi*(1)	22	MTR33822			MTR33822		
*Boana*_aff. *steinbachi*(2)	24	SCF395			SCF395		
Boana_albopunctata	5	ZUEC12053	AY549317				AY549370
Boana_alfaroi	9	QCAZ44528			QCAZ44528		
Boana_almendarizae	10	QCAZ31449			QCAZ31449		
Boana_calcarata	11	H2487			H2487		
Boana_dentei	12	AF2797			AF2797		
Boana_fasciata	13	QCAZ24866			QCAZ24866		
Boana_heilprini	14	AMNHA168405	AY843632		KF794126		AY843864
Boana_lanciformis	15	MJH564	AY843636				AY843870
Boana_leucocheila	6	MTR25723			MTR25723		
Boana_maculateralis	17	QCAZ43827			QCAZ43827		
Boana_multifasciata	8	ESTR00081		ESTR00081			
Boana_raniceps	19	MPEG36750			MPEG36750		
*Boana*_aff.courtoisae	20	AF0937			AF0937		
*Boana*_courtoisae	21	AF2584			AF2584		
*Boana*_sp. gr. *albopunctata* 3	18	AF2173			AF2173		
*Boana*_sp. gr. *albopunctata* 1	7	MTR25676		MTR25676			
*Boana*_sp. gr. *albopunctata* 2	3	BM044		BM044		BM044	
*Boana*_sp. gr. *albopunctata* 4	4	MPEG33422		MPEG33422			
Boana_steinbachi	23	MJ1301			MJ1301		
Boana_tetete	25	QCAZ40080			QCAZ40080		
*Aplastodiscus*_sp	Cophomantinae_OG	MTR26425			MTR26425		
Boana_boans	Boana_OG	AF1981			AF1981		
Boana_cinerascens	Boana_OG	TJC1100			TJC1100		
Boana_diabolica	Boana_OG	AF1827			AF1827		
Boana_ornatissima	Boana_OG	AF1912			AF1912		
Boana_pellucens	Boana_OG	WED53621	AY326058				
Boana_pulchella	Boana_OG	MACN37788	AY549352		KF794138		AY549405
Boana_punctata	Boana_OG	AF3280			AF3280		
Boana_riojana	Boana_OG	MACN37507	AY549356				
Boana_xerophylla	Boana_OG	AF1797			AF1797		
*Bokermannohyla*_sp	Cophomantinae_OG	MTR26423			MTR26423		
*Hyloscirtus*_sp	Cophomantinae_OG	AF4400			AF4400		
Myersiohyla_inparquesi	Cophomantinae_OG	RWM17688	AY843672				
Nesorohyla_kanaima	Cophomantinae_OG	ROM39582	AY843634		GQ366307		AY843868

Appendix 4. Detailed information on sound files analyzed for this study. Letters following numbers of recordings in AAG-UFU collection (e.g. 1a–e) indicate the number of sound files for each recorded male

Boana courtoisae

Sound file – MNHN-SO-2020-2943. Unvouchered recording. Recorded from Rorota, French Guiana.

Sound file – MNHN-SO-2020-2944. Unvouchered recording. Recorded from Rorota, French Guiana.

Sound file – MNHN-SO-2020-2946. Unvouchered recording. Recorded from Rorota, French Guiana.

Sound file – MNHN-SO-2020-2945. Unvouchered recording. Recorded from Rorota, French Guiana.

Sound file – MNHN-SO-2020-2947. Unvouchered recording. Recorded from Sipaliwini, Suriname.

Sound file – MNHN-SO-2020-2948. Unvouchered recording. Recorded from Paletuviers, French Guiana.

Boana eucharis

Sound files – Boana_eucharisAltaFlorestaMT1a–eDLB_AAGm671/ MNHN-SO-2020-2949–53; recorded on 11 January 2019, at 7:44 pm, air 24.5 °C. voucher: AAG-UFU 6503 (holotype). Recorded from Alta Floresta, Mato Grosso, Brazil.

Sound files – Boana_eucharisAltaFlorestaMT2a–cDLB_AAGm671/ MNHN-SO-2020-2954–56; recorded on 11 January 2019, at 8:04 pm, air 24.5 °C. Voucher: AAG-UFU 6504 (paratype). Recorded from Alta Floresta, Mato Grosso, Brazil.

Sound file – Boana_eucharisAltaFlorestaMT3a–cDLB_AAGm671/ MNHN-SO-2020-2957–59; recorded on 11 January 2019, at 8:10 pm, air 24.5 °C. Unvouchered recording. Recorded from Alta Floresta, Mato Grosso, Brazil.

Sound file – Boana_eucharisAltaFlorestaMT4a–bDLB_AAGm671/ MNHN-SO-2020-2960–61; recorded on 11 January 2019, at 9:05 pm, air 24.5 °C. Unvouchered recording. Recorded from Alta Floresta, Mato Grosso, Brazil.

Sound file – Boana_eucharisAltaFlorestaMT5a–iPM_AAGm671/ MNHN-SO-2020-2962–70; recorded on 20 January 2020, at 8:02 pm, air 25.1 °C. Voucher: AAG-UFU 6901 (paratype). Recorded from Alta Floresta, Mato Grosso, Brazil.

Sound file – Boana_eucharisAltaFlorestaMT6a–bAAGm671/ MNHN-SO-2020-2971–72; recorded on 20 January 2020, at 9:18 pm, air 25.0 °C. Unvouchered recording. Recorded from Alta Floresta, Mato Grosso, Brazil.

Sound file – Boana_eucharisAltaFlorestaMT7a–fAAGm671/ MNHN-SO-2020-2973–78 and MNHN-SO-2020-2980–81; recorded on 20 January 2020, at 9:48 pm, air 25.0 °C. Unvouchered recording. Recorded from Alta Floresta, Mato Grosso, Brazil.

Boana steinbachi

Sound file – MNHN-SO-2020-2934 . Voucher: SMF88394. Recorded from Buenavista, Sara province, Bolivia.

Sound file – MNHN-SO-2020-2935. Voucher: SMF88397. Recorded from Buenavista, Sara province, Bolivia.

Sound file – MNHN-SO-2020-2936. Unvouchered recording. Recorded from Rio Matos, Beni, Bolivia.

Sound file – MNHN-SO-2020-2937. Unvouchered recording. Recorded from Rio Matos, Beni, Bolivia.

Sound file – MNHN-SO-2020-2938. Unvouchered recording. Recorded from Tambopata, Madre de Dios, Peru.

Sound file – 14-Hyla fasciata. Unvouchered recording. Recorded from Tambopata, Madre de Dios, Peru.

Sound file – ML198328. Unvouchered recording. Recorded from Tambopata, Madre de Dios, Peru.

Sound file – ML198676. Unvouchered recording. Recorded from Tambopata, Madre de Dios, Peru.

Sound file – ML198677. Unvouchered recording. Recorded from Tambopata, Madre de Dios, Peru.

Sound file – ML222268. Unvouchered recording. Recorded from Cuzco Amazonico, Peru.

Sound file – Boana_steinbachiAssisBrasilAC1a–dTRC_AAGm671/ MNHN-SO-2020-2939–42; recorded on 12 February 2017, at 8:00 pm, air 26.2 °C. Voucher: AAG-UFU 5917. Recorded from Assis Brasil, Acre, Brazil.

Sound file – FNJV12840; recorded on 4 December 1986, at 8:00 pm, air 23.5 °C. Unvouchered recording. Recorded from Altamira, Pará, Brazil.

Sound file – FNJV12841; recorded on 7 December 1986, at 10:00 pm, air 23.5 °C. Unvouchered recording. Recorded from Altamira, Pará, Brazil.

Appendix 5. Details and justifications for the identification of these OTUs and their respective geographic ranges

Boana raniceps (1 OTU)

Boana raniceps is recovered as a single OTU, distantly related from the rest of the species and widely distributed latitudinally from Argentina to French Guiana and longitudinally from Bahia to central Amazonia throughout the Cerrado and Chaco. This distribution encompasses the type locality 'Paraguay'.

The *Boana albopunctata* clade (9 OTUs)

Boana albopunctata is restricted to a small range in the states of Sao Paulo and Minas Gerais, encompassing its type locality. However, additional data (Prado, Haddad, & Zamudio, 2012) indicate that the actual range of this OTU extends at least to the states of Goiás, Mato Grosso do Sul, and Paraná. However, the other populations previously identified as *B. albopunctata* further north in the Cerrado and in Amazonia probably belong to a distinct species, as already suggested by Prado et al. (2012).

Boana leucocheila is tentatively assigned to one of the OTU distributed in Mato Grosso, Rondônia, and Bolivia. This distribution encompasses the type locality (Caramaschi & de Niemeyer, 2003) and other populations also reported in Mato Grosso (Pansonato, Ávila, Kawashita-Ribeiro, & Morais, 2011). The examination of specimens (MTR) corroborated this identification.

Boana multifasciata was sampled at the type locality in Belém, Pará state, and in two localities (Carolina and Estreito) at the border between the states of Maranhão and Tocantins. This species may be circumscribed to the northern part of the Cerrado and adjacent parts of Amazonia. The range of this species probably extends further southward at least in northern Cerrado. However, the Amazonian populations previously identified as *B. multifasciata* are suggested to belong to a distinct species (see hereafter).

The populations previously identified as *Boana multifasciata* (*B.* aff. *albopunctata* 3) from the Guiana Shield, and as *Boana albopunctata* from Belo Monte, Pará (*B.* aff. *albopunctata* 2), Itaituba, Pará (*B.* aff. *albopunctata* 4), and Rondônia (*B.* aff. *albopunctata* 1) are suggested to belong to yet undescribed species. The two taxa (*B. paranaiba* and *B. caiapo*) that could not be included in our analysis are described from localities in the Cerrado (see Carvalho, Giaretta, & Facure, 2010; Pinheiro et al., 2018), and are thus unlikely to correspond to these Amazonian OTUs. Given the phenotypic differences observed among *B. leucocheila*, *B. albopunctata*, and *B. multifasciata*, these OTUs may also be phenotypically distinct from each other (Caramaschi & de Niemeyer, 2003; Carvalho et al., 2010). Nevertheless, we did not examine variation across these populations because it was outside the scope of our study. Therefore, these OTUs should be considered as Unconfirmed Candidate Species (UCS).

Boana lanciformis has a wide range in Western Amazonia (Peru, Ecuador Colombia, and Amazonas State in Brazil), encompassing its type locality in the District Pebas, Region of Loreto, Peru (incorrectly ascribed to Ecuador by Cope). However, one population from Téfé (Amazonas, Brazil), in central Amazonia, is found genetically distinct and identified as a separate OTU. We did not examine variation across these populations, thus, this OTU will be considered as UCS. Interestingly, the range of these two OTUs does not overlap with neither *Boana raniceps* nor any of the other OTU related to *B. albopunctata*.

The *Boana calcarata* clade (5 OTUs)

Boana calcarata is recovered as a single OTU largely distributed throughout Amazonia, thus encompassing its type locality in Guyana.

Boana almendarizae and *B. fasciata* display ranges circumscribed to the slopes of the Andes of Ecuador (type localities in Morona Santiago and Zamora-Chinchipe provinces, respectively) and northern Peru (Amazonas province), as already established by Caminer and Ron (2014). Similarly, *B. maculateralis* displays a small range in Ecuador, but in the lowlands. Its actual range extends at least to Meta (Acosta-Galvis et al., 2018) and Guaviare (Medina-Rangel, Méndez-Galeano, & Calderón-Espinosa, 2019) in Colombia, and probably to adjacent Peru. However, the populations from Loreto in northern Peru previously documented by Caminer and Ron (2014) as distinct from *B. maculateralis*, cluster with other populations from Loreto in northern Peru, and from Rio Içá (Amazonas) and Serra do Divisor (Acre) in north-western Brazil, forming a distinct OTU (*B.* aff. *maculateralis*). Populations from Leticia, in south-eastern Colombia (Acosta-Galvis et al., 2018), Japurá (Amazonas) in north-western Brazil (Rojas-Zamora et al., 2017), and from Manu National Park in southern Peru (Caminer & Ron, 2014) probably display this lineage as well. We did not examine variation across these populations, thus, this OTU will be considered as UCS.

The *Boana steinbachi* clade (9 OTUs)

Boana dentei displays a small range in the easternmost part of the Guiana Shield lowlands (Amapá and French Guiana) encompassing its type locality (Serra do Navio).

Boana alfaroi and *B. tetete* both display small ranges in Amazonian lowlands of Ecuador, as documented by Caminer and Ron (2014). Moreover, the range of *B. alfaroi* extends further north to Putumayo (Meza-Joya, Ramos-Pallares, & Hernández-Jaimes, 2019) and Caquetá (Medina-Rangel et al., 2019) in Colombia. However, the record from Acre provided by Carvalho et al. (2017) corresponds to *B.* aff. *steinbachi* 1 (see below). The range of *B. tetete* extends to Loreto, Peru,

confirming records from Acosta-Galvis et al. (2018). Nevertheless, their record from Leticia most likely corresponds to either *B. alfaroi* or *B*. aff. *steinbachi* 1.

Boana steinbachi occurs from Bolivia (type locality) to south-eastern Peru (Tambopata, Madre de Dios), and more surprisingly in eastern Brazilian Amazonia (Pará). This extensive range with a wide gap between Bolivia and Pará and the fact that acoustic data associated with voucher specimens were not available from the Pará populations did not allow us to confirm the taxonomic identity of these populations as conspecific with nominal *B. steinbachi* (see below). Another group of related populations extends widely in Western Amazonia of Peru, Colombia, and Brazil, forming a distinct OTU (*B*. aff. *steinbachi* 1). The populations previously identified as *Boana alfaroi* (Carvalho, Bang, Teixeira, & Giaretta, 2017) belong to this OTU, but since we did not find any phenotypic diagnosis among the OTUs within this clade, we treated them as conspecific with *B. steinbachi*. Additional populations from southern and eastern Peru (lower Madre de Dios River, Madre de Dios and Cocama, Ucayali) are identified as a distinct small-range OTU (*B*. aff. *steinbachi* 2). We examined the type series of *Boana steinbachi*, examined the morphology and analysed calls of a series of topotypes, and provided an amended diagnosis of the nominal species.

Populations from Rondônia (Pacaás Novos and Jirau) and Mato Grosso (Apiacás, Juruena, and Alta Floresta) form a distinct small-range lineage identified as a distinct OTU (*Boana* sp. 1). These populations were so far confused with *B. fasciata* (Avila & Kawashita-Ribeiro 2011; Lima, Keller, & Rebelo, 2017). We assessed the phylogenetic relationships and morphological and acoustic characters of *Boana* sp. 1, which led us to describe it herein as a new species (see below).

Populations from the Eastern Guiana Shield form two additional OTUs: *Boana* sp. 2 which extends throughout the region, and *Boana* sp. 3 which is circumscribed to coastal French Guiana. These populations were previously identified as *Boana fasciata* (Fouquet et al., 2007; Lescure & Marty 2000; Dewynter et al., 2008) and subsequently suggested to belong to an unnamed species (Funk et al., 2012; Caminer & Ron 2014; Cole, Townsend, Reynolds, MacCulloch, & Lathrop, 2013; Fouquet, Vidal, & Dewynter, 2019). We examined morphological and acoustic characters of specimens of *Boana* sp. 2 and described it herein as a new species (see below). However, we tentatively consider *Bana* sp. 3 as conspecific with *Boana* sp. 2 since no clear phenotypic differentiation was found across Guiana Shield populations.

Appendix 6A. Descriptive statistics of type 1 calls of the *Boana steinbachi* clade. Data presented as mean ± SD (range)

	***Boana eucharis* sp. nov.**	***Boana courtoisae* sp. nov.**	***Boana steinbachi***	***Boana dentei* (Marinho et al., 2020)**
Call duration (ms)	290 ± 42 (100–430)	120 ± 31 (140–240)	280 ± 49 (130–430)	70 ± 10 (60–90)
Number of notes	3–7	3–4	3–8	1
Note duration (ms)	13 ± 5 (3–60)	18 ± 3 (5–36)	15 ± 7 (4–52)	–
Note interval (ms)	61 ± 4 (27–82)	47 ± 5 (20–69)	41 ± 10 (1–67)	–
Dominant frequency (Hz)	2319.28 ± 113.18 (1981.10–2971.60)	2259.18 ± 216.22 (1636.50–2454.80)	2396.51 ± 312.85 (1687.50–3402.20)	2400.00 ± 300.00 (1900.00–2900.00)
Maximum frequency (Hz)	2841.46 ± 475.71 (2196.40–4220.50)	2860.05 ± 136.21 (2627.10–3100.80)	3336.38 ± 331.49 (2713.28–4478.90)	2800.00 ± 200.00 (2500.00–3100.00)
Minimum frequency (Hz)	1964.83 ± 109.88 (1722.70–2250.00)	1678.49 ± 230.85 (1335.10–1875.00)	1664. 90 ± 138.50 (1355.10–1981.10)	1600.00 ± 100.00 (1450.00–1800.00)
Call rise time (%)	45 ± 10 (2–97)	42 ± 18 (7–94)	48 ± 57 (2–98)	25 ± 7 (15 – 37)
Recorded males	7	5	13	9
Air temperature (°C)	25.1–25.4	–	–	24.5–25.5

Appendix 6~~A~~B. Descriptive statistics of type 1 calls of the analysed species. Data presented as mean ± SD (range)

	***Boana eucharis* sp. nov.**	***Boana courtoisae* sp. nov.**	***Boana steinbachi***	***Boana dentei* (Marinho et al., 2020)**
Call duration (ms)	48 ± 5 (29–64)	53 ± 16 (39–79)	48 ± 5 (29–64)	160 ± 30 (120–200)
Dominant frequency (Hz)	2515.11 ± 245.16 (1938.06–3143.80)	21912.14 ± 312.93 (1679.70–2411.70)	2469.43 ± 175.63 (1687.50–2812.50)	1900.00 ± 300.00 (1600.00–2200.00)
Maximum frequency (Hz)	3083.52 ± 142.57 (2712.20–3421.90)	2876.84 ± 186.20 (2627.10–3143.80)	3146.92 ± 353.97 (2713.20–4522.00)	2500.00 ± 100.00 (2300.00–2600.00)
Minimum frequency (Hz)	1861.25 ± 56.89 (1593.50–2067.20)	1533. 20 ± 112.30 (1464.30–1722.70)	1724.92 ± 62.75 (1453.10–2015.60)	1500.00 ± 100.00 (1300.00–1600.00)
Note rise time (%)	48 ± 7 (24–78)	57 ± 16 (39–82)	70 ± 7 (18–60)	41 ± 14 26–65
Recorded males	7	5	5	9
Air temperature (°C)	25.1–25.4	–	–	24.5–25.5

Appendix 7. Descriptive statistics of morphometric traits (in mm) from specimens of the *Boana steinbachi* clade: topotypes and additional specimens of *B. steinbachi*, and the type series of *B. eucharis* sp. nov. and *B. courtoisae* sp. nov. Data presented as mean ± SD (range). Abbreviations are: SVL = snout-vent length; FOOT = foot length; HL = head length; HW = head width; ED = eye diameter; TD = tympanum diameter; TL = tibia length; FL = femur length; CL = calcaneal appendage length. * sample sizes for CL are as follows: *B. steinbachi* (N = 6 males), *B. eucharis* sp. nov. (N = 7 males), and *B. courtoisae* sp. nov. (all specimens were measured)

	Boana steinbachi		*Boana eucharis* sp. nov.	*Boana courtoisae* sp. nov.	
	Males N = 18	Females N = 6	Males N = 7	Males N = 13	Females N = 3
SVL	33.6 ± 1.6 (30.4–37.4)	44.9 ± 2.1 (42.5–48.8)	32.7 ± 1.2 (30.8–34.7)	33.1 ± 1.9 (30.8–35.9)	44.2 ± 1.5 (43.0–45.9)
FL	14.0 ± 1.4 (11.4–16.6)	18.0 ± 0.8 (16.6–18.8)	13.3 ± 0.4 (12.7–13.7)	13.6 ± 1.1 (11.8–15.5)	19.0 ± 0.5 (18.6–19.5)
HL	11.5 ± 2.1 (7.9–13.4)	10.9 ± 0.3 (10.5–11.4)	12.1 ± 0.7 (10.7-12.9)	12.1 ± 0.8 (10.8–14.0)	15.5 ± 0.6 (15.0–16.1)
HW	10.8 ± 0.8 (9.2–12.1)	15.0 ± 0.4 (14.4–15.5)	10.7 ± 0.5 (10.1–11.8)	11.3 ± 1.0 (10.0–12.9)	14.5 ± 1.0 (13.6–15.6)
ED	4.0 ± 0.4 (3.2–4.9)	4.3 ± 0.4 (3.9–5.1)	4.2 ± 0.2 (3.8–4.7)	4.7 ± 0.4 (4.0–5.4)	5.1 ± 0.6 (4.4–5.5)
TD	2.1 ± 0.3 (1.3–2.5)	2.5 ± 0.5 (1.9–2.9)	2.0 ± 0.2 (1.6–2.2)	2.1 ± 0.2 (1.8–2.3)	2.4 ± 0.00
TL	18.7 ± 2.1 (14.2–21.7)	22.6 ± 1.4 (20.5–24.3)	18.4 ± 0.7 (17.1–19.6)	19.1 ± 1.1 (17.7–20.9)	26.1 ± 0.6 (25.6–26.7)
THL	18.8 ± 1.9 (14.8–21.1)	25.4 ± 0.9 (24.4–27.1)	16.7 ± 1.4 (14.9–18.6)	17.5 ± 1.2 (15.8–19.5)	23.7 ± 1.5 (22.1–25.1)
CAL*	0.5 ± 0.1 (0.3–0.6)	—	0.2 ± 0.0 (0.1–0.2)	0.5 ± 0.1 (0.3–0.6)	0.7 ± 0.1 (0.6–0.7)

Appendix 8. Additional *Boana courtoisae* sp. nov. specimens

Males:

AF1925, AF1934: French Guiana, Flat de la Waki
AF2319: French Guiana, Trinité,
AF3059, AF3070: French Guiana, Mitan
AF3694: French Guiana, Itoupe
AM008: French Guiana, Inini Tolenga
AF2115, AF2195: Suriname, Sipaliwini
AF3452, Suriname, Spari Creek
AF3775, AF3784: Suriname, Voltzberg, CI camp

Females:

AF2584, French Guiana, Sinnamary
AF1694, French Guiana, Saul – Limonade
AF1544, French Guiana, Saul – Gros arbre

Appendix 9. BioGeoBears models

Models	LnL	d	e	j	AIC	DAIC
DEC + J	**-46.445**	**6.89E-03**	**1.00E-12**	**0.040**	**98.89**	**0**
DIVAlike + J	−46.798	9.59E-03	2.00E-09	0.033	99.6	0.71
BAYAREA + J	−50.002	6.96E-3	1.00E-12	0.047	106	7.11
DEC	−52.78	0.015	1.00E-12	0	109.6	10.71
DIVAlike	−55.922	0.014	1.00E-12	0	115.8	16.91
BAYAREA	−61.097	0.014	0.147	0	126.2	27.31